Computers and Mathematics with Applications 71 (2016) 585–614

Contents lists available at ScienceDirect

Computers and Mathematics with Applications

journal homepage: www.elsevier.com/locate/camwa

A priori and a posteriori error analyses of a pseudostress-based mixed formulation for linear elasticity☆

Gabriel N. Gatica [a,b,*], Luis F. Gatica [a,c], Filánder A. Sequeira [d,1]

[a] *CI²MA, Universidad de Concepción, Concepción, Chile*

[b] *Departamento de Ingeniería Matemática, Universidad de Concepción, Casilla 160-C, Concepción, Chile*

[c] *Departamento de Matemática y Física Aplicadas, Facultad de Ingeniería, Universidad Católica de la Santísima Concepción, Casilla 297, Concepción, Chile*

[d] *Escuela de Matemática, Universidad Nacional de Costa Rica, Heredia, Costa Rica*

ARTICLE INFO

Article history:
Received 28 May 2015
Received in revised form 20 November 2015
Accepted 12 December 2015
Available online 5 January 2016

Keywords:
Pseudostress–displacement formulation
Linear elasticity
Mixed finite element method
3D high-order approximations

ABSTRACT

In this paper we present the a priori and a posteriori error analyses of a non-standard mixed finite element method for the linear elasticity problem with non-homogeneous Dirichlet boundary conditions. More precisely, the approach introduced here is based on a simplified interpretation of the pseudostress–displacement formulation originally proposed in Arnold and Falk (1988), which does not require symmetric tensor spaces in the finite element discretization. In addition, physical quantities such as the stress, the strain tensor of small deformations, and the rotation, are computed through a simple postprocessing in terms of the pseudostress variable. Furthermore, we also introduce a second element-by-element postprocessing formula for the stress, which yields an optimally convergent approximation of this unknown with respect to the broken $\mathbb{H}(\mathbf{div})$-norm. We apply the classical Babuška–Brezzi theory to prove that the corresponding continuous and discrete schemes are well-posed. In particular, Raviart–Thomas spaces of order $k \geq 0$ for the pseudostress and piecewise polynomials of degree $\leq k$ for the displacement can be utilized. Moreover, we remark that in the 3D case the number of unknowns behaves approximately as 9 times the number of elements (tetrahedra) of the triangulation when $k = 0$. This factor increases to 12.5 when one uses the classical PEERS. Next, we derive a reliable and efficient residual-based a posteriori error estimator for the mixed finite element scheme. Finally, several numerical results illustrating the performance of the method, confirming the theoretical properties of the estimator, and showing the expected behaviour of the associated adaptive algorithm, are provided.

1. Introduction

The introduction of further unknowns of physical interest, such as stresses, rotations, and tractions, and the need of locking-free numerical schemes when the corresponding Poisson ratio approaches 1/2, have historically been the main

☆ This work was partially supported by CONICYT-Chile through BASAL project CMM, Universidad de Chile, project Anillo ACT1118 (ANANUM), and the Becas-Conicyt Programme for foreign students; by Centro de Investigación en Ingeniería Matemática (CI²MA), Universidad de Concepción; and by Dirección de Investigación of the Universidad Católica de la Santísima Concepción, through the project DIN 07/2014.

* Corresponding author at: Departamento de Ingeniería Matemática, Universidad de Concepción, Casilla 160-C, Concepción, Chile.
E-mail addresses: ggatica@ci2ma.udec.cl (G.N. Gatica), lgatica@ucsc.cl (L.F. Gatica), filander.sequeira@una.cr, fsequeira@ci2ma.udec.cl (F.A. Sequeira).

1 Present address: CI²MA and Departamento de Ingeniería Matemática, Universidad de Concepción, Casilla 160-C, Concepción, Chile.

http://dx.doi.org/10.1016/j.camwa.2015.12.009
0898-1221/

reasons for the utilization of dual-mixed variational formulations and their associated mixed finite element methods to solve elasticity problems. The incompressible case can also be easily handled with this kind of formulations since the constants appearing in the stability and a priori error estimates do not depend on the unbounded Lamé parameter. Consequently, the derivation of appropriate finite element subspaces yielding corresponding well-posed Galerkin schemes has been extensively studied in the last three decades at least, and important early contributions with weakly imposed symmetry for the stress, which include the classical PEERS element and related approaches, were provided in [1–3], to name a few. However, since the appearing of those first works, the main challenge in this direction has been the development of mixed finite element methods that incorporate the symmetry of the stress into the definition of the respective continuous and discrete spaces. In fact, the first stable mixed finite element methods for linear elasticity, with symmetric and weakly symmetric stresses, were derived, thanks to the finite element exterior calculus, about a decade ago (see, e.g. [4–7]). In particular, the polynomial shape-functions provided in [7] yield the first stable elements for the symmetric stress–displacement approach in two dimensions. In this case, 24 degrees of freedom defining piecewise cubic polynomials for the stresses, and piecewise linear functions for the displacement, constitute the cheapest element. In turn, 162 degrees of freedom defining piecewise quartic stresses, and again piecewise linear displacements, form the lowest order element in 3D, which was introduced in [8]. Furthermore, stable elements with weak imposition of symmetric stresses have been derived in [4,6]. The corresponding element using the lowest polynomial degrees is determined by piecewise constants approximations for both the displacement and rotation, and piecewise linear functions for the stress. In addition, stable Stokes elements and interpolation operators keeping the reduced symmetry were employed in [9] to derive simpler proofs of the main results provided in [4,6].

On the other hand, an alternative way of dealing with dual-mixed variational formulations in continuum mechanics, without the need of imposing neither strong nor weak symmetry of the stresses, is given by the utilization of pseudostress-based approaches. In fact, this technique, which has become very popular, specially in fluid mechanics, has gained considerable attention in recent years due to its applicability to diverse linear as well as nonlinear problems. In particular, the velocity–pseudostress formulation of the Stokes equations was first studied in [10], and then reconsidered in [11], where further results, including the eventual incorporation of the pressure unknown and an associated a posteriori error analysis, were provided. In turn, augmented mixed finite element methods for pseudostress-based formulations of the stationary Stokes equations, which extend analogue results for linear elasticity problems (see [12–14]), were introduced and analysed in [15]. Furthermore, the velocity–pressure–pseudostress formulation has also been applied to nonlinear Stokes problems. In particular, a new mixed finite element method for a class of models arising in quasi-Newtonian fluids, was introduced in [16]. The results in [16] were extended in [17] to a setting in reflexive Banach spaces, thus allowing other nonlinear models such as the Carreau law for viscoplastic flows. Moreover, the dual-mixed approach from [16,17] was reformulated in [18] by restricting the space for the velocity gradient to that of trace-free tensors. For related contributions dealing with pseudostress-based formulations in incompressible flows, we refer to [19,20], and the references therein. In turn, the corresponding extension to the Navier–Stokes equations has been developed in [21,22]. More recently, a new dual-mixed method for the aforementioned problem, in which the main unknowns are given by the velocity, its gradient, and a modified nonlinear pseudostress tensor linking the usual stress and the convective term, has been proposed in [23]. The idea from [23] has been modified in [24] through the introduction of a nonlinear pseudostress tensor linking now the pseudostress (instead of the stress) and the convective term, which, together with the velocity, constitute the only unknowns. Lately, the approach from [24] has been further extended in [25,26], where new augmented mixed-primal formulations for the stationary Boussinesq problem and the Navier–Stokes equations with variable viscosity, respectively, have been proposed and analysed. In spite of the many aforedescribed works, it is quite surprising to realize that almost no contribution is available in the literature on the use of pseudostress-based formulations for the elasticity problem. Indeed, the search in MathScinet under the title words "*pseudostress*" and "*elasticity*" yields no results at all. Actually, up to the authors' knowledge, the only paper referring to this issue is [27], where a modified Hellinger–Reissner principle is employed to derive a new mixed variational formulation for the equations of linear elasticity. The resulting approach yields a pseudostress unknown defined in terms of the gradient of the displacement field, but depending also on a parameter to be chosen conveniently.

In the present paper we modify the approach from [27] by realizing that, under a suitable rewriting of the equilibrium equation, one can define a simpler pseudostress unknown in terms again of the gradient of the displacement field, but independent of any additional parameter. In addition, we introduce an element-by-element postprocessing formula for the symmetric stress, which yields an optimally convergent approximation of this unknown with respect to the broken $\mathbb{H}(\mathbf{div})$-norm. Moreover, a reliable and efficient residual-based a posteriori error estimator for the mixed finite element scheme is also derived. A very summarized version of the first part of this work is available in [28]. The rest of this paper is organized as follows. In Section 2 we describe the linear elasticity problem with non-homogeneous Dirichlet boundary conditions, derive its pseudostress-based dual-mixed formulation, and then show that it is well-posed. In Section 3 we introduce and analyse the associated mixed finite element method. In particular, we show that Raviart–Thomas spaces of order $k \geq 0$ for the pseudostress and piecewise polynomials of degree $\leq k$ for the displacement can be employed, which, in the 3D case, yields a global number of unknowns behaving approximately as only 9 times the number of tetrahedra of the triangulation when $k = 0$. Next, a reliable and efficient residual-based a posteriori error estimator is developed in Section 4. Finally, several numerical results showing the good performance of the mixed finite element method, confirming the reliability and efficiency of the estimator, and illustrating the expected behaviour of the associated adaptive algorithm, are reported in Section 5.

We end this section with some notations to be used below. Given $n \in \{2, 3\}$, we denote $\mathbf{R}^{n\times n}$ the space of square matrices of order n with real entries, $\mathbb{I} := (\delta_{ij})$ is the identity matrix of $\mathbf{R}^{n\times n}$, and for any $\boldsymbol{\tau} := (\tau_{ij})$, $\boldsymbol{\zeta} := (\zeta_{ij}) \in \mathbf{R}^{n\times n}$, we write as usual

$$\boldsymbol{\tau}^{\mathrm{t}} := (\tau_{ji}), \qquad \mathrm{tr}(\boldsymbol{\tau}) := \sum_{i=1}^{n} \tau_{ii}, \qquad \boldsymbol{\tau}^{\mathrm{d}} := \boldsymbol{\tau} - \frac{1}{n}\,\mathrm{tr}(\boldsymbol{\tau})\,\mathbb{I}, \quad \text{and} \quad \boldsymbol{\tau} : \boldsymbol{\zeta} := \sum_{i,j=1}^{n} \tau_{ij}\zeta_{ij},$$

which corresponds, respectively, to the transpose, the trace, the deviator tensor of a tensor $\boldsymbol{\tau}$, and the tensorial product between $\boldsymbol{\tau}$ and $\boldsymbol{\zeta}$. In turn, in what follows we utilize standard simplified terminology for Sobolev spaces and norms. In particular, if $\mathcal{O} \subseteq \mathbf{R}^n$ is a domain, $\mathcal{S} \subseteq \mathbf{R}^n$ is an open or closed Lipschitz curve if $n = 2$ (resp. surface if $n = 3$), and $r \in \mathbf{R}$, we set

$$\mathbf{H}^r(\mathcal{O}) := [H^r(\mathcal{O})]^n, \qquad \mathbb{H}^r(\mathcal{O}) := [H^r(\mathcal{O})]^{n\times n}, \quad \text{and} \quad \mathbf{H}^r(\mathcal{S}) := [H^r(\mathcal{S})]^n.$$

However, when $r = 0$ we usually write $\mathbf{L}^2(\mathcal{O})$, $\mathbb{L}^2(\mathcal{O})$, and $\mathbf{L}^2(\mathcal{S})$ instead of $\mathbf{H}^0(\mathcal{O})$, $\mathbb{H}^0(\mathcal{O})$, and $\mathbf{H}^0(\mathcal{S})$, respectively. The corresponding norms are denoted by $\|\cdot\|_{r,\mathcal{O}}$ (for $H^r(\mathcal{O})$, $\mathbf{H}^r(\mathcal{O})$, and $\mathbb{H}^r(\mathcal{O})$) and $\|\cdot\|_{r,\mathcal{S}}$ (for $H^r(\mathcal{S})$ and $\mathbf{H}^r(\mathcal{S})$). In general, given any Hilbert space H, we use $\mathbf{H}$ and $\mathbb{H}$ to denote H^n and $H^{n\times n}$, respectively. In addition, $\langle\cdot,\cdot\rangle_{\mathcal{S}}$ stands for the usual duality pairing between $H^{-1/2}(\mathcal{S})$ and $H^{1/2}(\mathcal{S})$, and $\mathbf{H}^{-1/2}(\mathcal{S})$ and $\mathbf{H}^{1/2}(\mathcal{S})$. Furthermore, with div denoting the usual divergence operator, the Hilbert space

$$\mathbf{H}(\mathrm{div};\mathcal{O}) := \left\{\mathbf{w} \in \mathbf{L}^2(\mathcal{O}) : \mathrm{div}(\mathbf{w}) \in L^2(\mathcal{O})\right\},$$

is standard in the realm of mixed problems (see [29,30]). The space of matrix valued functions whose rows belong to $\mathbf{H}(\mathrm{div};\mathcal{O})$ will be denoted $\mathbb{H}(\mathbf{div};\mathcal{O})$, where **div** stands for the action of div along each row of a tensor. The Hilbert norms of $\mathbf{H}(\mathrm{div};\mathcal{O})$ and $\mathbb{H}(\mathbf{div};\mathcal{O})$ are denoted by $\|\cdot\|_{\mathrm{div};\mathcal{O}}$ and $\|\cdot\|_{\mathbf{div};\mathcal{O}}$, respectively. Note that if $\boldsymbol{\tau} \in \mathbb{H}(\mathbf{div};\mathcal{O})$, then $\mathbf{div}(\boldsymbol{\tau}) \in \mathbf{L}^2(\mathcal{O})$ and also $\boldsymbol{\tau}\mathbf{n} \in \mathbf{H}^{-1/2}(\partial\mathcal{O})$, where $\mathbf{n}$ denotes the outward unit vector normal to the boundary $\partial\mathcal{O}$. Finally, we employ $\mathbf{0}$ to denote a generic null vector (including the null functional and operator), and use C and c, with or without subscripts, bars, tildes or hats, to denote generic constants independent of the discretization parameters, which may take different values at different places.

2. The pseudostress–displacement formulation

2.1. The elasticity problem

Let Ω be a bounded and simply connected polyhedral domain in $\mathbf{R}^n$, $n \in \{2, 3\}$, and $\Gamma := \partial\Omega$ the boundary of Ω. Our goal is to determine the displacement $\mathbf{u}$ and stress tensor $\boldsymbol{\sigma}$ of a linear elastic material occupying the region Ω. In other words, given a volume force $\mathbf{f} \in \mathbf{L}^2(\Omega)$ and a Dirichlet datum $\mathbf{g} \in \mathbf{H}^{1/2}(\Gamma)$, we seek a symmetric tensor field $\boldsymbol{\sigma}$ and a vector field $\mathbf{u}$ such that

$$\begin{aligned} \boldsymbol{\sigma} &= 2\mu\,\mathbf{e}(\mathbf{u}) + \lambda\,\mathrm{tr}(\mathbf{e}(\mathbf{u}))\,\mathbb{I} \quad \text{in } \Omega, \\ \mathbf{div}(\boldsymbol{\sigma}) &= -\mathbf{f} \quad \text{in } \Omega, \quad \text{and} \quad \mathbf{u} = \mathbf{g} \quad \text{on } \Gamma, \end{aligned} \tag{2.1}$$

where $\mathbf{e}(\mathbf{u}) := \frac{1}{2}(\nabla\mathbf{u} + (\nabla\mathbf{u})^{\mathrm{t}})$ is the strain tensor of small deformations, and λ, $\mu > 0$ denote the corresponding Lamé constants. Next, from

$$\mathbf{div}(\boldsymbol{\sigma}) = 2\mu\,\mathbf{div}(\mathbf{e}(\mathbf{u})) + \lambda\,\nabla\mathrm{div}(\mathbf{u}), \quad \text{and} \quad \mathbf{div}(\mathbf{e}(\mathbf{u})) = \frac{1}{2}\,\Delta\mathbf{u} + \frac{1}{2}\,\nabla\mathrm{div}(\mathbf{u}),$$

we deduce that

$$\mathbf{div}(\boldsymbol{\sigma}) = \mu\,\Delta\mathbf{u} + (\lambda + \mu)\,\nabla\mathrm{div}(\mathbf{u}).$$

Consequently, the formulation in displacement of (2.1) reduces to: Find $\mathbf{u}$ such that

$$\begin{aligned} &\mu\,\Delta\mathbf{u} + (\lambda + \mu)\,\nabla\mathrm{div}(\mathbf{u}) = -\mathbf{f} \quad \text{in } \Omega, \\ &\mathbf{u} = \mathbf{g} \quad \text{on } \Gamma. \end{aligned}$$

Now, we define the non-symmetric pseudostress as the tensor

$$\boldsymbol{\rho} := \mu\,\nabla\mathbf{u} + (\lambda + \mu)\,\mathrm{div}(\mathbf{u})\,\mathbb{I}$$

or (since $\mathrm{div}(\mathbf{u}) = \mathrm{tr}(\nabla\mathbf{u})$), equivalently

$$\boldsymbol{\rho} := \mu\,\nabla\mathbf{u} + (\lambda + \mu)\,\mathrm{tr}(\nabla\mathbf{u})\,\mathbb{I}.$$

In this way, using that $\mathbf{div}(\boldsymbol{\rho}) = \mathbf{div}(\boldsymbol{\sigma})$, we can rewrite (2.1) as: Find the pseudostress $\boldsymbol{\rho}$ and the displacement $\mathbf{u}$ such that

$$\begin{aligned} &\boldsymbol{\rho} = \mu\,\nabla\mathbf{u} + (\lambda + \mu)\,\mathrm{tr}(\nabla\mathbf{u})\,\mathbb{I} \quad \text{in } \Omega, \\ &\mathbf{div}(\boldsymbol{\rho}) = -\mathbf{f} \quad \text{in } \Omega, \quad \text{and} \quad \mathbf{u} = \mathbf{g} \quad \text{on } \Gamma. \end{aligned} \tag{2.2}$$

Furthermore, we find from the first equation of (2.2) that

$$\mathrm{tr}(\nabla \mathbf{u}) = \frac{1}{n\,\lambda + (n+1)\,\mu}\,\mathrm{tr}(\boldsymbol{\rho}), \tag{2.3}$$

which implies that the constitutive equation of (2.2) can also be established as

$$\frac{1}{\mu}\left\{\boldsymbol{\rho} - \frac{\lambda+\mu}{n\,\lambda + (n+1)\,\mu}\,\mathrm{tr}(\boldsymbol{\rho})\,\mathbb{I}\right\} = \nabla\,\mathbf{u}.$$

Hence, the new formulation of the problem (2.1) is given by: Find $(\boldsymbol{\rho}, \mathbf{u})$ such that

$$\begin{aligned} &\frac{1}{\mu}\left\{\boldsymbol{\rho} - \frac{\lambda+\mu}{n\,\lambda + (n+1)\,\mu}\,\mathrm{tr}(\boldsymbol{\rho})\,\mathbb{I}\right\} = \nabla\,\mathbf{u} \quad \text{in } \Omega, \\ &\mathbf{div}(\boldsymbol{\rho}) = -\mathbf{f} \quad \text{in } \Omega, \quad \text{and} \quad \mathbf{u} = \mathbf{g} \quad \text{on } \Gamma. \end{aligned} \tag{2.4}$$

2.2. The dual-mixed variational formulation

Multiplying the first equation in (2.4) by $\boldsymbol{\tau} \in \mathbb{H}(\mathbf{div}; \Omega)$, integrating by parts in Ω, and using the Dirichlet boundary condition, we obtain

$$\frac{1}{\mu}\int_\Omega \boldsymbol{\rho} : \boldsymbol{\tau} - \frac{\lambda+\mu}{\mu(n\,\lambda + (n+1)\,\mu)}\int_\Omega \mathrm{tr}(\boldsymbol{\rho})\,\mathrm{tr}(\boldsymbol{\tau}) + \int_\Omega \mathbf{u}\cdot\mathbf{div}(\boldsymbol{\tau}) = \langle \boldsymbol{\tau}\mathbf{n}, \mathbf{g}\rangle_\Gamma,$$

which together with the equilibrium equation (second equation in (2.4)) tested against $\mathbf{v} \in \mathbf{L}^2(\Omega)$, yields the variational formulation of (2.4) given by: Find $(\boldsymbol{\rho}, \mathbf{u}) \in \mathbb{H} \times \mathbf{Q}$ such that

$$\begin{aligned} a(\boldsymbol{\rho}, \boldsymbol{\tau}) + b(\boldsymbol{\tau}, \mathbf{u}) &= F(\boldsymbol{\tau}) \quad \forall\, \boldsymbol{\tau} \in \mathbb{H}, \\ b(\boldsymbol{\rho}, \mathbf{v}) &= G(\mathbf{v}) \quad \forall\, \mathbf{v} \in \mathbf{Q}, \end{aligned} \tag{2.5}$$

where $\mathbb{H} := \mathbb{H}(\mathbf{div}; \Omega)$, $\mathbf{Q} := \mathbf{L}^2(\Omega)$, the bilinear forms $a : \mathbb{H} \times \mathbb{H} \to \mathbf{R}$ and $b : \mathbb{H} \times \mathbf{Q} \to \mathbf{R}$ are defined by

$$a(\boldsymbol{\xi}, \boldsymbol{\tau}) := \frac{1}{\mu}\int_\Omega \boldsymbol{\xi} : \boldsymbol{\tau} - \frac{\lambda+\mu}{\mu(n\,\lambda + (n+1)\,\mu)}\int_\Omega \mathrm{tr}(\boldsymbol{\xi})\,\mathrm{tr}(\boldsymbol{\tau}) \quad \forall\, \boldsymbol{\xi}, \boldsymbol{\tau} \in \mathbb{H}, \tag{2.6}$$

$$b(\boldsymbol{\tau}, \mathbf{v}) := \int_\Omega \mathbf{v}\cdot\mathbf{div}(\boldsymbol{\tau}) \quad \forall\, \boldsymbol{\tau} \in \mathbb{H},\ \forall\, \mathbf{v} \in \mathbf{Q}, \tag{2.7}$$

and the functionals $F \in \mathbb{H}'$ and $G \in \mathbf{Q}'$ are given by

$$F(\boldsymbol{\tau}) := \langle \boldsymbol{\tau}\mathbf{n}, \mathbf{g}\rangle_\Gamma \quad \text{and} \quad G(\mathbf{v}) := -\int_\Omega \mathbf{f}\cdot\mathbf{v}.$$

We noted from (2.6) that

$$a(\mathbb{I}, \boldsymbol{\tau}) = \frac{1}{(n\lambda + (n+1)\mu)}\int_\Omega \mathrm{tr}(\boldsymbol{\tau}) \quad \forall\, \boldsymbol{\tau} \in \mathbb{H}, \tag{2.8}$$

and from (2.7) that

$$b(\mathbb{I}, \mathbf{v}) = 0 \quad \forall\, \mathbf{v} \in \mathbf{Q}. \tag{2.9}$$

Moreover, replacing $\boldsymbol{\xi} = \boldsymbol{\xi}^{\mathrm{d}} + \frac{1}{n}\,\mathrm{tr}(\boldsymbol{\xi})\,\mathbb{I}$ in (2.6), and using that $\boldsymbol{\xi}^{\mathrm{d}} : \boldsymbol{\tau} = \boldsymbol{\xi}^{\mathrm{d}} : \boldsymbol{\tau}^{\mathrm{d}}$, and that $\mathrm{tr}(\boldsymbol{\xi}^{\mathrm{d}}) = 0$, for all $\boldsymbol{\xi} \in \mathbb{L}^2(\Omega)$, we arrive at the following equivalent expression for the bilinear form a

$$a(\boldsymbol{\xi}, \boldsymbol{\tau}) = \frac{1}{\mu}\int_\Omega \boldsymbol{\xi}^{\mathrm{d}} : \boldsymbol{\tau}^{\mathrm{d}} + \frac{1}{n(n\,\lambda + (n+1)\,\mu)}\int_\Omega \mathrm{tr}(\boldsymbol{\xi})\,\mathrm{tr}(\boldsymbol{\tau}) \quad \forall\, \boldsymbol{\xi}, \boldsymbol{\tau} \in \mathbb{H}. \tag{2.10}$$

The convenience of writing a in the form (2.10) will become clear later on when we analyse the solvability of (2.5).

We now define $\mathbb{H}_0 := \left\{\boldsymbol{\tau} \in \mathbb{H}(\mathbf{div}; \Omega) : \int_\Omega \mathrm{tr}(\boldsymbol{\tau}) = 0\right\}$ and note that $\mathbb{H} = \mathbb{H}_0 \oplus \mathbf{R}\mathbb{I}$, that is for any $\boldsymbol{\tau} \in \mathbb{H}$ there exist unique $\boldsymbol{\tau}_0 \in \mathbb{H}_0$ and $d := \frac{1}{n|\Omega|}\int_\Omega \mathrm{tr}(\boldsymbol{\tau}) \in \mathbf{R}$, where $|\Omega|$ denotes the measure of Ω, such that $\boldsymbol{\tau} = \boldsymbol{\tau}_0 + d\,\mathbb{I}$. In particular, taking $\boldsymbol{\tau} = \mathbb{I}$ in the first equation of (2.5), we deduce that

$$\int_\Omega \mathrm{tr}(\boldsymbol{\rho}) = (n\,\lambda + (n+1)\,\mu)\int_\Gamma \mathbf{g}\cdot\mathbf{n},$$

which yields $\boldsymbol{\rho} = \boldsymbol{\rho}_0 + c\,\mathbb{I}$, with $\boldsymbol{\rho}_0 \in \mathbb{H}_0$ and the constant c given explicitly by

$$c := \frac{(n\lambda + (n+1)\mu)}{n\,|\Omega|}\int_\Gamma \mathbf{g}\cdot\mathbf{n}. \tag{2.11}$$

In this way, replacing $\boldsymbol{\rho}$ by the expression $\boldsymbol{\rho}_0 + c\,\mathbb{I}$ in (2.5), with the bilinear form a given by (2.10), applying the identities (2.8) and (2.9), using that $\boldsymbol{\rho}^{\mathrm{d}} = \boldsymbol{\rho}_0^{\mathrm{d}}$ and $\mathbf{div}(\boldsymbol{\rho}) = \mathbf{div}(\boldsymbol{\rho}_0)$, and denoting from now on the remaining unknown $\boldsymbol{\rho}_0 \in \mathbb{H}_0$ simply by $\boldsymbol{\rho}$, we find that the dual-mixed variational formulation (2.5) is equivalent to the following saddle point problem: Find $(\boldsymbol{\rho}, \mathbf{u}) \in \mathbb{H}_0 \times \mathbf{Q}$ such that

$$\begin{aligned} a(\boldsymbol{\rho}, \boldsymbol{\tau}) + b(\boldsymbol{\tau}, \mathbf{u}) &= F(\boldsymbol{\tau}) \quad \forall\, \boldsymbol{\tau} \in \mathbb{H}_0, \\ b(\boldsymbol{\rho}, \mathbf{v}) &= G(\mathbf{v}) \quad \forall\, \mathbf{v} \in \mathbf{Q}. \end{aligned} \tag{2.12}$$

Lemma 2.1. *Problems (2.5) and (2.12) are equivalent in the following sense:*

(i) *If $(\boldsymbol{\rho}, \mathbf{u}) \in \mathbb{H} \times \mathbf{Q}$ is a solution of (2.5), and $\boldsymbol{\rho} = \boldsymbol{\rho}_0 + c\,\mathbb{I}$, with $\boldsymbol{\rho}_0 \in \mathbb{H}_0$ and $c \in \mathbf{R}$, then $(\boldsymbol{\rho}_0, \mathbf{u}) \in \mathbb{H}_0 \times \mathbf{Q}$ is a solution of (2.12).*

(ii) *If $(\boldsymbol{\rho}_0, \mathbf{u}) \in \mathbb{H}_0 \times \mathbf{Q}$ is a solution of (2.12), and $\boldsymbol{\rho} := \boldsymbol{\rho}_0 + c\,\mathbb{I}$, with c given by (2.11), then $(\boldsymbol{\rho}, \mathbf{u}) \in \mathbb{H} \times \mathbf{Q}$ is a solution of (2.5).*

Proof. Let $(\boldsymbol{\rho}, \mathbf{u}) \in \mathbb{H} \times \mathbf{Q}$ be a solution of (2.5), such that $\boldsymbol{\rho} = \boldsymbol{\rho}_0 + c\,\mathbb{I}$, with $\boldsymbol{\rho}_0 \in \mathbb{H}_0$ and $c \in \mathbf{R}$. Then from the first equation of (2.5) we have

$$a(\boldsymbol{\rho}_0, \boldsymbol{\tau}) + b(\boldsymbol{\tau}, \mathbf{u}) = F(\boldsymbol{\tau}) - c\, a(\mathbb{I}, \boldsymbol{\tau}) \quad \forall\, \boldsymbol{\tau} \in \mathbb{H},$$

which using (2.8), yields

$$a(\boldsymbol{\rho}_0, \boldsymbol{\tau}) + b(\boldsymbol{\tau}, \mathbf{u}) = F(\boldsymbol{\tau}) \quad \forall\, \boldsymbol{\tau} \in \mathbb{H}_0.$$

In turn, from the second equation of (2.5) we can write

$$b(\boldsymbol{\rho}_0, \mathbf{v}) + c\, b(\mathbb{I}, \mathbf{v}) = G(\mathbf{v}) \quad \forall\, \mathbf{v} \in \mathbf{Q},$$

which according to (2.9), gives

$$b(\boldsymbol{\rho}_0, \mathbf{v}) = G(\mathbf{v}) \quad \forall\, \mathbf{v} \in \mathbf{Q},$$

and hence $(\boldsymbol{\rho}_0, \mathbf{u}) \in \mathbb{H}_0 \times \mathbf{Q}$ is a solution of (2.12). Conversely, let $(\boldsymbol{\rho}_0, \mathbf{u}) \in \mathbb{H}_0 \times \mathbf{Q}$ be a solution of (2.12), and set $\boldsymbol{\rho} := \boldsymbol{\rho}_0 + c\,\mathbb{I}$, with c given by (2.11). Then, given $\boldsymbol{\tau} = \boldsymbol{\tau}_0 + d\,\mathbb{I} \in \mathbb{H}$, with $\boldsymbol{\tau}_0 \in \mathbb{H}_0$ and $d \in \mathbf{R}$, we deduce

$$\begin{aligned} a(\boldsymbol{\rho}, \boldsymbol{\tau}) + b(\boldsymbol{\tau}, \mathbf{u}) &= a(\boldsymbol{\rho}_0, \boldsymbol{\tau}_0) + b(\boldsymbol{\tau}_0, \mathbf{u}) + d\, a(\mathbb{I}, c\,\mathbb{I}) = F(\boldsymbol{\tau}_0) + d \int_\Gamma \mathbf{g} \cdot \mathbf{n} \\ &= F(\boldsymbol{\tau}_0) + d\, F(\mathbb{I}) = F(\boldsymbol{\tau}). \end{aligned}$$

On the other hand, using (2.9) we deduce

$$b(\boldsymbol{\rho}, \mathbf{v}) = b(\boldsymbol{\rho}_0, \mathbf{v}) + c\, b(\mathbb{I}, \mathbf{v}) = G(\mathbf{v}) \quad \forall\, \mathbf{v} \in \mathbf{Q},$$

which shows that $(\boldsymbol{\rho}, \mathbf{u}) \in \mathbb{H} \times \mathbf{Q}$ is a solution of (2.5). □

Furthermore, according to the new meaning of $\boldsymbol{\rho}$, we deduce from (2.4) and (2.11) that the constitutive equation in (2.4) now becomes

$$\frac{1}{\mu}\left\{\boldsymbol{\rho} - \frac{\lambda + \mu}{n\,\lambda + (n+1)\,\mu}\,\mathrm{tr}(\boldsymbol{\rho})\,\mathbb{I}\right\} + \left\{\frac{1}{n\,|\Omega|}\int_\Gamma \mathbf{g} \cdot \mathbf{n}\right\}\mathbb{I} = \nabla\,\mathbf{u} \quad \text{in } \Omega,$$

whereas the equilibrium equation remains the same, that is

$$\mathbf{div}(\boldsymbol{\rho}) = -\mathbf{f} \quad \text{in } \Omega. \tag{2.13}$$

At this point we remark that the stress $\boldsymbol{\sigma}$ can be expressed in terms of the pseudostress $\boldsymbol{\rho}$ and displacement $\mathbf{u}$ as

$$\boldsymbol{\sigma} = \boldsymbol{\rho} + \boldsymbol{\rho}^{\mathrm{t}} - (\lambda + 2\mu)\,\mathrm{tr}(\nabla \mathbf{u})\,\mathbb{I},$$

whence using the identity (2.3) we can calculate the symmetric stress tensor field in terms of the pseudostress $\boldsymbol{\rho}$ by

$$\boldsymbol{\sigma} = \boldsymbol{\rho} + \boldsymbol{\rho}^{\mathrm{t}} - \left\{\frac{\lambda + 2\mu}{n\lambda + (n+1)\mu}\right\}\mathrm{tr}(\boldsymbol{\rho})\,\mathbb{I}. \tag{2.14}$$

In addition, other physical quantities of interest such as the strain tensor of small deformations $\mathbf{e}(\mathbf{u})$ and the rotation $\boldsymbol{\gamma} := \frac{1}{2}(\nabla\,\mathbf{u} - (\nabla\,\mathbf{u})^{\mathrm{t}})$, can be computed in terms of the pseudostress $\boldsymbol{\rho}$ by

$$\mathbf{e}(\mathbf{u}) = \frac{1}{2\,\mu}\left\{\boldsymbol{\rho} + \boldsymbol{\rho}^{\mathrm{t}} - \frac{2(\lambda + \mu)}{n\lambda + (n+1)\mu}\,\mathrm{tr}(\boldsymbol{\rho})\,\mathbb{I}\right\}, \quad \text{and} \quad \boldsymbol{\gamma} = \frac{1}{2\mu}(\boldsymbol{\rho} - \boldsymbol{\rho}^{\mathrm{t}}),$$

respectively. On the other hand, in terms of the $\mathbb{H}_0$-component of pseudostress, the stress is given by

$$\boldsymbol{\sigma} = \boldsymbol{\rho} + \boldsymbol{\rho}^{\mathrm{t}} - \left(\frac{\lambda + 2\mu}{n\lambda + (n+1)\mu}\,\mathrm{tr}(\boldsymbol{\rho}) - \frac{n\lambda + 2\mu}{n|\Omega|}\int_\Gamma \mathbf{g} \cdot \mathbf{n}\right)\mathbb{I}. \tag{2.15}$$

2.3. Analysis of the dual-mixed formulation

In this section we show the well-posedness of (2.12) by using the classical Babuška–Brezzi theory (see, e.g., [29,31]). The following lemma will be required.

Lemma 2.2. *There exists $c_1 > 0$, depending only on Ω, such that*

$$c_1 \|\boldsymbol{\tau}\|_{0,\Omega}^2 \leq \|\boldsymbol{\tau}^{\mathrm{d}}\|_{0,\Omega}^2 + \|\mathbf{div}(\boldsymbol{\tau})\|_{0,\Omega}^2 \quad \forall\, \boldsymbol{\tau} \in \mathbb{H}_0. \tag{2.16}$$

Proof. It is analogous to the corresponding proof for the two-dimensional case (see [32, Lemma 3.1] or [29, Proposition 3.1 of Chapter IV]). □

We note that, the inequality (2.16), being valid only in $\mathbb{H}_0$, explains the need of replacing (2.5) by the variational formulation (2.12). Thus, the following theorem provides the well-posedness of (2.12).

Theorem 2.1. *Assume that $\mathbf{f} \in \mathbf{L}^2(\Omega)$ and $\mathbf{g} \in \mathbf{H}^{1/2}(\Gamma)$. Then, there exists a unique solution $(\boldsymbol{\rho}, \mathbf{u}) \in \mathbb{H}_0 \times \mathbf{Q}$ to (2.12). In addition, there exists $c_2 > 0$, independent of λ, such that*

$$\|\boldsymbol{\rho}\|_{\mathbf{div};\Omega} + \|\mathbf{u}\|_{0,\Omega} \leq c_2 \left\{ \|\mathbf{f}\|_{0,\Omega} + \|\mathbf{g}\|_{1/2,\Gamma} \right\}.$$

Proof. It suffices to check that the bilinear forms a and b satisfy the hypotheses of the Babuška–Brezzi theory. The proof is similar to that of [11, Theorem 2.1]. For sake of completeness we now provide the details. We first observe from (2.6) and (2.7) that a and b are bounded with $\|a\| = \frac{2}{\mu}$ and $\|b\| = 1$, respectively. In fact, applying the Cauchy–Schwarz inequality and using that $\frac{\lambda+\mu}{n\lambda+(n+1)\mu} < \frac{1}{n}$, we find from definition of bilinear form a (cf. (2.6)) that

$$\begin{aligned} |a(\boldsymbol{\xi}, \boldsymbol{\tau})| &= \left| \frac{1}{\mu} \int_\Omega \boldsymbol{\xi} : \boldsymbol{\tau} - \frac{\lambda+\mu}{\mu\,(n\,\lambda + (n+1)\,\mu)} \int_\Omega \mathrm{tr}(\boldsymbol{\xi})\,\mathrm{tr}(\boldsymbol{\tau}) \right| \\ &\leq \frac{1}{\mu} \|\boldsymbol{\xi}\|_{0,\Omega} \|\boldsymbol{\tau}\|_{0,\Omega} + \frac{1}{n\mu} \|\mathrm{tr}(\boldsymbol{\xi})\|_{0,\Omega} \|\mathrm{tr}(\boldsymbol{\tau})\|_{0,\Omega} \\ &\leq \frac{2}{\mu} \|\boldsymbol{\xi}\|_{0,\Omega} \|\boldsymbol{\tau}\|_{0,\Omega} \leq \frac{2}{\mu} \|\boldsymbol{\xi}\|_{\mathbf{div};\Omega} \|\boldsymbol{\tau}\|_{\mathbf{div};\Omega} \quad \forall\, \boldsymbol{\xi}, \boldsymbol{\tau} \in \mathbb{H}_0. \end{aligned}$$

Analogously, applying the Cauchy–Schwarz inequality, we obtain from definition of bilinear form b (cf. (2.7)) that

$$|b(\boldsymbol{\tau}, \mathbf{v})| = \left| \int_\Omega \mathbf{v} \cdot \mathbf{div}(\boldsymbol{\tau}) \right| \leq \|\mathbf{div}(\boldsymbol{\tau})\|_{0,\Omega}\, \|\mathbf{v}\|_{0,\Omega} \leq \|\boldsymbol{\tau}\|_{\mathbf{div};\Omega}\, \|\mathbf{v}\|_{0,\Omega} \quad \forall\, \boldsymbol{\tau} \in \mathbb{H}_0,\ \forall\, \mathbf{v} \in \mathbf{Q}.$$

On the other hand, we deduce that $\mathbb{V} := \{\boldsymbol{\tau} \in \mathbb{H}_0 : \mathbf{div}(\boldsymbol{\tau}) = \mathbf{0}\}$ is the null space of b, whence (2.10) and Lemma 2.2 imply

$$a(\boldsymbol{\tau}, \boldsymbol{\tau}) \geq \frac{1}{\mu} \|\boldsymbol{\tau}^{\mathrm{d}}\|_{0,\Omega}^2 \geq \frac{c_1}{\mu} \|\boldsymbol{\tau}\|_{0,\Omega}^2 = \frac{c_1}{\mu} \|\boldsymbol{\tau}\|_{\mathbf{div};\Omega}^2 \quad \forall\, \boldsymbol{\tau} \in \mathbb{V}. \tag{2.17}$$

This shows that a is $\mathbb{V}$-elliptic, with constant $\alpha := \frac{c_1}{\mu}$ independent of the Lamé constant λ. Finally, given $\mathbf{v} \in \mathbf{Q}$, $\mathbf{v} \neq \mathbf{0}$, we let $\mathbf{z} \in \mathbf{H}_0^1(\Omega)$ be the unique weak solution of the auxiliary problem

$$\Delta\, \mathbf{z} = \mathbf{v} \quad \text{in } \Omega, \quad \mathbf{z} = \mathbf{0} \quad \text{on } \Gamma.$$

Then, we let $\widehat{\boldsymbol{\tau}}$ be the $\mathbb{H}_0$-component of $\nabla \mathbf{z}$, which implies $\mathbf{div}(\widehat{\boldsymbol{\tau}}) = \mathbf{div}(\nabla \mathbf{z}) = \mathbf{v}$ in Ω. This shows that the bounded linear operator $\mathbf{div} : \mathbb{H}_0 \to \mathbf{Q}$ is surjective, which completes the proof. □

3. The mixed finite element method

In this section, we define explicit finite element subspaces $\mathbb{H}_{0,h}$ of $\mathbb{H}_0(\mathbf{div}; \Omega)$, and $\mathbf{Q}_h$ of $\mathbf{L}^2(\Omega)$ such that the corresponding mixed finite element scheme associated with the continuous formulation (2.12) is well-posed and stable.

3.1. Preliminaries

Let $\{\mathcal{T}_h\}_{h>0}$ be a regular family of triangulations of the region $\bar{\Omega} \subset \mathbf{R}^n$ by tetrahedrons T of diameter h_T such that $\bar{\Omega} = \cup\{T : T \in \mathcal{T}_h\}$, and define $h := \max\{h_T : T \in \mathcal{T}_h\}$. The faces of the tetrahedrons of $\mathcal{T}_h$ are denoted by e and their corresponding diameters by h_e. Certainly, we are assuming here that $n = 3$. In the case $n = 2$ we just need to replace

tetrahedrons by triangles and faces by edges in what follows. Now, given an integer $\ell \geq 0$ and a subset U of $\mathbf{R}^n$, we denote by $\mathrm{P}_\ell(U)$ the space of polynomials defined in U of total degree at most ℓ. According to the notational convention given in the introduction, we denote $\mathbf{P}_\ell(U) := [\mathrm{P}_\ell(U)]^n$ and $\mathbb{P}_\ell(U) := [\mathrm{P}_\ell(U)]^{n\times n}$. Then, for each integer $k \geq 0$ and for each $T \in \mathcal{T}_h$, we define the local Raviart–Thomas space of order k (see, e.g. [29])

$$\mathbf{RT}_k(T) := \mathbf{P}_k(T) \oplus \mathrm{P}_k(T)\,\mathbf{x}$$

where $\mathbf{x} = \begin{pmatrix} x_1 \\ \vdots \\ x_n \end{pmatrix}$ is a generic vector of $\mathbf{R}^n$, and let $\mathbb{RT}_k(\mathcal{T}_h)$ be the corresponding global space, that is,

$$\mathbb{RT}_k(\mathcal{T}_h) := \left\{ \boldsymbol{\tau} \in \mathbb{H}(\mathbf{div};\Omega) : (\tau_{i1},\ldots,\tau_{in})^{\mathrm{t}}|_T \in \mathbf{RT}_k(T)\ \forall\, i \in \{1,\ldots,n\},\ \forall\, T \in \mathcal{T}_h \right\}.$$

We also let $\mathrm{P}_k(\mathcal{T}_h)$ be the global space of piecewise polynomials of degree $\leq k$, that is

$$\mathrm{P}_k(\mathcal{T}_h) := \left\{ v \in L^2(\Omega) : v|_T \in \mathrm{P}_k(T)\ \forall\, T \in \mathcal{T}_h \right\}. \tag{3.1}$$

We now introduce the following finite element subspaces of $\mathbb{H}_0$, and $\mathbf{Q}$, respectively,

$$\begin{aligned} \mathbb{H}_{0,h} &:= \mathbb{RT}_k(\mathcal{T}_h) \cap \mathbb{H}_0(\mathbf{div};\Omega) = \left\{ \boldsymbol{\tau}_h \in \mathbb{RT}_k(\mathcal{T}_h) : \int_\Omega \mathrm{tr}(\boldsymbol{\tau}_h) = 0 \right\}, \\ \mathbf{Q}_h &:= \mathbf{P}_k(\mathcal{T}_h). \end{aligned} \tag{3.2}$$

Then, the mixed finite element scheme associated with (2.12) reads: Find $(\boldsymbol{\rho}_h, \mathbf{u}_h) \in \mathbb{H}_{0,h} \times \mathbf{Q}_h$, such that

$$\begin{aligned} a(\boldsymbol{\rho}_h, \boldsymbol{\tau}_h) + b(\boldsymbol{\tau}_h, \mathbf{u}_h) &= \langle \boldsymbol{\tau}_h \mathbf{n}, \mathbf{g} \rangle_\Gamma \quad \forall\, \boldsymbol{\tau}_h \in \mathbb{H}_{0,h}, \\ b(\boldsymbol{\rho}_h, \mathbf{v}_h) &= -\int_\Omega \mathbf{f}\cdot\mathbf{v}_h \quad \forall\, \mathbf{v}_h \in \mathbf{Q}_h. \end{aligned} \tag{3.3}$$

We remark at this point that when $k = 0$ and $n = 3$ the number of unknowns N involved in (3.3) behaves approximately as 9 times the number of tetrahedra of the triangulation. In fact, having in mind that: each row of $\boldsymbol{\tau}_h \in \mathbb{RT}_0(\mathcal{T}_h)$ is locally defined by 4 degrees of freedom, most of the sides of the triangulation belong to 2 tetrahedra each, and each $\mathbf{v}_h \in \mathbf{P}_0(\mathcal{T}_h)$ is locally determined by 3 degrees of freedom, we find that N is asymptotically given by

$$\left(\frac{4\times 3}{2} + 3 \right) \times \text{number of tetrahedra} = 9 \times \text{number of tetrahedra}. \tag{3.4}$$

In turn, it is easy to show (see, e.g. formulae given in [31, Section 3.3]) that the factor 9 changes to 39 and 102 when $k = 1$ and $k = 2$, respectively. On the other hand, it is important to notice that the identity (2.15) certainly suggests to approximate the symmetric stress tensor field $\boldsymbol{\sigma}$ by the postprocessing formula

$$\boldsymbol{\sigma}_h = \boldsymbol{\rho}_h + \boldsymbol{\rho}_h^{\mathrm{t}} - \left(\frac{\lambda + 2\mu}{n\lambda + (n+1)\mu} \mathrm{tr}(\boldsymbol{\rho}_h) - \frac{n\lambda + 2\mu}{n|\Omega|} \int_\Gamma \mathbf{g}\cdot\mathbf{n} \right) \mathbb{I}. \tag{3.5}$$

Moreover, in Section 3.3 we propose a second-step postprocessed approximation of $\boldsymbol{\sigma}_h$ and provide the corresponding error estimate.

3.2. Solvability analysis

In order to provide the unique solvability of the Galerkin scheme (3.3), we need to introduce the Raviart–Thomas interpolation operator (see [29]), $\mathscr{E}_h^k : \mathbb{H}^1(\Omega) \to \mathbb{RT}_k(\mathcal{T}_h)$, which, given $\boldsymbol{\tau} \in \mathbb{H}^1(\Omega)$, and denoting by $\mathbf{n}$ the outward unit normal on each face/edge of the triangulation, is characterized by the following identities:

$$\int_e \mathscr{E}_h^k(\boldsymbol{\tau})\mathbf{n}\cdot\mathbf{p} = \int_e \boldsymbol{\tau}\mathbf{n}\cdot\mathbf{p} \quad \forall\, \text{face/edge } e \in \mathcal{T}_h, \forall\, \mathbf{p} \in \mathbf{P}_k(e),\ \text{when } k \geq 0, \tag{3.6}$$

and

$$\int_T \mathscr{E}_h^k(\boldsymbol{\tau}) : \boldsymbol{\xi} = \int_T \boldsymbol{\tau} : \boldsymbol{\xi} \quad \forall\, T \in \mathcal{T}_h,\ \forall\, \boldsymbol{\xi} \in \mathbb{P}_{k-1}(T),\ \text{when } k \geq 1. \tag{3.7}$$

Then, using (3.6) and (3.7), it is easy to show that

$$\mathbf{div}(\mathscr{E}_h^k(\boldsymbol{\tau})) = \mathscr{P}_h^k(\,\mathbf{div}(\boldsymbol{\tau})\,), \tag{3.8}$$

where $\mathscr{P}_h^k : \mathbf{L}^2(\Omega) \to \mathbf{Q}_h$ is the $\mathbf{L}^2(\Omega)$–orthogonal projector. The interpolation operator $\mathscr{E}_h^k$ can also be defined as a bounded linear operator from the larger space $\mathbb{H}^s(\Omega) \cap \mathbb{H}(\mathbf{div};\Omega)$ into $\mathbb{RT}_k(\mathcal{T}_h)$ for all $s \in (0, 1]$ (see, e.g. Theorem 3.16 in [33]), and

in this case there holds the following interpolation error estimate

$$\|\boldsymbol{\tau} - \mathscr{E}_h^k(\boldsymbol{\tau})\|_{0,T} \leq C\, h_T^s \left\{ \|\boldsymbol{\tau}\|_{s,T} + \|\mathbf{div}(\boldsymbol{\tau})\|_{0,T} \right\} \quad \forall\, T \in \mathcal{T}_h. \tag{3.9}$$

Furthermore, we need the following approximation properties of the operators $\mathscr{P}_h^k$ and $\mathscr{E}_h^k$. It is well known (see, e.g. [34]) that for each $\mathbf{v} \in \mathbf{H}^m(\Omega)$, with $0 \leq m \leq k+1$, there holds

$$\|\mathbf{v} - \mathscr{P}_h^k(\mathbf{v})\|_{0,T} \leq C\, h_T^m\, |\mathbf{v}|_{m,T} \quad \forall\, T \in \mathcal{T}_h. \tag{3.10}$$

In addition, the operator $\mathscr{E}_h^k$ satisfies the following approximation properties (see, e.g. [29]): For each $\boldsymbol{\tau} \in \mathbb{H}^m(\Omega)$, with $1 \leq m \leq k+1$,

$$\|\boldsymbol{\tau} - \mathscr{E}_h^k(\boldsymbol{\tau})\|_{0,T} \leq C\, h_T^m\, |\boldsymbol{\tau}|_{m,T} \quad \forall\, T \in \mathcal{T}_h. \tag{3.11}$$

For each $\boldsymbol{\tau} \in \mathbb{H}^1(\Omega)$ such that $\mathbf{div}(\boldsymbol{\tau}) \in \mathbf{H}^m(\Omega)$, with $0 \leq m \leq k+1$,

$$\|\mathbf{div}(\boldsymbol{\tau} - \mathscr{E}_h^k(\boldsymbol{\tau}))\|_{0,T} \leq C\, h_T^m\, |\mathbf{div}(\boldsymbol{\tau})|_{m,T} \quad \forall\, T \in \mathcal{T}_h. \tag{3.12}$$

For each $\boldsymbol{\tau} \in \mathbb{H}^1(\Omega)$, where T_e is any tetrahedron/triangle of $\mathcal{T}_h$ having e as a face/edge,

$$\|\boldsymbol{\tau}\mathbf{n} - \mathscr{E}_h^k(\boldsymbol{\tau})\mathbf{n}\|_{0,e} \leq C\, h_e^{1/2}\, \|\boldsymbol{\tau}\|_{1,T_e} \quad \forall\, \text{face/edge}\ e \in \mathcal{T}_h. \tag{3.13}$$

In particular, note that (3.12) follows easily from the properties (3.8) and (3.10).

Then, as a consequence of (3.9), (3.10), (3.11), (3.12), (3.13), and the usual interpolation estimates, we find that $\mathbb{H}_{0,h}$ and $\mathbf{Q}_h$ satisfy the following approximation properties:

($\mathrm{AP}_h^{\boldsymbol{\rho}}$) For each $s \in (0, k+1]$ and for each $\boldsymbol{\tau} \in \mathbb{H}^s(\Omega) \cap \mathbb{H}_0(\mathbf{div};\Omega)$ with $\mathbf{div}(\boldsymbol{\tau}) \in \mathbf{H}^s(\Omega)$ there exists $\boldsymbol{\tau}_h \in \mathbb{H}_{0,h}$ such that

$$\|\boldsymbol{\tau} - \boldsymbol{\tau}_h\|_{\mathbf{div};\Omega} \leq C\, h^s \left\{ \|\boldsymbol{\tau}\|_{s,\Omega} + \|\mathbf{div}(\boldsymbol{\tau})\|_{s,\Omega} \right\}.$$

($\mathrm{AP}_h^{\mathbf{u}}$) For each $s \in [0, k+1]$ and for each $\mathbf{v} \in \mathbf{H}^s(\Omega)$, there exists $\mathbf{v}_h \in \mathbf{Q}_h$ such that

$$\|\mathbf{v} - \mathbf{v}_h\|_{0,\Omega} \leq C\, h^s\, \|\mathbf{v}\|_{s,\Omega}.$$

Next, we establish the unique solvability, stability, and convergence of the Galerkin scheme (3.3) with the finite element subspaces given by (3.2). We begin with the proof of the discrete inf–sup condition for the bilinear form b.

Lemma 3.1. *Let $\mathbb{H}_{0,h}$ and $\mathbf{Q}_h$ be given by (3.2). Then, there exists $\beta > 0$, independent of h and λ, such that*

$$\sup_{\substack{\boldsymbol{\tau}_h \in \mathbb{H}_{0,h} \\ \boldsymbol{\tau}_h \neq \mathbf{0}}} \frac{b(\boldsymbol{\tau}_h, \mathbf{v}_h)}{\|\boldsymbol{\tau}_h\|_{\mathbf{div};\Omega}} \geq \beta\, \|\mathbf{v}_h\|_{0,\Omega} \quad \forall\ \mathbf{v}_h \in \mathbf{Q}_h.$$

Proof. See [11, Lemma 3.2]. □

The following theorem establishes the well-posedness of (3.3) and the associated Céa estimate.

Theorem 3.1. *The Galerkin scheme (3.3) has a unique solution $(\boldsymbol{\rho}_h, \mathbf{u}_h) \in \mathbb{H}_{0,h} \times \mathbf{Q}_h$, which satisfies the corresponding stability and Céa estimates, i.e. there exist positive constants C, $\widetilde{C}$, independent of h and λ, such that*

$$\|(\boldsymbol{\rho}_h,\ \mathbf{u}_h)\|_{\mathbb{H}_0 \times \mathbf{Q}} \leq C \left\{ \|\mathbf{f}\|_{0,\Omega} + \|\mathbf{g}\|_{1/2,\Gamma} \right\},$$

and

$$\|(\boldsymbol{\rho},\ \mathbf{u}) - (\boldsymbol{\rho}_h,\ \mathbf{u}_h)\|_{\mathbb{H}_0 \times \mathbf{Q}} \leq \widetilde{C} \inf_{(\boldsymbol{\tau}_h, \mathbf{v}_h) \in \mathbb{H}_{0,h} \times \mathbf{Q}_h} \|(\boldsymbol{\rho},\ \mathbf{u}) - (\boldsymbol{\tau}_h,\ \mathbf{v}_h)\|_{\mathbb{H}_0 \times \mathbf{Q}}. \tag{3.14}$$

Proof. Since $\mathbf{div}(\mathbb{H}_{0,h}) \subseteq \mathbf{Q}_h$, we find that the discrete kernel of b is given by

$$\mathbb{V}_h := \left\{ \boldsymbol{\tau}_h \in \mathbb{H}_{0,h} : b(\boldsymbol{\tau}_h, \mathbf{v}_h) = 0 \quad \forall\, \mathbf{v}_h \in \mathbf{Q}_h \right\} = \left\{ \boldsymbol{\tau}_h \in \mathbb{H}_{0,h} : \mathbf{div}(\boldsymbol{\tau}_h) = \mathbf{0} \text{ in } \Omega \right\} \subseteq \mathbb{V},$$

which, thanks to (2.17), shows that a is strongly coercive in $\mathbb{V}_h$. This fact, Lemma 3.1, and a direct application of the discrete Babuška–Brezzi theory (see, e.g. [30, Theorem 1.1, Chapter II] or [29, Theorem II.1.1]) complete the proof. □

The following theorem provides the theoretical rate of convergence of the Galerkin scheme (3.3), under suitable regularity assumptions on the exact solution.

Theorem 3.2. *Let $(\boldsymbol{\rho}, \mathbf{u}) \in \mathbb{H}_0 \times \mathbf{Q}$ and $(\boldsymbol{\rho}_h, \mathbf{u}_h) \in \mathbb{H}_{0,h} \times \mathbf{Q}_h$ be the unique solutions of the continuous and discrete formulations (2.12) and (3.3), respectively. Assume that $\boldsymbol{\rho} \in \mathbb{H}^s(\Omega)$, $\mathbf{div}(\boldsymbol{\rho}) \in \mathbf{H}^s(\Omega)$ and $\mathbf{u} \in \mathbf{H}^s(\Omega)$, for some $s \in (0, k+1]$. Then, there exists $C > 0$, independent of h, such that*

$$\|(\boldsymbol{\rho}, \mathbf{u}) - (\boldsymbol{\rho}_h, \mathbf{u}_h)\|_{\mathbb{H}_0 \times \mathbf{Q}} \leq C\, h^s \left\{ \|\boldsymbol{\rho}\|_{s,\Omega} + \|\mathbf{div}(\boldsymbol{\rho})\|_{s,\Omega} + \|\mathbf{u}\|_{s,\Omega} \right\}.$$

Proof. It is a straightforward consequence of the Céa estimate (3.14) and the approximation properties $(\mathrm{AP}_h^{\boldsymbol{\rho}})$ and $(\mathrm{AP}_h^{\mathbf{u}})$. □

3.3. A fully postprocessed stress

We end this section by proposing a second-step postprocessed stress and deriving the corresponding a priori error estimate. To do that, we first observe from (2.15) and (3.5) that there holds

$$\|\boldsymbol{\sigma}-\boldsymbol{\sigma}_h\|_{0,\Omega} \leq (2+n)\,\|\boldsymbol{\rho}-\boldsymbol{\rho}_h\|_{0,\Omega}, \tag{3.15}$$

which shows that the rate of convergence of $\|\boldsymbol{\sigma}-\boldsymbol{\sigma}_h\|_{0,\Omega}$ is the same of $\|\boldsymbol{\rho}-\boldsymbol{\rho}_h\|_{0,\Omega}$. Unfortunately, numerical experiments (cf. Section 5) confirm that the rate of convergence of $\sum_{T\in\mathcal{T}_h}\|\boldsymbol{\sigma}-\boldsymbol{\sigma}_h\|^2_{\mathbf{div};T}$ is of lower order than $\sum_{T\in\mathcal{T}_h}\|\boldsymbol{\rho}-\boldsymbol{\rho}_h\|^2_{\mathbf{div};T}$. This fact has motivated the construction of a second approximation for the stress variable $\boldsymbol{\sigma}$, which has a better rate of convergence in the broken $\mathbb{H}(\mathbf{div})$-norm. Indeed, we first note that $\boldsymbol{\sigma}_h$ gives us a good approximation for $\boldsymbol{\sigma}$ in the $\mathbb{L}^2$-norm (cf. (3.15)). Hence, the problem lies on the approximation that $\mathbf{div}(\boldsymbol{\sigma}_h)$ implies for $\mathbf{div}(\boldsymbol{\sigma})$. Furthermore, we know from (2.1) that $\mathbf{div}(\boldsymbol{\sigma}) = -\mathbf{f}$, and then we try to approximate $\mathbf{div}(\boldsymbol{\sigma}_h)$ by $-\mathbf{f}$ in each $T\in\mathcal{T}_h$. The above discussion suggests to define the following postprocessed approximation for $\boldsymbol{\sigma}$: Given $T\in\mathcal{T}_h$, we find $\boldsymbol{\sigma}_h^\star|_T := \boldsymbol{\sigma}_{h,T}^\star \in \mathbb{RT}_k(T)$ such that

$$\langle\boldsymbol{\sigma}_{h,T}^\star,\,\boldsymbol{\tau}_h\rangle_{\mathbf{div};T} := \int_T \boldsymbol{\sigma}_{h,T}^\star : \boldsymbol{\tau}_h + \int_T \mathbf{div}(\boldsymbol{\sigma}_{h,T}^\star)\cdot\mathbf{div}(\boldsymbol{\tau}_h) = \int_T \boldsymbol{\sigma}_h : \boldsymbol{\tau}_h - \int_T \mathbf{f}\cdot\mathbf{div}(\boldsymbol{\tau}_h), \tag{3.16}$$

for all $\boldsymbol{\tau}_h \in \mathbb{RT}_k(T) := \left\{\boldsymbol{\tau}\in\mathbb{L}^2(T) : (\tau_{i1},\ldots,\tau_{in})^{\mathrm{t}}|_T \in \mathbf{RT}_k(T)\ \forall\, i\in\{1,\ldots,n\}\right\}$. It is important to note that $\boldsymbol{\sigma}_{h,T}^\star$ can be explicitly (and efficiently) calculated for each $T\in\mathcal{T}_h$ independently. Moreover, the following result establishes an estimate for the local error $\|\boldsymbol{\sigma}-\boldsymbol{\sigma}_{h,T}^\star\|_{\mathbf{div};T}$.

Lemma 3.2. *Assume that $\boldsymbol{\sigma}|_T \in \mathbb{H}^1(T)$ for each $T\in\mathcal{T}_h$. Then there holds*

$$\|\boldsymbol{\sigma}-\boldsymbol{\sigma}_{h,T}^\star\|_{\mathbf{div};T} \leq \|\boldsymbol{\sigma}-\boldsymbol{\sigma}_h\|_{0,T} + 2\,\|\boldsymbol{\sigma}-\mathscr{E}_{h,T}^k(\boldsymbol{\sigma})\|_{\mathbf{div};T}, \tag{3.17}$$

where $\mathscr{E}_{h,T}^k$ is the local Raviart–Thomas interpolation operator on T.

Proof. We first notice, using that $\mathbf{div}(\boldsymbol{\sigma}) = -\mathbf{f}$ in Ω, that there holds

$$\langle\boldsymbol{\sigma},\,\boldsymbol{\tau}_h\rangle_{\mathbf{div};T} = \int_T \boldsymbol{\sigma} : \boldsymbol{\tau}_h - \int_T \mathbf{f}\cdot\mathbf{div}(\boldsymbol{\tau}_h) \quad \forall\,\boldsymbol{\tau}_h\in\mathbb{RT}_k(T),$$

which, using (3.16), implies the error equation:

$$\langle\boldsymbol{\sigma}-\boldsymbol{\sigma}_{h,T}^\star,\,\boldsymbol{\tau}_h\rangle_{\mathbf{div};T} = \int_T (\boldsymbol{\sigma}-\boldsymbol{\sigma}_h) : \boldsymbol{\tau}_h \quad \forall\,\boldsymbol{\tau}_h\in\mathbb{RT}_k(T),$$

and then, adding $\mathscr{E}_{h,T}^k(\boldsymbol{\sigma})$ to both sides and rearranging, we find that

$$\langle\mathscr{E}_{h,T}^k(\boldsymbol{\sigma})-\boldsymbol{\sigma}_{h,T}^\star,\,\boldsymbol{\tau}_h\rangle_{\mathbf{div};T} = \int_T (\boldsymbol{\sigma}-\boldsymbol{\sigma}_h) : \boldsymbol{\tau}_h + \langle\mathscr{E}_{h,T}^k(\boldsymbol{\sigma})-\boldsymbol{\sigma},\,\boldsymbol{\tau}_h\rangle_{\mathbf{div};T} \quad \forall\,\boldsymbol{\tau}_h\in\mathbb{RT}_k(T).$$

Next, taking $\boldsymbol{\tau}_h := \mathscr{E}_{h,T}^k(\boldsymbol{\sigma})-\boldsymbol{\sigma}_{h,T}^\star \in \mathbb{RT}_k(T)$ in the above identity, and applying the Cauchy–Schwarz inequality, we deduce that

$$\|\mathscr{E}_{h,T}^k(\boldsymbol{\sigma})-\boldsymbol{\sigma}_{h,T}^\star\|_{\mathbf{div};T} \leq \|\boldsymbol{\sigma}-\boldsymbol{\sigma}_h\|_{0,T} + \|\boldsymbol{\sigma}-\mathscr{E}_{h,T}^k(\boldsymbol{\sigma})\|_{\mathbf{div};T}. \tag{3.18}$$

Finally, from the triangle inequality we note that

$$\|\boldsymbol{\sigma}-\boldsymbol{\sigma}_{h,T}^\star\|_{\mathbf{div};T} \leq \|\boldsymbol{\sigma}-\mathscr{E}_{h,T}^k(\boldsymbol{\sigma})\|_{\mathbf{div};T} + \|\mathscr{E}_{h,T}^k(\boldsymbol{\sigma})-\boldsymbol{\sigma}_{h,T}^\star\|_{\mathbf{div};T},$$

which, together with (3.18), yields (3.17) and completes the proof. □

A straightforward consequence of the previous lemma is given by the following global rate of convergence for $\boldsymbol{\sigma}_h^\star$.

Theorem 3.3. *Let $(\boldsymbol{\rho},\mathbf{u}) \in \mathbb{H}_0\times\mathbf{Q}$ and $(\boldsymbol{\rho}_h,\mathbf{u}_h)\in\mathbb{H}_{0,h}\times\mathbf{Q}_h$ be the unique solutions of the continuous and discrete formulations (2.12) and (3.3), respectively. In addition, let $\boldsymbol{\sigma}$ be the stress tensor given by (2.15), and let $\boldsymbol{\sigma}_h$ and $\boldsymbol{\sigma}_h^\star$ be its discrete approximations introduced in (3.5) and (3.16), respectively. Assume that $\boldsymbol{\rho}\in\mathbb{H}^s(\Omega)$, $\mathbf{div}(\boldsymbol{\rho})\in\mathbf{H}^s(\Omega)$, and $\mathbf{u}\in\mathbf{H}^s(\Omega)$, for some $s\in(0,k+1]$. Then, there exists $C>0$, independent of h, such that*

$$\left\{\sum_{T\in\mathcal{T}_h}\|\boldsymbol{\sigma}-\boldsymbol{\sigma}_h^\star\|^2_{\mathbf{div};T}\right\}^{1/2} \leq C\,h^s\left\{\|\boldsymbol{\rho}\|_{s,\Omega}+\|\mathbf{div}(\boldsymbol{\rho})\|_{s,\Omega}+\|\mathbf{u}\|_{s,\Omega}\right\}.$$

Proof. We first observe from (2.15) that the regularity of $\boldsymbol{\sigma}$ depends on the regularity of $\boldsymbol{\rho}$. Indeed, given $\boldsymbol{\rho} \in \mathbb{H}^s(\Omega)$, this establish that $\boldsymbol{\rho}^{\mathrm{t}} \in \mathbb{H}^s(\Omega)$ and $\mathrm{tr}(\boldsymbol{\rho}) \in H^s(\Omega)$, which imply that $\boldsymbol{\sigma} \in \mathbb{H}^s(\Omega)$. In addition, from the fact that $\mathbf{div}(\boldsymbol{\sigma}) = \mathbf{div}(\boldsymbol{\rho})$, we deduce that $\mathbf{div}(\boldsymbol{\sigma}) \in \mathbf{H}^s(\Omega)$. Then, the proof follows straightforwardly from the estimate (3.17), after summing up over $T \in \mathcal{T}_h$, using (3.11), (3.12) and (3.15) together with Theorem 3.2. □

We end this section by emphasizing, as it has become clear from the foregoing analysis, that the present pseudostress-based formulation for linear elasticity is very suitable to handle corresponding Dirichlet boundary conditions. In other words, as long as no tractions are imposed on Γ or part of it, there is no need of introducing the symmetric stress tensor $\boldsymbol{\sigma}$ as the main unknown of the associated mixed formulation. In spite of it, and if approximations of $\boldsymbol{\sigma}$ are anyway required, we also showed that this can be easily obtained through a simple postprocessing procedure yielding optimal rates of convergence in the broken $\mathbb{H}(\mathbf{div}; \Omega)$-norm. Nevertheless, it is still not clear whether the pseudostress-based approach can also be applied/adapted to Neumann or mixed boundary conditions, so that additional work in this direction needs certainly to be done. Perhaps, as a first attempt, one could try to explore a further use of formula (2.14) expressing $\boldsymbol{\sigma}$ in terms of the pseudostress $\boldsymbol{\rho}$. More precisely, assuming for instance that one has the Neumann boundary condition: $\boldsymbol{\sigma}\,\mathbf{n} = \mathbf{g}_{\mathbf{N}} \in \mathbf{H}^{-1/2}(\Gamma)$ on Γ, we find from (2.14) that

$$\boldsymbol{\rho}\,\mathbf{n} = \mathbf{g}_{\mathbf{N}} - \left(\boldsymbol{\rho}^{\mathrm{t}} - \left\{ \frac{\lambda + 2\mu}{n\lambda + (n+1)\mu} \right\} \mathrm{tr}(\boldsymbol{\rho})\, \mathbb{I} \right) \mathbf{n} \quad \text{on } \Gamma,$$

and hence, the resulting Neumann boundary value problem arising now from (2.4) becomes: Find $(\boldsymbol{\rho}, \mathbf{u})$ such that

$$\begin{aligned} &\frac{1}{\mu} \left\{ \boldsymbol{\rho} - \frac{\lambda + \mu}{n\,\lambda + (n+1)\,\mu} \mathrm{tr}(\boldsymbol{\rho})\, \mathbb{I} \right\} = \nabla\, \mathbf{u} \quad \text{in } \Omega, \quad \mathbf{div}(\boldsymbol{\rho}) = -\mathbf{f} \quad \text{in } \Omega, \\ &\boldsymbol{\rho}\,\mathbf{n} = \mathbf{g}_{\mathbf{N}} - \left(\boldsymbol{\rho}^{\mathrm{t}} - \left\{ \frac{\lambda + 2\mu}{n\lambda + (n+1)\mu} \right\} \mathrm{tr}(\boldsymbol{\rho})\, \mathbb{I} \right) \mathbf{n} \quad \text{on } \Gamma. \end{aligned} \tag{3.19}$$

In this way, a fixed-point strategy based on the unknown $\boldsymbol{\rho}$ could be suggested to analyse the well-posedness of (3.19) and its Galerkin approximation. We plan to address this and other eventual approaches arising from (2.14) and (3.19), at least numerically, in a future work.

4. A residual-based a posteriori error estimator

In this section we develop a residual-based a posteriori error analysis for the mixed finite element scheme (3.3) with the subspaces $\mathbb{H}_{0,h}$ and $\mathbf{Q}_h$ defined by (3.2) for $n = 3$. To this end, we require additional notations. We first recall that the curl of a 3D vector $\mathbf{v} := (v_1, v_2, v_3)$ is the 3D vector

$$\mathrm{curl}(\mathbf{v}) = \nabla \times \mathbf{v} := \left(\frac{\partial v_3}{\partial x_2} - \frac{\partial v_2}{\partial x_3}, \frac{\partial v_1}{\partial x_3} - \frac{\partial v_3}{\partial x_1}, \frac{\partial v_2}{\partial x_1} - \frac{\partial v_1}{\partial x_2} \right).$$

Then, given a tensor function $\boldsymbol{\tau} := (\tau_{ij})_{3\times 3}$, the operator $\underline{\mathbf{curl}}$ denotes curl acting along each row of $\boldsymbol{\tau}$, that is, $\underline{\mathbf{curl}}(\boldsymbol{\tau})$ is the 3×3 tensor whose rows are given by

$$\underline{\mathbf{curl}}(\boldsymbol{\tau}) := \begin{pmatrix} \mathrm{curl}(\tau_{11}, \tau_{12}, \tau_{13}) \\ \mathrm{curl}(\tau_{21}, \tau_{22}, \tau_{23}) \\ \mathrm{curl}(\tau_{31}, \tau_{32}, \tau_{33}) \end{pmatrix}.$$

Also, we denote by $\boldsymbol{\tau} \times \mathbf{n}$, the 3×3 tensor whose rows are given by the tangential components of each row of $\boldsymbol{\tau}$, that is,

$$\boldsymbol{\tau} \times \mathbf{n} := \begin{pmatrix} (\tau_{11}, \tau_{12}, \tau_{13}) \times \mathbf{n} \\ (\tau_{21}, \tau_{22}, \tau_{23}) \times \mathbf{n} \\ (\tau_{31}, \tau_{32}, \tau_{33}) \times \mathbf{n} \end{pmatrix}.$$

In addition, we define the Sobolev space

$$\mathbb{H}(\underline{\mathbf{curl}}; \Omega) := \left\{ \mathbf{w} \in \mathbb{L}^2(\Omega) : \underline{\mathbf{curl}}(\mathbf{w}) \in \mathbb{L}^2(\Omega) \right\}.$$

On the other hand, given $T \in \mathcal{T}_h$, we let $\mathcal{E}(T)$ be the set of its faces, and let $\mathcal{E}_h$ be the set of all faces of the triangulation $\mathcal{T}_h$. Then, we write $\mathcal{E}_h = \mathcal{E}_h(\Omega) \cup \mathcal{E}_h(\Gamma)$, where $\mathcal{E}_h(\Omega) := \{e \in \mathcal{E}_h : e \subseteq \Omega\}$ and $\mathcal{E}_h(\Gamma) := \{e \in \mathcal{E}_h : e \subseteq \Gamma\}$. Also, for each face $e \in \mathcal{E}_h$ we fix a unit normal $\mathbf{n}_e$ to e. In addition, given $\boldsymbol{\tau} \in \mathbb{H}(\underline{\mathbf{curl}}; \Omega)$ and $e \in \mathcal{E}_h(\Omega)$, we let $[\![\boldsymbol{\tau} \times \mathbf{n}_e]\!]$ be the corresponding jump of the tangential traces (which exist in a variational sense) across e, that is, $[\![\boldsymbol{\tau} \times \mathbf{n}_e]\!] := (\boldsymbol{\tau}|_T - \boldsymbol{\tau}|_{T'})|_e \times \mathbf{n}_e$, where T and T' are the elements of $\mathcal{T}_h$ having e as a common face. From now on, when no confusion arises, we simply write $\mathbf{n}$ instead of $\mathbf{n}_e$.

4.1. The a posteriori error estimator

Given $(\boldsymbol{\rho}, \mathbf{u}) \in \mathbb{H}_0 \times \mathbf{Q}$ and $(\boldsymbol{\rho}_h, \mathbf{u}_h) \in \mathbb{H}_{0,h} \times \mathbf{Q}_h$ be the unique solutions of the continuous and discrete formulations (2.12) and (3.3), respectively, we define for each $T \in \mathcal{T}_h$ a local error indicator θ_T as follows:

$$\begin{aligned}
\theta_T^2 &:= \|\mathbf{f} + \mathbf{div}(\boldsymbol{\rho}_h)\|_{0,T}^2 + h_T^2 \left\| \nabla \mathbf{u}_h - \frac{1}{\mu}\left\{\boldsymbol{\rho}_h - \frac{\lambda+\mu}{3\lambda+4\mu}\,\mathrm{tr}(\boldsymbol{\rho}_h)\,\mathbb{I}\right\} - c_{\mathbf{g}}\,\mathbb{I}\right\|_{0,T}^2 \\
&\quad + h_T^2 \left\| \underline{\mathbf{curl}}\left(\frac{1}{\mu}\left\{\boldsymbol{\rho}_h - \frac{\lambda+\mu}{3\lambda+4\mu}\,\mathrm{tr}(\boldsymbol{\rho}_h)\,\mathbb{I}\right\}\right)\right\|_{0,T}^2 \\
&\quad + \sum_{e \in \mathcal{E}(T) \cap \mathcal{E}_h(\Omega)} h_e \left\| \left[\!\left[\left(\frac{1}{\mu}\left\{\boldsymbol{\rho}_h - \frac{\lambda+\mu}{3\lambda+4\mu}\,\mathrm{tr}(\boldsymbol{\rho}_h)\,\mathbb{I}\right\} + c_{\mathbf{g}}\,\mathbb{I}\right) \times \mathbf{n} \right]\!\right] \right\|_{0,e}^2 \\
&\quad + \sum_{e \in \mathcal{E}(T) \cap \mathcal{E}_h(\Gamma)} h_e \left\{ \left\| \nabla \mathbf{g} \times \mathbf{n} - \left(\frac{1}{\mu}\left\{\boldsymbol{\rho}_h - \frac{\lambda+\mu}{3\lambda+4\mu}\,\mathrm{tr}(\boldsymbol{\rho}_h)\,\mathbb{I}\right\} + c_{\mathbf{g}}\,\mathbb{I}\right) \times \mathbf{n} \right\|_{0,e}^2 + \|\mathbf{g} - \mathbf{u}_h\|_{0,e}^2 \right\},
\end{aligned} \tag{4.1}$$

where

$$c_{\mathbf{g}} := \frac{1}{3|\Omega|}\int_{\Gamma} \mathbf{g} \cdot \mathbf{n}. \tag{4.2}$$

The residual character of each term on the right hand side of (4.1) is quite clear from the continuous identities provided in Section 2. As usual the expression

$$\boldsymbol{\theta} := \left\{ \sum_{T \in \mathcal{T}_h} \theta_T^2 \right\}^{1/2} \tag{4.3}$$

is employed as the global residual error estimator.

The following theorem constitutes the main result of this section.

Theorem 4.1. *Assume that Ω is a polyhedral domain and that $\mathbf{g} \in \mathbf{H}^1(\Gamma)$. In addition, let $(\boldsymbol{\rho}, \mathbf{u}) \in \mathbb{H}_0 \times \mathbf{Q}$ and $(\boldsymbol{\rho}_h, \mathbf{u}_h) \in \mathbb{H}_{0,h} \times \mathbf{Q}_h$ be the unique solutions of (2.12) and (3.3), respectively. Then, there exist positive constants $C_{\mathtt{eff}}$ and $C_{\mathtt{rel}}$, independent of h and λ, such that*

$$C_{\mathtt{eff}}\,\boldsymbol{\theta} + h.o.t. \leq \|(\boldsymbol{\rho}, \mathbf{u}) - (\boldsymbol{\rho}_h, \mathbf{u}_h)\|_{\mathbb{H}_0 \times \mathbf{Q}} \leq C_{\mathtt{rel}}\,\boldsymbol{\theta}, \tag{4.4}$$

where h.o.t. stands for one or several terms of higher order.

The proof of Theorem 4.1 is separated into the parts given by the next subsections. Firstly, we prove the reliability (upper bound in (4.4)) of the global error estimator, and then in Section 4.3 we show the efficiency of the global error estimator (lower bound in (4.4)).

4.2. Reliability

We begin with the following preliminary estimate.

Lemma 4.1. *Let $(\boldsymbol{\rho}, \mathbf{u}) \in \mathbb{H}_0 \times \mathbf{Q}$ and $(\boldsymbol{\rho}_h, \mathbf{u}_h) \in \mathbb{H}_{0,h} \times \mathbf{Q}_h$ be the unique solutions of (2.12) and (3.3), respectively. Then there exists $C > 0$, independent of h, such that*

$$C\,\|(\boldsymbol{\rho} - \boldsymbol{\rho}_h, \mathbf{u} - \mathbf{u}_h)\|_{\mathbb{H}_0 \times \mathbf{Q}} \leq \sup_{\substack{\boldsymbol{\tau} \in \mathbb{H}_0 \\ \boldsymbol{\tau} \neq \mathbf{0}}} \frac{|E(\boldsymbol{\tau})|}{\|\boldsymbol{\tau}\|_{\mathbb{H}_0}} + \|\mathbf{f} + \mathbf{div}(\boldsymbol{\rho}_h)\|_{0,\Omega}, \tag{4.5}$$

where

$$E(\boldsymbol{\tau}) := a(\boldsymbol{\rho} - \boldsymbol{\rho}_h, \boldsymbol{\tau}) + b(\boldsymbol{\tau}, \mathbf{u} - \mathbf{u}_h) \quad \forall\, \boldsymbol{\tau} \in \mathbb{H}_0. \tag{4.6}$$

Proof. We first observe from Theorem 2.1 that the bounded linear operator $\mathcal{A} : \mathbb{H}_0 \times \mathbf{Q} \to (\mathbb{H}_0 \times \mathbf{Q})' \equiv \mathbb{H}_0' \times \mathbf{Q}'$, which is induced by the left-hand side of the equations in (2.12), is an isomorphism. Then there exists $C > 0$ such that

$$\|\mathcal{A}(\boldsymbol{\xi}, \mathbf{w})\|_{\mathbb{H}_0' \times \mathbf{Q}'} \geq C\,\|(\boldsymbol{\xi}, \mathbf{w})\|_{\mathbb{H}_0 \times \mathbf{Q}} \quad \forall\, (\boldsymbol{\xi}, \mathbf{w}) \in \mathbb{H}_0 \times \mathbf{Q}.$$

Equivalently

$$C\,\|(\boldsymbol{\xi},\mathbf{w})\|_{\mathbb{H}_0\times\mathbf{Q}} \leq \sup_{\substack{(\boldsymbol{\tau},\mathbf{v})\in\mathbb{H}_0\times\mathbf{Q}\\(\boldsymbol{\tau},\mathbf{v})\neq\mathbf{0}}} \frac{a(\boldsymbol{\xi},\boldsymbol{\tau})+b(\boldsymbol{\tau},\mathbf{w})+b(\boldsymbol{\xi},\mathbf{v})}{\|(\boldsymbol{\tau},\mathbf{v})\|_{\mathbb{H}_0\times\mathbf{Q}}} \quad \forall\,(\boldsymbol{\xi},\mathbf{w})\in\mathbb{H}_0\times\mathbf{Q}.$$

In particular, for the error $(\boldsymbol{\xi},\mathbf{w}):=(\boldsymbol{\rho}-\boldsymbol{\rho}_h,\mathbf{u}-\mathbf{u}_h)$, and using the notation introduced by (4.6) we have

$$\begin{aligned} C\,\|(\boldsymbol{\rho}-\boldsymbol{\rho}_h,\mathbf{u}-\mathbf{u}_h)\|_{\mathbb{H}_0\times\mathbf{Q}} &\leq \sup_{\substack{(\boldsymbol{\tau},\mathbf{v})\in\mathbb{H}_0\times\mathbf{Q}\\(\boldsymbol{\tau},\mathbf{v})\neq\mathbf{0}}} \frac{a(\boldsymbol{\rho}-\boldsymbol{\rho}_h,\boldsymbol{\tau})+b(\boldsymbol{\tau},\mathbf{u}-\mathbf{u}_h)+b(\boldsymbol{\rho}-\boldsymbol{\rho}_h,\mathbf{v})}{\|(\boldsymbol{\tau},\mathbf{v})\|_{\mathbb{H}_0\times\mathbf{Q}}} \\ &\leq \sup_{\substack{(\boldsymbol{\tau},\mathbf{v})\in\mathbb{H}_0\times\mathbf{Q}\\(\boldsymbol{\tau},\mathbf{v})\neq\mathbf{0}}} \left\{\frac{E(\boldsymbol{\tau})}{\|\boldsymbol{\tau}\|_{\mathbb{H}_0}}+\frac{b(\boldsymbol{\rho}-\boldsymbol{\rho}_h,\mathbf{v})}{\|\mathbf{v}\|_{\mathbf{Q}}}\right\} \leq \sup_{\substack{\boldsymbol{\tau}\in\mathbb{H}_0\\\boldsymbol{\tau}\neq\mathbf{0}}}\frac{E(\boldsymbol{\tau})}{\|\boldsymbol{\tau}\|_{\mathbb{H}_0}}+\sup_{\substack{\mathbf{v}\in\mathbf{Q}\\\mathbf{v}\neq\mathbf{0}}}\frac{b(\boldsymbol{\rho}-\boldsymbol{\rho}_h,\mathbf{v})}{\|\mathbf{v}\|_{\mathbf{Q}}}. \end{aligned}$$

In turn, according to the definition of the bilinear operator b (cf. (2.7)), and using the Cauchy–Schwarz inequality, and the second equation of (2.5), we get

$$\sup_{\substack{\mathbf{v}\in\mathbf{Q}\\\mathbf{v}\neq\mathbf{0}}}\frac{b(\boldsymbol{\rho}-\boldsymbol{\rho}_h,\mathbf{v})}{\|\mathbf{v}\|_{\mathbf{Q}}}=\sup_{\substack{\mathbf{v}\in\mathbf{Q}\\\mathbf{v}\neq\mathbf{0}}}\frac{-\int_\Omega \mathbf{v}\cdot\{\mathbf{f}+\mathbf{div}(\boldsymbol{\rho}_h)\}}{\|\mathbf{v}\|_{\mathbf{Q}}}\leq\|\mathbf{f}+\mathbf{div}(\boldsymbol{\rho}_h)\|_{0,\Omega},$$

which, completes the proof of (4.5). □

Our next goal is to estimate the supremum in (4.5). For this purpose, we now deduce from the first equations of (2.12) and (3.3) that

$$E(\boldsymbol{\tau})=F(\boldsymbol{\tau})-a(\boldsymbol{\rho}_h,\boldsymbol{\tau})-b(\boldsymbol{\tau},\mathbf{u}_h)\quad\forall\,\boldsymbol{\tau}\in\mathbb{H}_0,\quad\text{and}\quad E(\boldsymbol{\tau}_h)=0\quad\forall\,\boldsymbol{\tau}_h\in\mathbb{H}_{0,h},$$

whence, given a particular $\boldsymbol{\tau}_h\in\mathbb{H}_{0,h}$, and denoting $\widehat{\boldsymbol{\tau}}:=\boldsymbol{\tau}-\boldsymbol{\tau}_h$, we can write

$$E(\boldsymbol{\tau})=E(\widehat{\boldsymbol{\tau}})=\langle\widehat{\boldsymbol{\tau}}\mathbf{n},\mathbf{g}\rangle_\Gamma-\frac{1}{\mu}\int_\Omega\boldsymbol{\rho}_h^{\mathrm{d}}:\widehat{\boldsymbol{\tau}}^{\mathrm{d}}-\frac{1}{3(3\lambda+4\mu)}\int_\Omega\mathrm{tr}(\boldsymbol{\rho}_h)\,\mathrm{tr}(\widehat{\boldsymbol{\tau}})-\int_\Omega\mathbf{u}_h\cdot\mathbf{div}(\widehat{\boldsymbol{\tau}}).\tag{4.7}$$

In this way, estimating the supremum in (4.5) reduces now to bound $|E(\widehat{\boldsymbol{\tau}})|$ for a suitable choice of $\boldsymbol{\tau}_h\in\mathbb{H}_{0,h}$ (cf. (3.2)). To this end, we will need the Clément interpolation operator $I_h:H^1(\Omega)\to X_h$ (cf. [35]), where

$$X_h:=\left\{v\in C(\bar\Omega):v|_T\in\mathrm{P}_1(T)\;\forall\,T\in\mathcal{T}_h\right\}.$$

A vectorial version of I_h, say $\mathbf{I}_h:\mathbf{H}^1(\Omega)\to\mathbf{X}_h:=[X_h]^3$, which is defined componentwise by I_h, is also required. The following lemma establishes the local approximation properties of I_h.

Lemma 4.2. *There exist constants $c_1,c_2>0$, independent of h, such that for all $v\in H^1(\Omega)$ there holds*

$$\|v-I_h(v)\|_{0,T}\leq c_1\,h_T\,\|v\|_{1,\triangle(T)}\quad\forall\,T\in\mathcal{T}_h,$$

and

$$\|v-I_h(v)\|_{0,e}\leq c_2\,h_e^{1/2}\,\|v\|_{1,\triangle(e)}\quad\forall\,e\in\mathcal{E}_h,$$

where $\triangle(T):=\cup\{T'\in\mathcal{T}_h:T'\cap T\neq\varnothing\}$ and $\triangle(e):=\cup\{T'\in\mathcal{T}_h:T'\cap e\neq\varnothing\}$.

Proof. See [35]. □

In turn, we now establish a suitable Helmholtz decomposition for $\mathbb{H}(\mathbf{div};\Omega)$.

Lemma 4.3. *For each $\boldsymbol{\tau}\in\mathbb{H}(\mathbf{div};\Omega)$ there exist $\mathbf{z}\in\mathbf{H}^2(\Omega)$ and $\boldsymbol{\chi}\in\mathbb{H}^1(\Omega)$ such that*

$$\boldsymbol{\tau}=\nabla\mathbf{z}+\underline{\mathbf{curl}}(\boldsymbol{\chi})\quad\text{in }\Omega\quad\text{and}\quad\|\mathbf{z}\|_{2,\Omega}+\|\boldsymbol{\chi}\|_{1,\Omega}\leq c\,\|\boldsymbol{\tau}\|_{\mathbf{div};\Omega},\tag{4.8}$$

where c is a positive constant independent of all the foregoing variables.

Proof. We begin by introducing a sufficiently large convex domain $\widetilde{\Omega}$ such that $\overline{\Omega}\subset\widetilde{\Omega}$. Then, we proceed as in the second part of the proof of [36, Lemma 3.3] and perform a suitable extension of $\boldsymbol{\tau}$ to the whole domain $\widetilde{\Omega}$. More precisely, given $\boldsymbol{\tau}\in\mathbb{H}(\mathbf{div};\Omega)$, we consider the boundary value problem:

$$\Delta\mathbf{w}=\mathbf{0}\quad\text{in }\widetilde{\Omega}\setminus\overline{\Omega},\quad\frac{\partial\mathbf{w}}{\partial\mathbf{n}}=\boldsymbol{\tau}\,\mathbf{n}\text{ on }\Gamma,\qquad\mathbf{w}=\mathbf{0}\quad\text{on }\partial\widetilde{\Omega},\tag{4.9}$$

where $\mathbf{n}$ stands here for the inward unit normal on Γ. It follows, thanks to the Lax–Milgram Theorem, that (4.9) has a unique solution $\mathbf{w}\in\mathbf{H}^1(\widetilde{\Omega}\setminus\overline{\Omega})$, which satisfies

$$\|\mathbf{w}\|_{1,\widetilde{\Omega}\setminus\overline{\Omega}}\leq\widetilde{c}\,\|\boldsymbol{\tau}\,\mathbf{n}\|_{-1/2,\Gamma}\leq\widetilde{c}\,\|\boldsymbol{\tau}\|_{\mathbf{div};\Omega},\tag{4.10}$$

with a constant $\widetilde{c} > 0$, independent of $\boldsymbol{\tau}$. Then, we define $\widetilde{\boldsymbol{\tau}} := \begin{cases} \boldsymbol{\tau} & \text{in } \Omega \\ \nabla \mathbf{w} & \text{in } \widetilde{\Omega} \setminus \overline{\Omega} \end{cases}$, and observe, according to (4.9) and (4.10), that $\widetilde{\boldsymbol{\tau}} \in \mathbb{H}(\mathbf{div}; \widetilde{\Omega})$ and

$$\|\widetilde{\boldsymbol{\tau}}\|_{\mathbf{div};\widetilde{\Omega}} \leq \left\{1 + \widetilde{c}^2\right\}^{1/2} \|\boldsymbol{\tau}\|_{\mathbf{div};\Omega}. \tag{4.11}$$

In this way, applying the Helmholtz decomposition provided by [37, Proposition 4.52] (see also [38, Theorems 2.17 and 3.12] for the original reference) to the convex region $\widetilde{\Omega}$ and $\widetilde{\boldsymbol{\tau}} \in \mathbb{H}(\mathbf{div}; \widetilde{\Omega})$, we deduce that there exist $\widetilde{\mathbf{z}} \in \mathbf{H}^2(\widetilde{\Omega})$ and $\widetilde{\boldsymbol{\chi}} := \begin{pmatrix} \widetilde{\boldsymbol{\chi}}_1 \\ \widetilde{\boldsymbol{\chi}}_2 \\ \widetilde{\boldsymbol{\chi}}_3 \end{pmatrix} \in \mathbb{H}^1(\widetilde{\Omega})$, with $\widetilde{\boldsymbol{\chi}}_i := (\widetilde{\chi}_{i1}, \widetilde{\chi}_{i2}, \widetilde{\chi}_{i3})^{\mathrm{t}} \in \mathbf{H}^1(\widetilde{\Omega})$, $i \in \{1, 2, 3\}$, such that

$$\widetilde{\boldsymbol{\tau}} = \nabla \widetilde{\mathbf{z}} + \underline{\mathbf{curl}}(\widetilde{\boldsymbol{\chi}}) \quad \text{in } \widetilde{\Omega} \quad \text{and} \quad \|\widetilde{\mathbf{z}}\|_{2,\widetilde{\Omega}} + \|\widetilde{\boldsymbol{\chi}}\|_{1,\widetilde{\Omega}} \leq C \|\widetilde{\boldsymbol{\tau}}\|_{\mathbf{div};\widetilde{\Omega}} \leq \widetilde{C} \|\boldsymbol{\tau}\|_{\mathbf{div};\Omega}, \tag{4.12}$$

where the last inequality makes use of (4.11), thus yielding $\widetilde{C} = C \left\{1 + \widetilde{c}^2\right\}^{1/2}$. Finally, defining $\mathbf{z} := \widetilde{\mathbf{z}}|_{\Omega} \in \mathbf{H}^2(\Omega)$ and $\boldsymbol{\chi} := \widetilde{\boldsymbol{\chi}}|_{\Omega} \in \mathbb{H}^1(\Omega)$, noting that certainly $\widetilde{\boldsymbol{\tau}}|_{\Omega} = \boldsymbol{\tau}$, and employing (4.12), we arrive at (4.8) and conclude the proof. □

Now we are in conditions to estimate $E(\widehat{\boldsymbol{\tau}})$ (cf. (4.7)). To do that, we let $\boldsymbol{\tau} \in \mathbb{H}_0$ and bound $|E(\widehat{\boldsymbol{\tau}})|$ for a specific choice of $\boldsymbol{\tau}_h \in \mathbb{H}_{0,h}$. More precisely, the Helmholtz decomposition of $\boldsymbol{\tau}$ given by Lemma 4.3 suggests to define $\boldsymbol{\tau}_h$ through what we call a discrete Helmholtz decomposition. In other words, with the notations employed in the above proof we now let $\boldsymbol{\chi}_h := \begin{pmatrix} \boldsymbol{\chi}_{1h} \\ \boldsymbol{\chi}_{2h} \\ \boldsymbol{\chi}_{3h} \end{pmatrix}$, where $\boldsymbol{\chi}_{ih} := \mathbf{I}_h(\boldsymbol{\chi}_i)$, $i \in \{1, 2, 3\}$, and define

$$\boldsymbol{\tau}_h := \mathscr{E}_h^k(\nabla \mathbf{z}) + \underline{\mathbf{curl}}(\boldsymbol{\chi}_h) - d_h \mathbb{I}, \tag{4.13}$$

where $\mathscr{E}_h^k$ is the Raviart–Thomas interpolation operator introduced before (cf. (3.6) and (3.7)), and the constant d_h is chosen so that $\boldsymbol{\tau}_h$, which is already in $\mathbb{RT}_k(\mathcal{T}_h)$, belongs to $\mathbb{H}_{0,h}$. Equivalently, $\boldsymbol{\tau}_h$ is the $\mathbb{H}_0$-component of $\mathscr{E}_h^k(\nabla \mathbf{z}) + \underline{\mathbf{curl}}(\boldsymbol{\chi}_h) \in \mathbb{RT}_k(\mathcal{T}_h)$, which yields

$$d_h = \frac{1}{3\,|\Omega|} \int_{\Omega} \mathrm{tr}\big(\mathscr{E}_h^k(\nabla \mathbf{z}) + \underline{\mathbf{curl}}(\boldsymbol{\chi}_h)\big) = -\frac{1}{3\,|\Omega|} \int_{\Omega} \mathrm{tr}\big(\nabla \mathbf{z} - \mathscr{E}_h^k(\nabla \mathbf{z}) + \underline{\mathbf{curl}}(\boldsymbol{\chi} - \boldsymbol{\chi}_h)\big), \tag{4.14}$$

where the second equality makes use of the fact that $\boldsymbol{\tau} = \nabla \mathbf{z} + \underline{\mathbf{curl}}(\boldsymbol{\chi})$ is taken in $\mathbb{H}_0$. According to the aforementioned Helmholtz decomposition of $\boldsymbol{\tau}$, we refer to (4.13) as the announced discrete Helmholtz decomposition of $\boldsymbol{\tau}_h$. Therefore, we can write

$$\widehat{\boldsymbol{\tau}} := \nabla \mathbf{z} - \mathscr{E}_h^k(\nabla \mathbf{z}) + \underline{\mathbf{curl}}(\boldsymbol{\chi} - \boldsymbol{\chi}_h) + d_h \mathbb{I}, \tag{4.15}$$

which, using the property (3.8), yields

$$\mathbf{div}(\widehat{\boldsymbol{\tau}}) = \mathbf{div}(\nabla \mathbf{z} - \mathscr{E}_h^k(\nabla \mathbf{z})) = (\mathbf{I} - \mathscr{P}_h^k)(\mathbf{div}(\nabla \mathbf{z})) = (\mathbf{I} - \mathscr{P}_h^k)(\mathbf{div}(\boldsymbol{\tau})).$$

In this way, since $\mathscr{P}_h^k : \mathbf{L}^2(\Omega) \to \mathbf{Q}_h$ is the orthogonal projector and $\mathbf{u}_h \in \mathbf{Q}_h$, we readily see from the foregoing equation that

$$\int_{\Omega} \mathbf{u}_h \cdot \mathbf{div}(\widehat{\boldsymbol{\tau}}) = \int_{\Omega} \mathbf{u}_h \cdot (\mathbf{I} - \mathscr{P}_h^k)(\mathbf{div}(\boldsymbol{\tau})) = 0. \tag{4.16}$$

In turn, taking into account that $\boldsymbol{\rho}_h \in \mathbb{H}_{0,h}$, and recalling the expressions for $c_{\mathbf{g}}$ and d_h given by (4.2) and (4.14), respectively, we easily deduce from the definition of E (cf. (4.7)) that

$$E(d_h \mathbb{I}) = d_h \int_{\Gamma} \mathbf{g} \cdot \mathbf{n} = -c_{\mathbf{g}} \int_{\Omega} \mathrm{tr}\big(\nabla \mathbf{z} - \mathscr{E}_h^k(\nabla \mathbf{z}) + \underline{\mathbf{curl}}(\boldsymbol{\chi} - \boldsymbol{\chi}_h)\big). \tag{4.17}$$

Hence, replacing (4.15) into (4.7), and employing (4.16) and (4.17), we find that $E(\widehat{\boldsymbol{\tau}})$ can be decomposed as

$$E(\widehat{\boldsymbol{\tau}}) = E_1(\mathbf{z}) + E_2(\boldsymbol{\chi}), \tag{4.18}$$

where

$$E_1(\mathbf{z}) := \langle (\nabla \mathbf{z} - \mathscr{E}_h^k(\nabla \mathbf{z}))\mathbf{n}, \mathbf{g} \rangle_{\Gamma} - c_{\mathbf{g}} \int_{\Omega} \mathrm{tr}(\nabla \mathbf{z} - \mathscr{E}_h^k(\nabla \mathbf{z})) - \frac{1}{\mu} \int_{\Omega} \boldsymbol{\rho}_h^{\mathrm{d}} : (\nabla \mathbf{z} - \mathscr{E}_h^k(\nabla \mathbf{z})) - \frac{1}{3(3\lambda + 4\mu)} \int_{\Omega} \mathrm{tr}(\boldsymbol{\rho}_h)\, \mathrm{tr}(\nabla \mathbf{z} - \mathscr{E}_h^k(\nabla \mathbf{z})),$$

and

$$E_2(\boldsymbol{\chi}) := \langle \underline{\mathbf{curl}}(\boldsymbol{\chi}-\boldsymbol{\chi}_h)\mathbf{n}, \mathbf{g}\rangle_{\Gamma} - c_{\mathbf{g}} \int_{\Omega} \mathrm{tr}(\underline{\mathbf{curl}}(\boldsymbol{\chi}-\boldsymbol{\chi}_h)) - \frac{1}{\mu}\int_{\Omega} \boldsymbol{\rho}_h^{\mathrm{d}} : \underline{\mathbf{curl}}(\boldsymbol{\chi}-\boldsymbol{\chi}_h) - \frac{1}{3(3\lambda+4\mu)}\int_{\Omega} \mathrm{tr}(\boldsymbol{\rho}_h)\,\mathrm{tr}(\underline{\mathbf{curl}}(\boldsymbol{\chi}-\boldsymbol{\chi}_h)).$$

Furthermore, we note from the definition of $\boldsymbol{\rho}_h^{\mathrm{d}}$ and the equality $\mathrm{tr}(\boldsymbol{\xi}) = \boldsymbol{\xi} : \mathbb{I}$, that

$$E_1(\mathbf{z}) = \langle (\nabla \mathbf{z} - \mathscr{E}_h^k(\nabla \mathbf{z}))\mathbf{n}, \mathbf{g}\rangle_{\Gamma} - \int_{\Omega} \left(\frac{1}{\mu}\left\{ \boldsymbol{\rho}_h - \frac{\lambda+\mu}{3\lambda+4\mu}\,\mathrm{tr}(\boldsymbol{\rho}_h)\,\mathbb{I}\right\} + c_{\mathbf{g}}\,\mathbb{I}\right) : (\nabla \mathbf{z} - \mathscr{E}_h^k(\nabla \mathbf{z})), \tag{4.19}$$

and

$$E_2(\boldsymbol{\chi}) = \langle \underline{\mathbf{curl}}(\boldsymbol{\chi}-\boldsymbol{\chi}_h)\mathbf{n}, \mathbf{g}\rangle_{\Gamma} - \int_{\Omega} \left(\frac{1}{\mu}\left\{ \boldsymbol{\rho}_h - \frac{\lambda+\mu}{3\lambda+4\mu}\,\mathrm{tr}(\boldsymbol{\rho}_h)\,\mathbb{I}\right\} + c_{\mathbf{g}}\,\mathbb{I}\right) : \underline{\mathbf{curl}}(\boldsymbol{\chi}-\boldsymbol{\chi}_h). \tag{4.20}$$

The following two lemmas provide upper bounds for $|E_1(\mathbf{z})|$ and $|E_2(\boldsymbol{\chi})|$.

Lemma 4.4. *There exists $C > 0$, independent of λ and h, such that*

$$|E_1(\mathbf{z})| \leq C \left\{ \sum_{T\in\mathcal{T}_h} \theta_{1,T}^2 \right\}^{1/2} \|\boldsymbol{\tau}\|_{\mathbf{div};\Omega}, \tag{4.21}$$

where

$$\theta_{1,T}^2 := h_T^2 \left\| \nabla \mathbf{u}_h - \left(\frac{1}{\mu}\left\{ \boldsymbol{\rho}_h - \frac{\lambda+\mu}{3\lambda+4\mu}\,\mathrm{tr}(\boldsymbol{\rho}_h)\,\mathbb{I}\right\} + c_{\mathbf{g}}\,\mathbb{I}\right)\right\|_{0,T}^2 + \sum_{e\in\mathcal{E}(T)\cap\mathcal{E}_h(\Gamma)} h_e \|\mathbf{g} - \mathbf{u}_h\|_{0,e}^2.$$

Proof. Since $\nabla\mathbf{z} \in \mathbb{H}^1(\Omega)$, it follows that $(\nabla\mathbf{z} - \mathscr{E}_h^k(\nabla\mathbf{z}))\mathbf{n}|_{\Gamma}$ belongs to $\mathbf{L}^2(\Gamma)$, whence $E_1(\mathbf{z})$ (cf. (4.19)) can be redefined as:

$$E_1(\mathbf{z}) = \sum_{e\in\mathcal{E}_h(\Gamma)} \int_e (\nabla\mathbf{z} - \mathscr{E}_h^k(\nabla\mathbf{z}))\mathbf{n}\cdot\mathbf{g} - \int_{\Omega} \left(\frac{1}{\mu}\left\{ \boldsymbol{\rho}_h - \frac{\lambda+\mu}{3\lambda+4\mu}\,\mathrm{tr}(\boldsymbol{\rho}_h)\,\mathbb{I}\right\} + c_{\mathbf{g}}\,\mathbb{I}\right) : (\nabla\mathbf{z} - \mathscr{E}_h^k(\nabla\mathbf{z})). \tag{4.22}$$

On the other hand, since $\mathbf{u}_h|_e \in \mathbf{P}_k(e)$ for each face $e \in \mathcal{E}_h$ (in particular for each face $e \in \mathcal{E}_h(\Gamma)$), and $\nabla\mathbf{u}_h|_T \in \mathbb{P}_{k-1}(T)$ for each $T \in \mathcal{T}_h$, the identities (3.6) and (3.7) characterizing $\mathscr{E}_h^k$, yield, respectively,

$$\int_e (\nabla\mathbf{z} - \mathscr{E}_h^k(\nabla\mathbf{z}))\,\mathbf{n}\cdot\mathbf{u}_h = 0 \quad \forall\, e \in \mathcal{E}_h(\Gamma),$$

and

$$\int_T (\nabla\mathbf{z} - \mathscr{E}_h^k(\nabla\mathbf{z})) : \nabla\mathbf{u}_h = 0 \quad \forall\, T \in \mathcal{T}_h.$$

Hence, introducing the above expressions into (4.22), we can write $E_1(\mathbf{z})$ as

$$E_1(\mathbf{z}) = \sum_{e\in\mathcal{E}_h(\Gamma)} \int_e (\nabla\mathbf{z} - \mathscr{E}_h^k(\nabla\mathbf{z}))\mathbf{n}\cdot(\mathbf{g} - \mathbf{u}_h) + \sum_{T\in\mathcal{T}_h} \int_T \left[\nabla\mathbf{u}_h - \left(\frac{1}{\mu}\left\{ \boldsymbol{\rho}_h - \frac{\lambda+\mu}{3\lambda+4\mu}\,\mathrm{tr}(\boldsymbol{\rho}_h)\,\mathbb{I}\right\} + c_{\mathbf{g}}\,\mathbb{I}\right)\right] : (\nabla\mathbf{z} - \mathscr{E}_h^k(\nabla\mathbf{z})).$$

Finally, applying the Cauchy–Schwarz inequality, the approximation properties (3.11) (with $m = 1$) and (3.13), and then the fact that $\|\nabla\mathbf{z}\|_{1,\Omega} \leq \|\mathbf{z}\|_{2,\Omega} \leq C\|\boldsymbol{\tau}\|_{\mathbf{div};\Omega}$ by (4.8), we obtain the upper bound (4.21). □

Lemma 4.5. *Assume that $\mathbf{g} \in \mathbf{H}^1(\Gamma)$. Then, there exists $C > 0$, independent of λ and h, such that*

$$|E_2(\boldsymbol{\chi})| \leq C \left\{ \sum_{T\in\mathcal{T}_h} \theta_{2,T}^2 \right\}^{1/2} \|\boldsymbol{\tau}\|_{\mathbf{div};\Omega}, \tag{4.23}$$

where

$$\theta_{2,T}^2 := h_T^2 \left\| \underline{\mathbf{curl}} \left(\frac{1}{\mu} \left\{ \boldsymbol{\rho}_h - \frac{\lambda+\mu}{3\lambda+4\mu} \operatorname{tr}(\boldsymbol{\rho}_h)\, \mathbb{I} \right\} \right) \right\|_{0,T}^2 + \sum_{e \in \mathcal{E}(T) \cap \mathcal{E}_h(\Omega)} h_e \left\| \left[\!\left[\left(\frac{1}{\mu} \left\{ \boldsymbol{\rho}_h - \frac{\lambda+\mu}{3\lambda+4\mu} \operatorname{tr}(\boldsymbol{\rho}_h)\, \mathbb{I} \right\} + c_{\mathbf{g}}\, \mathbb{I} \right) \times \mathbf{n} \right]\!\right] \right\|_{0,e}^2 + \sum_{e \in \mathcal{E}(T) \cap \mathcal{E}_h(\Gamma)} h_e \left\| \nabla \mathbf{g} \times \mathbf{n} - \left(\frac{1}{\mu} \left\{ \boldsymbol{\rho}_h - \frac{\lambda+\mu}{3\lambda+4\mu} \operatorname{tr}(\boldsymbol{\rho}_h)\, \mathbb{I} \right\} + c_{\mathbf{g}}\, \mathbb{I} \right) \times \mathbf{n} \right\|_{0,e}^2 .$$

Proof. Using the fact that $\underline{\mathbf{curl}}(\boldsymbol{\chi} - \boldsymbol{\chi}_h)\, \mathbf{n} = \mathbf{div}\left((\boldsymbol{\chi} - \boldsymbol{\chi}_h) \times \mathbf{n}\right)$, and then integrating by parts on Γ, we find that

$$\langle \underline{\mathbf{curl}}(\boldsymbol{\chi} - \boldsymbol{\chi}_h)\, \mathbf{n}, \mathbf{g} \rangle_{\Gamma} = \langle \boldsymbol{\chi} - \boldsymbol{\chi}_h, \nabla \mathbf{g} \times \mathbf{n} \rangle_{\Gamma} = \sum_{e \in \mathcal{E}_h(\Gamma)} \int_e (\boldsymbol{\chi} - \boldsymbol{\chi}_h) : (\nabla \mathbf{g} \times \mathbf{n}).$$

Next, integrating by parts on each $T \in \mathcal{T}_h$, we obtain that

$$\begin{aligned} &\int_{\Omega} \left(\frac{1}{\mu} \left\{ \boldsymbol{\rho}_h - \frac{\lambda+\mu}{3\lambda+4\mu} \operatorname{tr}(\boldsymbol{\rho}_h)\, \mathbb{I} \right\} + c_{\mathbf{g}}\, \mathbb{I} \right) : \underline{\mathbf{curl}}(\boldsymbol{\chi} - \boldsymbol{\chi}_h) \\ &= \sum_{T \in \mathcal{T}_h} \left[\int_T \underline{\mathbf{curl}} \left(\frac{1}{\mu} \left\{ \boldsymbol{\rho}_h - \frac{\lambda+\mu}{3\lambda+4\mu} \operatorname{tr}(\boldsymbol{\rho}_h)\, \mathbb{I} \right\} \right) : (\boldsymbol{\chi} - \boldsymbol{\chi}_h) \right. \\ &\quad \left. + \int_{\partial T} \left(\frac{1}{\mu} \left\{ \boldsymbol{\rho}_h - \frac{\lambda+\mu}{3\lambda+4\mu} \operatorname{tr}(\boldsymbol{\rho}_h)\, \mathbb{I} \right\} + c_{\mathbf{g}}\, \mathbb{I} \right) \times \mathbf{n} : (\boldsymbol{\chi} - \boldsymbol{\chi}_h) \right] \\ &= \sum_{T \in \mathcal{T}_h} \int_T \underline{\mathbf{curl}} \left(\frac{1}{\mu} \left\{ \boldsymbol{\rho}_h - \frac{\lambda+\mu}{3\lambda+4\mu} \operatorname{tr}(\boldsymbol{\rho}_h)\, \mathbb{I} \right\} \right) : (\boldsymbol{\chi} - \boldsymbol{\chi}_h) \\ &\quad + \sum_{e \in \mathcal{E}_h(\Omega)} \int_e \left[\!\left[\left(\frac{1}{\mu} \left\{ \boldsymbol{\rho}_h - \frac{\lambda+\mu}{3\lambda+4\mu} \operatorname{tr}(\boldsymbol{\rho}_h)\, \mathbb{I} \right\} + c_{\mathbf{g}}\, \mathbb{I} \right) \times \mathbf{n} \right]\!\right] : (\boldsymbol{\chi} - \boldsymbol{\chi}_h) \\ &\quad + \sum_{e \in \mathcal{E}_h(\Gamma)} \int_e \left(\frac{1}{\mu} \left\{ \boldsymbol{\rho}_h - \frac{\lambda+\mu}{3\lambda+4\mu} \operatorname{tr}(\boldsymbol{\rho}_h)\, \mathbb{I} \right\} + c_{\mathbf{g}}\, \mathbb{I} \right) \times \mathbf{n} : (\boldsymbol{\chi} - \boldsymbol{\chi}_h). \end{aligned}$$

Hence, replacing the above expressions into (4.20), we can write

$$\begin{aligned} E_2(\boldsymbol{\chi}) = &- \sum_{T \in \mathcal{T}_h} \int_T \underline{\mathbf{curl}} \left(\frac{1}{\mu} \left\{ \boldsymbol{\rho}_h - \frac{\lambda+\mu}{3\lambda+4\mu} \operatorname{tr}(\boldsymbol{\rho}_h)\, \mathbb{I} \right\} \right) : (\boldsymbol{\chi} - \boldsymbol{\chi}_h) \\ &- \sum_{e \in \mathcal{E}_h(\Omega)} \int_e \left[\!\left[\left(\frac{1}{\mu} \left\{ \boldsymbol{\rho}_h - \frac{\lambda+\mu}{3\lambda+4\mu} \operatorname{tr}(\boldsymbol{\rho}_h)\, \mathbb{I} \right\} + c_{\mathbf{g}}\, \mathbb{I} \right) \times \mathbf{n} \right]\!\right] : (\boldsymbol{\chi} - \boldsymbol{\chi}_h) \\ &+ \sum_{e \in \mathcal{E}_h(\Gamma)} \int_e \left[\nabla \mathbf{g} \times \mathbf{n} - \left(\frac{1}{\mu} \left\{ \boldsymbol{\rho}_h - \frac{\lambda+\mu}{3\lambda+4\mu} \operatorname{tr}(\boldsymbol{\rho}_h)\, \mathbb{I} \right\} + c_{\mathbf{g}}\, \mathbb{I} \right) \times \mathbf{n} \right] : (\boldsymbol{\chi} - \boldsymbol{\chi}_h). \end{aligned}$$

In addition, since $\boldsymbol{\chi}_h := \mathbf{I}_h(\boldsymbol{\chi})$, the approximation properties of $\mathbf{I}_h$ (cf. Lemma 4.2) yield

$$\|\boldsymbol{\chi} - \boldsymbol{\chi}_h\|_{0,T} \leq c_1\, h_T\, \|\boldsymbol{\chi}\|_{1,\triangle(T)} \quad \forall\, T \in \mathcal{T}_h, \tag{4.24}$$

and

$$\|\boldsymbol{\chi} - \boldsymbol{\chi}_h\|_{0,e} \leq c_2\, h_e^{1/2}\, \|\boldsymbol{\chi}\|_{1,\triangle(e)} \quad \forall\, e \in \mathcal{E}_h. \tag{4.25}$$

Thus, applying the Cauchy–Schwarz inequality to each term in the above expression for $E_2(\boldsymbol{\chi})$, and making use of the estimates (4.24), (4.25) and (4.8), together with the fact that $\triangle(T)$ and $\triangle(e)$ are bounded (since $\{\mathcal{T}_h\}_{h>0}$ is shape-regular), we derive the upper bound (4.23). □

Finally, it follows from the decomposition (4.18) of E and Lemmas 4.4 and 4.5 that

$$|E(\widehat{\boldsymbol{\tau}})| \leq C \left\{ \sum_{T \in \mathcal{T}_h} (\theta_{1,T}^2 + \theta_{2,T}^2) \right\}^{1/2} \|\boldsymbol{\tau}\|_{\mathbf{div};\Omega} \quad \forall\, \boldsymbol{\tau} \in \mathbb{H}_0,$$

which, gives an upper bound for the supremum on the right hand side of (4.5) (cf. Lemma 4.1).

In this way, and noting that

$$\|\mathbf{f}+\mathbf{div}(\boldsymbol{\rho}_h)\|^2_{0,\Omega}=\sum_{T\in\mathcal{T}_h}\|\mathbf{f}+\mathbf{div}(\boldsymbol{\rho}_h)\|^2_{0,T},$$

we conclude from Lemma 4.1 the reliability of $\boldsymbol{\theta}$ (upper bound in (4.4)).

4.3. Efficiency

In this section we prove the efficiency of our a posteriori error estimator $\boldsymbol{\theta}$ (lower bound in (4.4)). In other words, we derive suitable upper bounds for the six terms defining the local error indicator θ_T^2 (cf. (4.1)). We first notice, using that $\mathbf{f}=-\mathbf{div}(\boldsymbol{\rho})$ in Ω, that there holds

$$\|\mathbf{f}+\mathbf{div}(\boldsymbol{\rho}_h)\|^2_{0,T}=\|\mathbf{div}(\boldsymbol{\rho}-\boldsymbol{\rho}_h)\|^2_{0,T}\leq\|\boldsymbol{\rho}-\boldsymbol{\rho}_h\|^2_{\mathbf{div};T}. \tag{4.26}$$

Next, in order to bound the terms involving the mesh parameters h_T and h_e, we proceed similarly as in [39,40] (see also [41]), and apply results ultimately based on inverse inequalities (see [34]) and the localization technique introduced in [42], which is based on tetrahedron-bubble and face–bubble functions. To this end, we now introduce further notations and preliminary results. Given $T\in\mathcal{T}_h$ and $e\in\mathcal{E}(T)$, we let ψ_T and ψ_e be the usual tetrahedron-bubble and face–bubble functions, respectively (see (1.5) and (1.6) in [42]), which satisfy:

(i) $\psi_T\in\mathrm{P}_4(T)$, $\mathrm{supp}(\psi_T)\subseteq T$, $\psi_T=0$ on ∂T, and $0\leq\psi_T\leq 1$ in T.
(ii) $\psi_e|_T\in\mathrm{P}_3(T)$, $\mathrm{supp}(\psi_e)\subseteq\omega_e:=\cup\{T'\in\mathcal{T}_h : e\in\mathcal{E}(T')\}$, $\psi_e=0$ on $\partial T\setminus e$, and $0\leq\psi_e\leq 1$ in ω_e.

We also recall from [43] that, given $k\in\mathbf{N}\cup\{0\}$, there exists a linear operator $L : C(e)\to C(T)$ that satisfies $L(p)\in\mathrm{P}_k(T)$ and $L(p)|_e=p\,\forall\,p\in\mathrm{P}_k(e)$. A corresponding vectorial version of L, that is the componentwise application of L, is denoted by $\mathbf{L}$. Additional properties of ψ_T, ψ_e and L are collected in the following lemma.

Lemma 4.6. *Given $k\in\mathbf{N}\cup\{0\}$, there exist positive constants c_1, c_2, and c_3, depending only on k and the shape regularity of the triangulations (minimum angle condition), such that for each $T\in\mathcal{T}_h$ and $e\in\mathcal{E}(T)$, there hold*

$$\|q\|^2_{0,T}\leq c_1\,\|\psi_T^{1/2}\,q\|^2_{0,T}\quad\forall\,q\in\mathrm{P}_k(T), \tag{4.27}$$

$$\|p\|^2_{0,e}\leq c_2\,\|\psi_e^{1/2}\,p\|^2_{0,e}\quad\forall\,p\in\mathrm{P}_k(e), \tag{4.28}$$

and

$$\|\psi_e^{1/2}\,L(p)\|^2_{0,T}\leq c_3\,h_e\,\|p\|^2_{0,e}\quad\forall\,p\in\mathrm{P}_k(e). \tag{4.29}$$

Proof. See [43, Lemma 4.1]. □

The following inverse estimate will also be used.

Lemma 4.7. *Let $\ell,m\in\mathbf{N}\cup\{0\}$ such that $\ell\leq m$. Then, there exists $c_4>0$, depending only on k, ℓ, m and the shape regularity of the triangulations, such that for each $T\in\mathcal{T}_h$ there holds*

$$|q|_{m,T}\leq c_4\,h_T^{\ell-m}\,|q|_{\ell,T}\quad\forall\,q\in\mathrm{P}_k(T). \tag{4.30}$$

Proof. See [34, Theorem 3.2.6]. □

In order to bound the boundary term of the local error estimator θ_T given by $h_e\,\|\mathbf{g}-\mathbf{u}_h\|^2_{0,e}$, $e\in\mathcal{E}_h(\Gamma)$, we will need the following discrete trace inequality.

Lemma 4.8. *There exists $c_5>0$, depending only on the shape regularity of the triangulations, such that for each $T\in\mathcal{T}_h$ and $e\in\mathcal{E}(T)$, there holds*

$$\|v\|^2_{0,e}\leq c_5\,\left\{h_e^{-1}\,\|v\|^2_{0,T}+h_e\,|v|^2_{1,T}\right\}\quad\forall\,v\in H^1(T). \tag{4.31}$$

Proof. See [44, equation (2.4)]. □

Lemma 4.9. *Let $\boldsymbol{\zeta}_h\in\mathbb{L}^2(\Omega)$ be a piecewise polynomial of degree $k\geq 0$ on each $T\in\mathcal{T}_h$. In addition, let $\boldsymbol{\zeta}\in\mathbb{L}^2(\Omega)$ be such that $\underline{\mathbf{curl}}(\boldsymbol{\zeta})=\mathbf{0}$ on each $T\in\mathcal{T}_h$. Then, there exists $c_6>0$, independent of h, such that*

$$\|\underline{\mathbf{curl}}(\boldsymbol{\zeta}_h)\|_{0,T}\leq c_6\,h_T^{-1}\,\|\boldsymbol{\zeta}-\boldsymbol{\zeta}_h\|_{0,T}\quad\forall\,T\in\mathcal{T}_h. \tag{4.32}$$

Proof. We adapt the proof of [45, Lemma 4.3]. Indeed, applying (4.27), integrating by parts, recalling that $\psi_T = 0$ on ∂T, and using the Cauchy–Schwarz inequality, we obtain

$$\begin{aligned}\|\underline{\mathbf{curl}}(\boldsymbol{\zeta}_h)\|_{0,T}^2 &\leq c_1 \|\psi_T^{1/2}\underline{\mathbf{curl}}(\boldsymbol{\zeta}_h)\|_{0,T}^2 = c_1 \int_T \underline{\mathbf{curl}}(\boldsymbol{\zeta}_h - \boldsymbol{\zeta}) : \psi_T\, \underline{\mathbf{curl}}(\boldsymbol{\zeta}_h) \\ &= c_1 \int_T (\boldsymbol{\zeta}_h - \boldsymbol{\zeta}) : \underline{\mathbf{curl}}(\psi_T\, \underline{\mathbf{curl}}(\boldsymbol{\zeta}_h)) \leq c_1 \|\boldsymbol{\zeta} - \boldsymbol{\zeta}_h\|_{0,T} \|\underline{\mathbf{curl}}(\psi_T\, \underline{\mathbf{curl}}(\boldsymbol{\zeta}_h))\|_{0,T}.\end{aligned}$$

From the inverse estimate (4.30) and the fact that $0 \leq \psi_T \leq 1$, it follows

$$\|\underline{\mathbf{curl}}(\psi_T\, \underline{\mathbf{curl}}(\boldsymbol{\zeta}_h))\|_{0,T} \leq \widetilde{c}_4\, h_T^{-1} \|\psi_T\, \underline{\mathbf{curl}}(\boldsymbol{\zeta}_h)\|_{0,T} \leq \widetilde{c}_4\, h_T^{-1}\, \|\underline{\mathbf{curl}}(\boldsymbol{\zeta}_h)\|_{0,T},$$

where $\widetilde{c}_4$ depends only on c_4 (see (4.30)). This proves the lemma with $c_6 := c_1\widetilde{c}_4$. □

Lemma 4.10. *Let $\boldsymbol{\zeta}_h \in \mathbb{L}^2(\Omega)$ be a piecewise polynomial of degree $k \geq 0$ on each $T \in \mathcal{T}_h$, and let $\boldsymbol{\zeta} \in \mathbb{L}^2(\Omega)$ be such that $\underline{\mathbf{curl}}(\boldsymbol{\zeta}) = \mathbf{0}$ in Ω. Then, there exists $c_7 > 0$, independent of h, such that*

$$\|[\![\boldsymbol{\zeta}_h \times \mathbf{n}]\!]\|_{0,e} \leq c_7\, h_e^{-1/2}\, \|\boldsymbol{\zeta} - \boldsymbol{\zeta}_h\|_{0,\omega_e} \quad \forall\, e \in \mathcal{E}_h. \tag{4.33}$$

Proof. We adapt the proof of [45, Lemma 4.4]. Given a face $e \in \mathcal{E}_h$, we denote $\mathbf{r}_h := [\![\boldsymbol{\zeta}_h \times \mathbf{n}]\!]$ the corresponding tangential jump of $\boldsymbol{\zeta}_h$. Then, employing (4.28) and integrating by parts on each tetrahedron of ω_e, we obtain

$$\begin{aligned}c_2^{-1}\|\mathbf{r}_h\|_{0,e}^2 &\leq \|\psi_e^{1/2}\mathbf{r}_h\|_{0,e}^2 = \|\psi_e^{1/2}\mathbf{L}(\mathbf{r}_h)\|_{0,e}^2 = \int_e \psi_e \mathbf{L}(\mathbf{r}_h) : [\![\boldsymbol{\zeta}_h \times \mathbf{n}]\!] \\ &= -\int_{\omega_e} \psi_e \mathbf{L}(\mathbf{r}_h) : \underline{\mathbf{curl}}(\boldsymbol{\zeta}_h) + \int_{\omega_e} \underline{\mathbf{curl}}(\psi_e \mathbf{L}(\mathbf{r}_h)) : \boldsymbol{\zeta}_h.\end{aligned}$$

Next, since $[\![\boldsymbol{\zeta} \times \mathbf{n}]\!] = \mathbf{0}$, we deduce that

$$0 = -\int_{\omega_e} \psi_e \mathbf{L}(\mathbf{r}_h) : \underline{\mathbf{curl}}(\boldsymbol{\zeta}) + \int_{\omega_e} \underline{\mathbf{curl}}(\psi_e \mathbf{L}(\mathbf{r}_h)) : \boldsymbol{\zeta},$$

and therefore

$$\begin{aligned}c_2^{-1}\|\mathbf{r}_h\|_{0,e}^2 &\leq \int_{\omega_e} \psi_e \mathbf{L}(\mathbf{r}_h) : \underline{\mathbf{curl}}(\boldsymbol{\zeta} - \boldsymbol{\zeta}_h) - \int_{\omega_e} \underline{\mathbf{curl}}(\psi_e \mathbf{L}(\mathbf{r}_h)) : (\boldsymbol{\zeta} - \boldsymbol{\zeta}_h) \\ &= -\int_{\omega_e} \psi_e \mathbf{L}(\mathbf{r}_h) : \underline{\mathbf{curl}}(\boldsymbol{\zeta}_h) - \int_{\omega_e} \underline{\mathbf{curl}}(\psi_e \mathbf{L}(\mathbf{r}_h)) : (\boldsymbol{\zeta} - \boldsymbol{\zeta}_h),\end{aligned}$$

which, using the Cauchy–Schwarz inequality, yields

$$c_2^{-1}\|\mathbf{r}_h\|_{0,e}^2 \leq \|\psi_e \mathbf{L}(\mathbf{r}_h)\|_{0,\omega_e} \|\underline{\mathbf{curl}}(\boldsymbol{\zeta}_h)\|_{0,\omega_e} + \|\underline{\mathbf{curl}}(\psi_e \mathbf{L}(\mathbf{r}_h))\|_{0,\omega_e} \|\boldsymbol{\zeta} - \boldsymbol{\zeta}_h\|_{0,\omega_e}.$$

Now, applying Lemma 4.9 to each element of ω_e, and using the fact that $h_{T_e}^{-1} \leq h_e^{-1}$, it follows the existence of a constant $\widetilde{c}_6 > 0$ that depends only on c_6 (see (4.32)) such that

$$\|\underline{\mathbf{curl}}(\boldsymbol{\zeta}_h)\|_{0,\omega_e} \leq \widetilde{c}_6\, h_e^{-1}\, \|\boldsymbol{\zeta} - \boldsymbol{\zeta}_h\|_{0,\omega_e}. \tag{4.34}$$

On the other hand, from inverse estimate (4.30) applied to each element of ω_e, there exists a constant $\widetilde{c}_4 > 0$ that depends only on c_4 (see (4.30)) such that

$$\|\underline{\mathbf{curl}}(\psi_e \mathbf{L}(\mathbf{r}_h))\|_{0,\omega_e} \leq \widetilde{c}_4\, h_e^{-1} \|\psi_e \mathbf{L}(\mathbf{r}_h)\|_{0,\omega_e}, \tag{4.35}$$

whereas employing (4.29) and the fact that $0 \leq \psi_e \leq 1$, we deduce that

$$\|\psi_e \mathbf{L}(\mathbf{r}_h)\|_{0,\omega_e} \leq c_3^{1/2}\, h_e^{1/2} \|\mathbf{r}_h\|_{0,e}. \tag{4.36}$$

Finally (4.33) follows easily from (4.34)–(4.36), with $c_7 := c_2 c_3^{1/2} \max\{\widetilde{c}_4, \widetilde{c}_6\}$. □

We now apply Lemmas 4.9 and 4.10 to bound the other two terms defining θ_T^2. For this purpose, we define for each $T \in \mathcal{T}_h$ the tensors

$$\boldsymbol{\zeta}_h := \frac{1}{\mu}\left\{\boldsymbol{\rho}_h - \frac{\lambda + \mu}{3\lambda + 4\mu}\, \mathrm{tr}(\boldsymbol{\rho}_h)\, \mathbb{I}\right\} + c_{\mathbf{g}}\, \mathbb{I} \quad \text{in } T \tag{4.37}$$

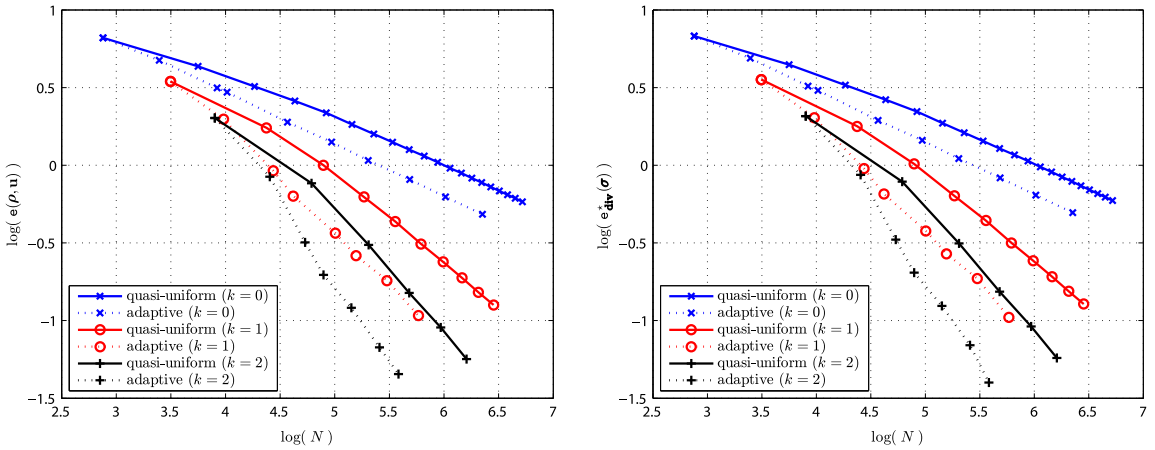

Fig. 5.1. Example 2, $\mathbf{e}(\boldsymbol{\rho}, \mathbf{u})$ vs. N (left) and $\mathbf{e}^{\star}_{\mathbf{div}}(\boldsymbol{\sigma})$ vs. N (right).

and

$$\boldsymbol{\zeta} := \frac{1}{\mu}\left\{\boldsymbol{\rho} - \frac{\lambda+\mu}{3\lambda+4\mu}\,\mathrm{tr}(\boldsymbol{\rho})\,\mathbb{I}\right\} + c_{\mathbf{g}}\,\mathbb{I} \quad \text{in } T, \tag{4.38}$$

then, using the triangle inequality, the fact that $\frac{\lambda+\mu}{3\lambda+4\mu} < 1$, and the continuity of $\boldsymbol{\tau} \mapsto \mathrm{tr}(\boldsymbol{\tau})$, we readily deduce that

$$\|\boldsymbol{\zeta} - \boldsymbol{\zeta}_h\|_{0,T} \leq \frac{4}{\mu}\|\boldsymbol{\rho} - \boldsymbol{\rho}_h\|_{0,T} \quad \forall\, T \in \mathcal{T}_h. \tag{4.39}$$

Lemma 4.11. *There exist $C_1, C_2 > 0$, independent of h and λ, such that*

$$h_T^2 \left\| \underline{\mathbf{curl}}\left(\frac{1}{\mu}\left\{\boldsymbol{\rho}_h - \frac{\lambda+\mu}{3\lambda+4\mu}\,\mathrm{tr}(\boldsymbol{\rho}_h)\,\mathbb{I}\right\}\right)\right\|^2_{0,T} \leq C_1\,\|\boldsymbol{\rho} - \boldsymbol{\rho}_h\|^2_{0,T} \quad \forall\, T \in \mathcal{T}_h \tag{4.40}$$

and

$$h_e \left\| \left[\left[\left(\frac{1}{\mu}\left\{\boldsymbol{\rho}_h - \frac{\lambda+\mu}{3\lambda+4\mu}\,\mathrm{tr}(\boldsymbol{\rho}_h)\,\mathbb{I}\right\} + c_{\mathbf{g}}\,\mathbb{I}\right) \times \mathbf{n}\right]\right] \right\|^2_{0,e} \leq C_2\,\|\boldsymbol{\rho} - \boldsymbol{\rho}_h\|^2_{0,\omega_e} \quad \forall\, e \in \mathcal{E}_h(\Omega). \tag{4.41}$$

Proof. We begin by applying Lemma 4.9 to the tensors (4.37) and (4.38), and then using (4.39), we obtain (4.40) with $C_1 := \frac{16}{\mu^2}c_6$. Analogously, applying Lemma 4.10 to the tensors (4.37) and (4.38), and then using (4.39), we obtain (4.41) with $C_2 := \frac{16}{\mu^2}c_7$. □

The remaining three terms are bounded next. For this purpose, we will apply Lemmas 4.6–4.8.

Lemma 4.12. *There exists $C_3 > 0$, independent of h and λ, such that for each $T \in \mathcal{T}_h$*

$$h_T^2 \left\| \nabla \mathbf{u}_h - \left(\frac{1}{\mu}\left\{\boldsymbol{\rho}_h - \frac{\lambda+\mu}{3\lambda+4\mu}\,\mathrm{tr}(\boldsymbol{\rho}_h)\,\mathbb{I}\right\} + c_{\mathbf{g}}\,\mathbb{I}\right)\right\|^2_{0,T} \leq C_3\,\left\{\|\mathbf{u} - \mathbf{u}_h\|^2_{0,T} + h_T^2\,\|\boldsymbol{\rho} - \boldsymbol{\rho}_h\|^2_{0,T}\right\}. \tag{4.42}$$

Proof. We adapt the proof of [46, Lemma 4.13]. In fact, given $T \in \mathcal{T}_h$, we denote $\boldsymbol{\chi}_T := \nabla \mathbf{u}_h - \boldsymbol{\zeta}_h$ in T, where $\boldsymbol{\zeta}_h$ is given by (4.37). Then, applying (4.27), using that $\nabla \mathbf{u} = \boldsymbol{\zeta}$ in Ω, where $\boldsymbol{\zeta}$ is given by (4.38), and integrating by parts, we find that

$$\begin{aligned}
\|\boldsymbol{\chi}_T\|^2_{0,T} &\leq c_1\,\|\psi_T^{1/2}\,\boldsymbol{\chi}_T\|^2_{0,T} = c_1 \int_T \psi_T\,\boldsymbol{\chi}_T : \left(\nabla \mathbf{u}_h - \boldsymbol{\zeta}_h\right) \\
&= c_1 \int_T \psi_T\,\boldsymbol{\chi}_T : \left\{\nabla(\mathbf{u}_h - \mathbf{u}) + (\boldsymbol{\zeta} - \boldsymbol{\zeta}_h)\right\} \\
&= c_1 \left\{\int_T \mathbf{div}(\psi_T\,\boldsymbol{\chi}_T)\cdot(\mathbf{u} - \mathbf{u}_h) + \int_T \psi_T\,\boldsymbol{\chi}_T : \left(\boldsymbol{\zeta} - \boldsymbol{\zeta}_h\right)\right\}.
\end{aligned}$$

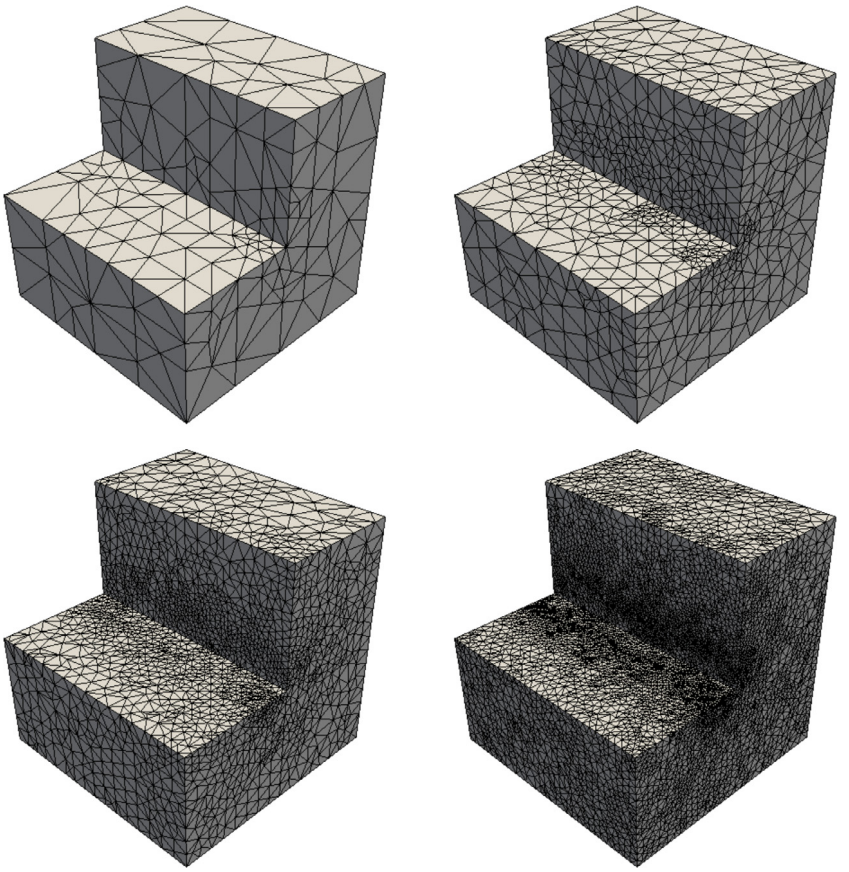

Fig. 5.2. Example 2, adapted meshes for $k = 0$ with 10 348, 93 637, 485 527, and 2 251 543 degrees of freedom.

Then, applying the Cauchy–Schwarz inequality, the inverse estimate (4.30), the fact that $0 \leq \psi_T \leq 1$, and the estimate (4.39), we get

$$\|\boldsymbol{\chi}_T\|_{0,T}^2 \leq c_1 \left\{ (3\bar{c}_4)^{1/2} h_T^{-1} \|\mathbf{u} - \mathbf{u}_h\|_{0,T} + \frac{4}{\mu} \|\boldsymbol{\rho} - \boldsymbol{\rho}_h\|_{0,T} \right\} \|\boldsymbol{\chi}_T\|_{0,T},$$

where $\bar{c}_4$ is a constant that depends only on c_4 (see (4.30)). Hence,

$$h_T^2 \|\boldsymbol{\chi}_T\|_{0,T} \leq C_3 \left\{ \|\mathbf{u} - \mathbf{u}_h\|_{0,T}^2 + h_T^2 \|\boldsymbol{\rho} - \boldsymbol{\rho}_h\|_{0,T}^2 \right\},$$

where $C_3 := c_1^2 \left(\frac{4\sqrt{3\bar{c}_4}}{\mu} + \max\left\{ 3\bar{c}_4, \frac{16}{\mu^2} \right\} \right)$ is independent of h and λ, which completes the proof. □

Lemma 4.13. *Assume that* $\mathbf{g}$ *is piecewise polynomial. Then, there exists* $C_4 > 0$*, independent of* h *and* λ*, such that for each* $e \in \mathcal{E}_h(\Gamma)$ *there holds*

$$h_e \left\| \left(\nabla \mathbf{g} - \frac{1}{\mu} \left\{ \boldsymbol{\rho}_h - \frac{\lambda + \mu}{3\lambda + 4\mu} \operatorname{tr}(\boldsymbol{\rho}_h) \mathbb{I} \right\} - c_{\mathbf{g}} \mathbb{I} \right) \times \mathbf{n} \right\|_{0,e}^2 \leq C_4 \|\boldsymbol{\rho} - \boldsymbol{\rho}_h\|_{0,T_e}^2, \tag{4.43}$$

where T_e *is the tetrahedron of* $\mathcal{T}_h$ *having* e *as a face.*

Proof. Given $e \in \mathcal{E}_h(\Gamma)$ we denote $\boldsymbol{\chi}_e := (\nabla \mathbf{g} - \boldsymbol{\zeta}_h) \times \mathbf{n}$ on e. Then, applying (4.28) and the extension operator $\mathbf{L} : \mathbf{C}(e) \to \mathbf{C}(T)$, we obtain that

$$\begin{aligned} \|\boldsymbol{\chi}_e\|_{0,e}^2 &\leq c_2 \|\psi_e^{1/2} \boldsymbol{\chi}_e\|_{0,e}^2 = c_2 \int_e \psi_e \, \boldsymbol{\chi}_e : \left\{ (\nabla \mathbf{g} - \boldsymbol{\zeta}_h) \times \mathbf{n} \right\} \\ &= c_2 \int_{\partial T_e} \psi_e \, \mathbf{L}(\boldsymbol{\chi}_e) : \left\{ (\nabla \mathbf{u} - \boldsymbol{\zeta}_h) \times \mathbf{n} \right\}. \end{aligned}$$

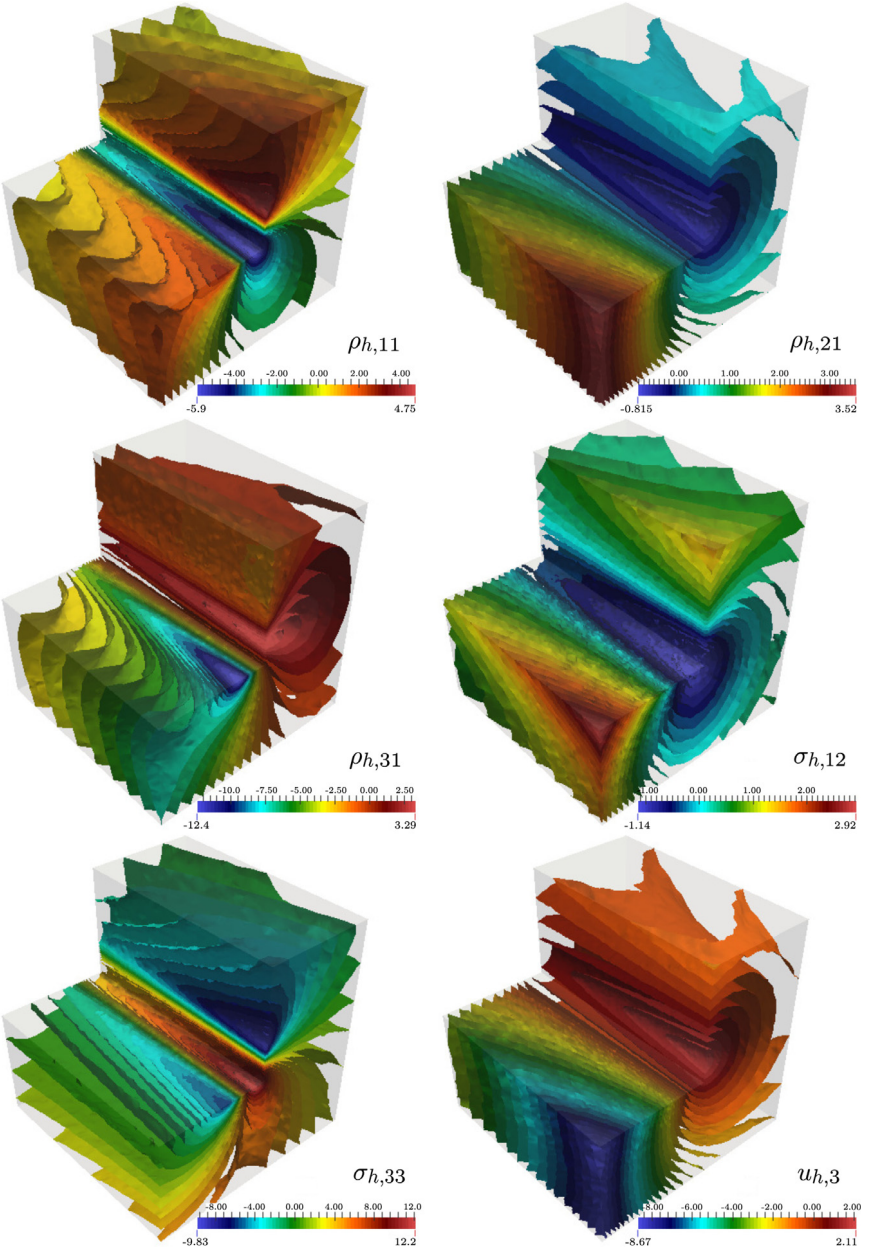

Fig. 5.3. Example 2, iso-surfaces of some components of the approximate solutions ($k = 0$ and $N = 2\,251\,543$) for adaptive scheme.

Now, integrating by parts, and using that $\nabla \mathbf{u} = \boldsymbol{\zeta}$ in T_e, we find that

$$\int_{\partial T_e} \psi_e \, \mathbf{L}(\boldsymbol{\chi}_e) : \{(\nabla \mathbf{u} - \boldsymbol{\zeta}_h) \times \mathbf{n}\} = \int_{T_e} (\boldsymbol{\zeta} - \boldsymbol{\zeta}_h) : \underline{\mathbf{curl}}(\psi_e \, \mathbf{L}(\boldsymbol{\chi}_e)) + \int_{T_e} \underline{\mathbf{curl}}(\boldsymbol{\zeta}_h) : \psi_e \, \mathbf{L}(\boldsymbol{\chi}_e).$$

Then, applying the Cauchy–Schwarz inequality, the inverse estimate (4.30) and Lemma 4.9, we deduce that

$$\|\boldsymbol{\chi}_e\|_{0,e}^2 \leq c_2(c_4 + c_6)\, h_{T_e}^{-1} \, \|\boldsymbol{\zeta} - \boldsymbol{\zeta}_h\|_{0,T_e} \|\psi_e \mathbf{L}(\boldsymbol{\chi}_e)\|_{0,T_e}.$$

In turn, recalling that $0 \leq \psi_e \leq 1$ and using (4.29), we can write

$$\|\psi_e \mathbf{L}(\boldsymbol{\chi}_e)\|_{0,T_e} \leq \|\psi_e^{1/2} \mathbf{L}(\boldsymbol{\chi}_e)\|_{0,T_e} \leq c_3^{1/2} \, h_e^{1/2} \|\boldsymbol{\chi}_e\|_{0,T_e},$$

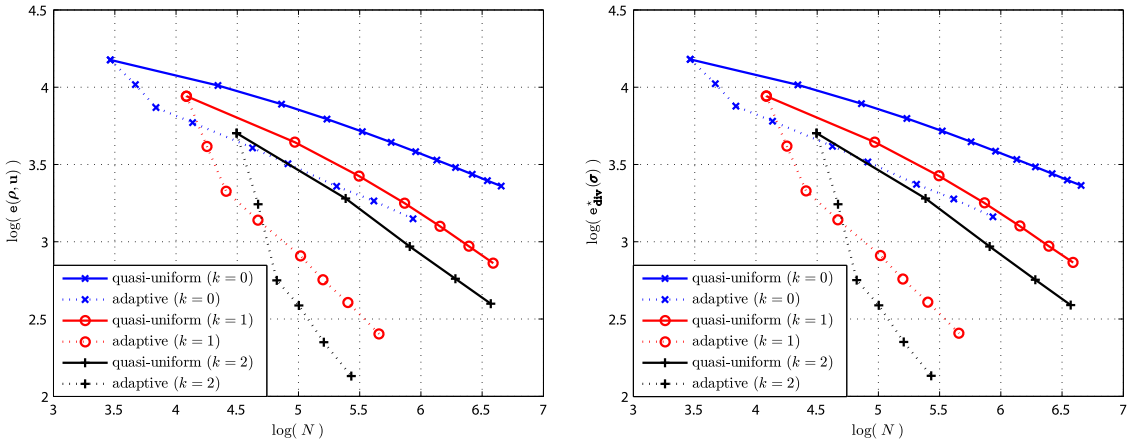

Fig. 5.4. Example 3, $\mathrm{e}(\boldsymbol{\rho}, \mathbf{u})$ vs. N (left) and $\mathrm{e}^{\star}_{\mathbf{div}}(\boldsymbol{\sigma})$ vs. N (right).

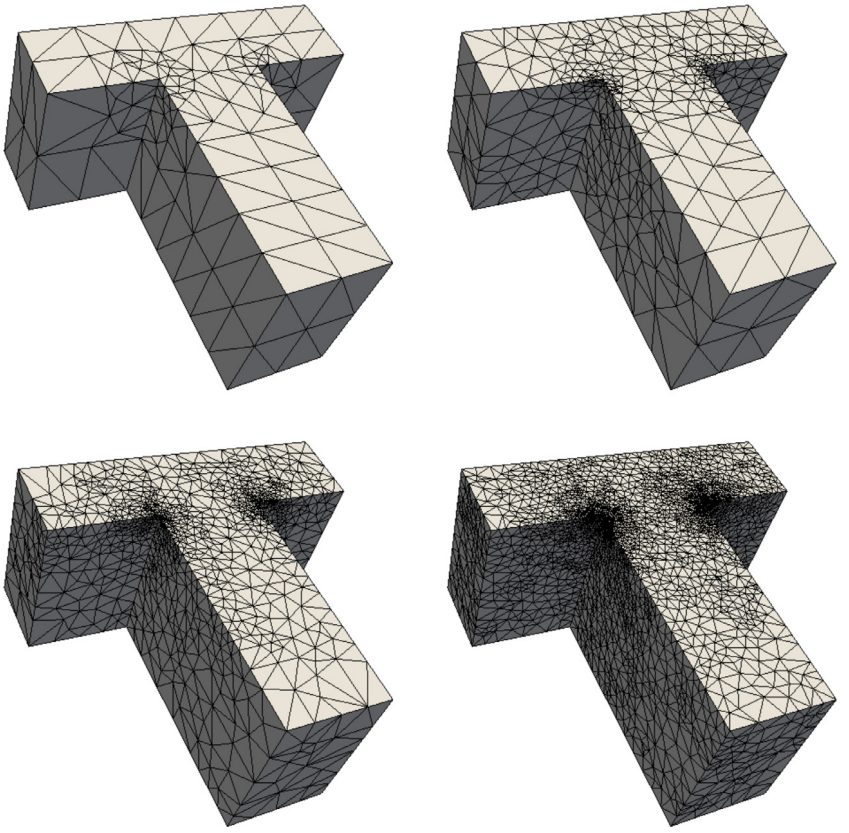

Fig. 5.5. Example 3, adapted meshes for $k = 0$ with 6868, 42 169, 204 958, and 861 778 degrees of freedom.

which, combined with the foregoing inequality, the fact that $h_e \leq h_{T_e}$, and the estimate (4.39), yield

$$h_e \, \|\boldsymbol{\chi}_e\|^2_{0,e} \leq \frac{16}{\mu^2} c_2^2 c_3 (c_4 + c_6)^2 \, \|\boldsymbol{\rho} - \boldsymbol{\rho}_h\|^2_{0,T_e}.$$

This completes the proof of (4.43) with $C_4 := \frac{16}{\mu^2} c_2^2 c_3 (c_4 + c_6)^2$. □

We remark here that if $\mathbf{g}$ were not piecewise polynomial but sufficiently smooth, then higher order terms given by the errors arising from suitable polynomial approximations would appear in (4.4). This explains the eventual expression *h.o.t.* in (4.4).

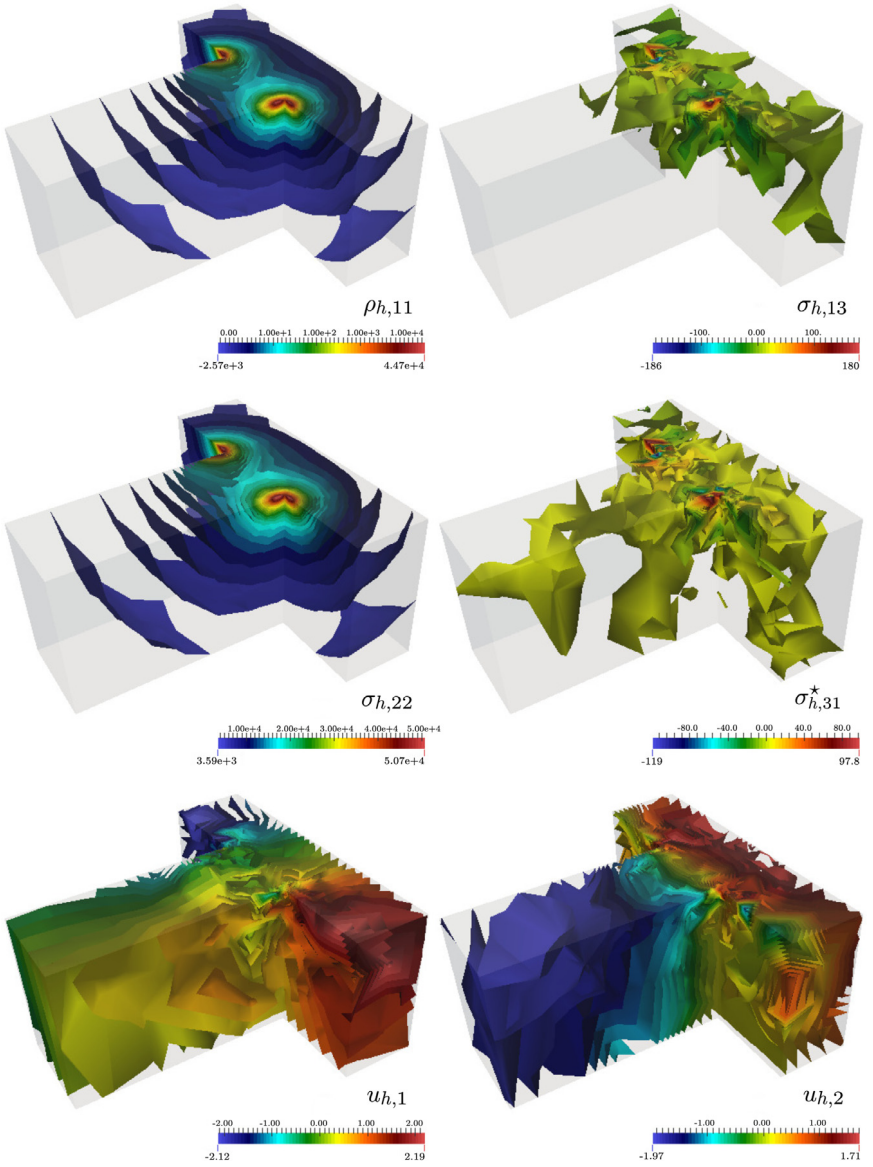

Fig. 5.6. Example 3, iso-surfaces of some components of the approximate solutions ($k = 2$ and $N = 270\,037$) for adaptive scheme.

Lemma 4.14. *There exists $C_5 > 0$, independent of h and λ, such that for each $e \in \mathcal{E}_h(\Gamma)$ there holds*

$$h_e \, \|\mathbf{g} - \mathbf{u}_h\|^2_{0,e} \leq C_5 \, \left\{ \|\mathbf{u} - \mathbf{u}_h\|^2_{0,T_e} + h^2_{T_e} \, \|\boldsymbol{\rho} - \boldsymbol{\rho}_h\|^2_{0,T_e} \right\}, \tag{4.44}$$

where T_e is the tetrahedron of $\mathcal{T}_h$ having e as a face.

Proof. We adapt the proof of [11, Lemma 4.14]. Indeed, applying the discrete trace inequality given by (4.31) of Lemma 4.8, together with the fact that $\mathbf{u} = \mathbf{g}$ on Γ and $\nabla \mathbf{u} = \boldsymbol{\zeta}$ in Ω, we easily obtain that for each $e \in \mathcal{E}_h(\Gamma)$ there holds

$$\begin{aligned}
\|\mathbf{g} - \mathbf{u}_h\|^2_{0,e} &= \|\mathbf{u} - \mathbf{u}_h\|^2_{0,e} \leq c_5 \, \left\{ h_e^{-1} \|\mathbf{u} - \mathbf{u}_h\|^2_{0,T_e} + h_e |\mathbf{u} - \mathbf{u}_h|^2_{1,T_e} \right\} \\
&= c_5 \, \left\{ h_e^{-1} \|\mathbf{u} - \mathbf{u}_h\|^2_{0,T_e} + h_e \|\nabla \mathbf{u} - \nabla \mathbf{u}_h\|^2_{0,T_e} \right\} \\
&= c_5 \, \left\{ h_e^{-1} \|\mathbf{u} - \mathbf{u}_h\|^2_{0,T_e} + h_e \|\boldsymbol{\zeta} - \boldsymbol{\zeta}_h + \boldsymbol{\zeta}_h - \nabla \mathbf{u}_h\|^2_{0,T_e} \right\} \\
&\leq c_5 \, \left\{ h_e^{-1} \|\mathbf{u} - \mathbf{u}_h\|^2_{0,T_e} + 2h_e \left\{ \|\boldsymbol{\zeta} - \boldsymbol{\zeta}_h\|^2_{0,T_e} + \|\nabla \mathbf{u}_h - \boldsymbol{\zeta}_h\|^2_{0,T_e} \right\} \right\},
\end{aligned}$$

which, using that $h_e \leq h_{T_e}$, gives

$$h_e \, \|\mathbf{g} - \mathbf{u}_h\|^2_{0,e} \leq c_5 \, \left\{ \|\mathbf{u} - \mathbf{u}_h\|^2_{0,T_e} + 2h^2_{T_e} \left\{ \|\boldsymbol{\zeta} - \boldsymbol{\zeta}_h\|^2_{0,T_e} + \|\nabla \mathbf{u}_h - \boldsymbol{\zeta}_h\|^2_{0,T_e} \right\} \right\}.$$

This estimate, the upper bound given by (4.39), and Lemma 4.12 yield (4.44) with $C_5 := c_5\,(2C_3 + \max\{1, \frac{32}{\mu}\})$. □

Finally, the efficiency of $\boldsymbol{\theta}$ follows straightforwardly from the estimate (4.26), together with Lemmas 4.11 throughout 4.14, after summing up over $T \in \mathcal{T}_h$ and using that the number of tetrahedra on each domain ω_e is bounded by two.

5. Numerical results

In this section, we present some numerical results in $\mathbf{R}^3$ illustrating the performance of the mixed finite element scheme (3.3), confirming the reliability and efficiency of the a posteriori error estimator $\boldsymbol{\theta}$ (cf. (4.3)) analysed in Section 4, and showing the behaviour of the associated adaptive algorithm. In all the computations we consider the specific finite element subspaces $\mathbb{H}_{0,h}$ and $\mathbf{Q}_h$ given by (3.2) with $k \in \{0, 1, 2\}$. In addition, similarly as in [15,12], the zero integral mean condition for tensors in the space $\mathbb{H}_{0,h}$ is imposed via a real Lagrange multiplier, which actually means that, instead of (3.3), we solve the modified discrete scheme given by: Find $(\boldsymbol{\rho}_h, (\mathbf{u}_h, \xi_h)) \in \mathbb{H}_h \times (\mathbf{Q}_h \times \mathbf{R})$ such that

$$\begin{aligned} a(\boldsymbol{\rho}_h, \boldsymbol{\tau}_h) + b(\boldsymbol{\tau}_h, \mathbf{u}_h) + \xi_h \int_\Omega \mathrm{tr}(\boldsymbol{\tau}_h) &= \langle \boldsymbol{\tau}_h \mathbf{n}, \mathbf{g} \rangle_\Gamma \quad \forall\, \boldsymbol{\tau}_h \in \mathbb{H}_h, \\ b(\boldsymbol{\rho}_h, \mathbf{v}_h) + \eta_h \int_\Omega \mathrm{tr}(\boldsymbol{\rho}_h) &= -\int_\Omega \mathbf{f} \cdot \mathbf{v}_h \quad \forall\, (\mathbf{v}_h, \eta_h) \in \mathbf{Q}_h \times \mathbf{R}. \end{aligned} \tag{5.1}$$

Notice that ξ_h, known in advance to be equal to $c_{\mathbf{g}}$ (cf. (4.2)), which arises after taking $\boldsymbol{\tau}_h = \mathbb{I}$ and $(\mathbf{v}_h, \eta_h) = (0, 1)$ in (5.1), is an artificial unknown introduced here just to keep the symmetry of (5.1).

We begin by introducing additional notations. In what follows N stands for the total number of degrees of freedom (unknowns) of (3.3), which, as proved by (3.4) for $k = 0$ (see also [14, Section 4]), behaves asymptotically as 9 times the number of tetrahedra of each triangulation. This factor increases to 12.5 when we use the three-dimensional PEERS (see, e.g. [47, Definition 3.1]). In order to confirm the above factor and those indicated for $k = 1$ and $k = 2$ right after (3.4), in all the numerical tables to be displayed below we include a column with the ratio N/m, where m is the number of tetrahedra of each triangulation. In turn, the individual and total errors of the unknowns pseudostress $\boldsymbol{\rho}$ and displacement $\mathbf{u}$ are given by

$$\mathtt{e}(\boldsymbol{\rho}) := \|\boldsymbol{\rho} - \boldsymbol{\rho}_h\|_{\mathbf{div};\Omega}, \qquad \mathtt{e}(\mathbf{u}) := \|\mathbf{u} - \mathbf{u}_h\|_{0,\Omega}, \quad \text{and} \quad \mathtt{e}(\boldsymbol{\rho}, \mathbf{u}) := \Big\{[\mathtt{e}(\boldsymbol{\rho})]^2 + [\mathtt{e}(\mathbf{u})]^2\Big\}^{1/2},$$

whereas the effectivity index with respect to $\boldsymbol{\theta}$ is defined by

$$\mathtt{eff}(\boldsymbol{\theta}) := \mathtt{e}(\boldsymbol{\rho}, \mathbf{u})/\boldsymbol{\theta}.$$

Then, we define the experimental rates of convergence

$$\mathtt{r}(\boldsymbol{\rho}) := \frac{\log(\mathtt{e}(\boldsymbol{\rho})/\mathtt{e}'(\boldsymbol{\rho}))}{\log(h/h')}, \qquad \mathtt{r}(\mathbf{u}) := \frac{\log(\mathtt{e}(\mathbf{u})/\mathtt{e}'(\mathbf{u}))}{\log(h/h')}, \quad \text{and} \quad \mathtt{r}(\boldsymbol{\rho}, \mathbf{u}) := \frac{\log(\mathtt{e}(\boldsymbol{\rho}, \mathbf{u})/\mathtt{e}'(\boldsymbol{\rho}, \mathbf{u}))}{\log(h/h')},$$

where $\mathtt{e}$ and $\mathtt{e}'$ denote the corresponding errors at two consecutive triangulations with mesh sizes h and h', respectively. However, when the adaptive algorithm is applied (see details below), the expression $\log(h/h')$ appearing in the computation of the above rates is replaced by $-\frac{1}{2}\log(N/N')$, where N and N', denote the corresponding degrees of freedom of each triangulation. In addition, we also define

$$\mathtt{e}_0(\boldsymbol{\sigma}) := \|\boldsymbol{\sigma} - \boldsymbol{\sigma}_h\|_{0,\Omega}, \qquad \mathtt{e}_{\mathbf{div}}(\boldsymbol{\sigma}) := \left\{\sum_{T \in \mathcal{T}_h} \|\boldsymbol{\sigma} - \boldsymbol{\sigma}_h\|^2_{\mathbf{div};T}\right\}^{1/2},$$

$$\mathtt{e}^\star_0(\boldsymbol{\sigma}) := \|\boldsymbol{\sigma} - \boldsymbol{\sigma}^\star_h\|_{0,\Omega}, \quad \text{and} \quad \mathtt{e}^\star_{\mathbf{div}}(\boldsymbol{\sigma}) := \left\{\sum_{T \in \mathcal{T}_h} \|\boldsymbol{\sigma} - \boldsymbol{\sigma}^\star_h\|^2_{\mathbf{div};T}\right\}^{1/2},$$

the corresponding errors of stress $\boldsymbol{\sigma}$. Hence, similarly as before, we also denote by $\mathtt{r}_0(\boldsymbol{\sigma})$, $\mathtt{r}_{\mathbf{div}}(\boldsymbol{\sigma})$, $\mathtt{r}^\star_0(\boldsymbol{\sigma})$ and $\mathtt{r}^\star_{\mathbf{div}}(\boldsymbol{\sigma})$, the experimental rates of convergence. Here, $\boldsymbol{\sigma}_h$ is the approximation given by the postprocessing formula (3.5), whereas $\boldsymbol{\sigma}^\star_h$ is introduced in (3.16).

Next, we recall that given the Young modulus E and the Poisson ratio ν of an isotropic linear elastic solid, the corresponding Lamé parameters are defined as

$$\mu := \frac{E}{2(1+\nu)} \quad \text{and} \quad \lambda := \frac{E\nu}{(1+\nu)(1-2\nu)}.$$

Table 5.1
Example 1, quasi-uniform scheme.

k	h	N	N/m	$\mathtt{e}(\boldsymbol{\rho})$	$\mathtt{r}(\boldsymbol{\rho})$	$\mathtt{e}(\mathbf{u})$	$\mathtt{r}(\mathbf{u})$	$\mathtt{e}(\boldsymbol{\rho},\mathbf{u})$	$\mathtt{r}(\boldsymbol{\rho},\mathbf{u})$	$\mathtt{eff}(\boldsymbol{\theta})$
0	0.4330	3745	9.753	8.89e+2	–	3.76e+1	–	8.90e+2	–	0.2035
	0.3464	7201	9.601	7.09e+2	1.01	2.61e+1	1.63	7.10e+2	1.01	0.1944
	0.2887	12313	9.501	5.89e+2	1.02	1.92e+1	1.69	5.89e+2	1.02	0.1878
	0.2474	19405	9.429	5.02e+2	1.03	1.47e+1	1.74	5.03e+2	1.03	0.1828
	0.2165	28801	9.375	4.38e+2	1.03	1.16e+1	1.77	4.38e+2	1.03	0.1790
	0.1925	40825	9.334	3.88e+2	1.03	9.39e−0	1.79	3.88e+2	1.03	0.1759
	0.1732	55801	9.300	3.48e+2	1.03	7.76e−0	1.81	3.48e+2	1.03	0.1735
	0.1575	74053	9.273	3.15e+2	1.03	6.52e−0	1.82	3.15e+2	1.03	0.1714
	0.1443	95905	9.250	2.88e+2	1.03	5.56e−0	1.83	2.88e+2	1.03	0.1697
	0.1332	121681	9.231	2.65e+2	1.03	4.80e−0	1.84	2.65e+2	1.03	0.1683
1	0.4330	15841	41.253	4.83e+1	–	1.12e−0	–	4.84e+1	–	0.0536
	0.3464	30601	40.801	3.09e+1	2.00	6.00e−1	2.80	3.09e+1	2.00	0.0523
	0.2887	52489	40.501	2.15e+1	2.00	3.59e−1	2.81	2.15e+1	2.00	0.0516
	0.2165	123265	40.125	1.21e+1	2.00	1.60e−1	2.81	1.21e+1	2.00	0.0506
	0.1925	174961	40.000	9.56e−0	2.00	1.15e−1	2.80	9.56e−0	2.00	0.0503
	0.1732	239401	39.900	7.74e−0	2.00	8.59e−2	2.78	7.74e−0	2.00	0.0501
	0.1575	317989	39.818	6.40e−0	2.00	6.60e−2	2.76	6.40e−0	2.00	0.0499
	0.1443	412129	39.750	5.38e−0	2.00	5.20e−2	2.74	5.38e−0	2.00	0.0497
	0.1332	523225	39.692	4.58e−0	2.00	4.19e−2	2.72	4.59e−0	2.00	0.0496
2	0.4330	40897	106.503	1.89e−0	–	3.17e−2	–	1.89e−0	–	0.0310
	0.3464	79201	105.601	9.68e−1	3.00	1.35e−2	3.81	9.68e−1	3.00	0.0304
	0.2887	136081	105.001	5.60e−1	3.00	6.77e−3	3.79	5.60e−1	3.00	0.0300
	0.2165	320257	104.250	2.36e−1	2.99	2.31e−3	3.72	2.37e−1	2.99	0.0296
	0.1925	454897	104.000	1.67e−1	2.98	1.49e−3	3.69	1.67e−1	2.98	0.0296
	0.1732	622801	103.800	1.22e−1	2.95	1.02e−3	3.64	1.22e−1	2.95	0.0296
	0.1575	827641	103.636	9.19e−2	2.98	7.20e−4	3.64	9.19e−2	2.98	0.0296
	0.1443	1073089	103.500	7.09e−2	2.98	5.25e−4	3.63	7.09e−2	2.98	0.0293
	0.1332	1362817	103.385	5.57e−2	3.01	3.93e−4	3.61	5.57e−2	3.01	0.0293

Table 5.2
Example 1, quasi-uniform scheme for the postprocessed unknowns: $\boldsymbol{\sigma}_h$ and $\boldsymbol{\sigma}_h^\star$.

k	h	N	$\mathtt{e}_0(\boldsymbol{\sigma})$	$\mathtt{r}_0(\boldsymbol{\sigma})$	$\mathtt{e}_{\mathbf{div}}(\boldsymbol{\sigma})$	$\mathtt{r}_{\mathbf{div}}(\boldsymbol{\sigma})$	$\mathtt{e}_0^\star(\boldsymbol{\sigma})$	$\mathtt{r}_0^\star(\boldsymbol{\sigma})$	$\mathtt{e}_{\mathbf{div}}^\star(\boldsymbol{\sigma})$	$\mathtt{r}_{\mathbf{div}}^\star(\boldsymbol{\sigma})$
0	0.4330	3745	6.44e+2	–	1.80e+3	–	6.08e+2	–	9.34e+2	–
	0.3464	7201	5.22e+2	0.94	1.71e+3	0.23	4.93e+2	0.94	7.52e+2	0.97
	0.2887	12313	4.37e+2	0.97	1.66e+3	0.17	4.13e+2	0.97	6.28e+2	0.99
	0.2165	28801	3.29e+2	1.00	1.60e+3	0.10	3.11e+2	1.00	4.72e+2	1.00
	0.1732	55801	2.62e+2	1.01	1.58e+3	0.06	2.48e+2	1.01	3.77e+2	1.00
	0.1575	74053	2.38e+2	1.01	1.57e+3	0.05	2.25e+2	1.02	3.43e+2	1.01
	0.1443	95905	2.18e+2	1.02	1.56e+3	0.05	2.06e+2	1.02	3.14e+2	1.01
	0.1332	121681	2.01e+2	1.02	1.56e+3	0.04	1.90e+2	1.02	2.90e+2	1.01
1	0.4330	15841	3.47e+1	–	6.91e+2	–	3.04e+1	–	5.09e+1	–
	0.3464	30601	2.26e+1	1.92	5.63e+2	0.92	1.98e+1	1.93	3.27e+1	1.97
	0.2887	52489	1.59e+1	1.94	4.75e+2	0.93	1.39e+1	1.94	2.28e+1	1.98
	0.2165	123265	9.05e−0	1.95	3.62e+2	0.95	7.94e−0	1.95	1.29e+1	1.98
	0.1925	174961	7.19e−0	1.96	3.23e+2	0.95	6.31e−0	1.96	1.02e+1	1.98
	0.1575	317989	4.85e−0	1.96	2.67e+2	0.96	4.26e−0	1.96	6.86e−0	1.99
	0.1443	412129	4.09e−0	1.97	2.45e+2	0.97	3.59e−0	1.96	5.77e−0	1.99
	0.1332	523225	3.49e−0	1.97	2.27e+2	0.97	3.06e−0	1.97	4.93e−0	1.99
2	0.4330	40897	1.41e−0	–	4.87e+1	–	1.21e−0	–	1.99e−0	–
	0.3464	79201	7.31e−1	2.94	3.16e+1	1.93	6.28e−1	2.94	1.02e−0	2.98
	0.2887	136081	4.27e−1	2.95	2.22e+1	1.94	3.66e−1	2.95	5.93e−1	2.98
	0.2474	215209	2.71e−1	2.96	1.64e+1	1.95	2.32e−1	2.96	3.74e−1	2.99
	0.2165	320257	1.82e−1	2.96	1.27e+1	1.96	1.56e−1	2.96	2.51e−1	2.99
	0.1732	622801	9.40e−2	2.97	8.16e−0	1.97	8.06e−2	2.97	1.29e−1	2.99
	0.1575	827641	7.07e−2	2.98	6.76e−0	1.97	6.07e−2	2.98	9.69e−2	2.99
	0.1443	1073089	5.46e−2	2.98	5.69e−0	1.97	4.68e−2	2.99	7.47e−2	3.00
	0.1332	1362817	4.29e−2	2.99	4.85e−0	2.00	3.68e−2	2.99	5.88e−2	3.00

In the examples we fix $E = 1$ and take $\nu \in \{0.3000, 0.4900, 0.4999\}$, which gives the following values of μ and λ:

ν	μ	λ
0.3000	0.3846	0.5769
0.4900	0.3356	16.4430
0.4999	0.3333	1666.4444

Table 5.3
Example 2, quasi-uniform scheme.

k	h	N	N/m	$\mathtt{e}(\boldsymbol{\rho})$	$\mathtt{r}(\boldsymbol{\rho})$	$\mathtt{e}(\mathbf{u})$	$\mathtt{r}(\mathbf{u})$	$\mathtt{e}(\boldsymbol{\rho},\mathbf{u})$	$\mathtt{r}(\boldsymbol{\rho},\mathbf{u})$	$\mathtt{eff}(\boldsymbol{\theta})$
0	0.7500	757	10.514	6.58e−0	–	6.65e−1	–	6.62e−0	–	0.3313
	0.3750	5617	9.752	4.32e−0	0.61	3.34e−1	1.00	4.34e−0	0.61	0.3322
	0.2500	18469	9.501	3.20e−0	0.74	2.21e−1	1.01	3.21e−0	0.74	0.3304
	0.1875	43201	9.375	2.59e−0	0.75	1.66e−1	1.00	2.59e−0	0.75	0.3342
	0.1500	83701	9.300	2.17e−0	0.78	1.33e−1	1.00	2.17e−0	0.78	0.3386
	0.1250	143857	9.250	1.83e−0	0.94	1.11e−1	0.99	1.83e−0	0.94	0.3335
	0.1071	227557	9.214	1.59e−0	0.91	9.49e−2	1.00	1.59e−0	0.91	0.3326
	0.0938	338689	9.188	1.40e−0	0.92	8.30e−2	1.00	1.41e−0	0.92	0.3321
	0.0833	481141	9.167	1.26e−0	0.93	7.38e−2	1.00	1.26e−0	0.93	0.3316
	0.0750	658801	9.150	1.14e−0	0.90	6.64e−2	1.01	1.15e−0	0.90	0.3342
	0.0682	875557	9.136	1.04e−0	0.96	6.03e−2	1.00	1.05e−0	0.96	0.3337
	0.0625	1135297	9.125	9.57e−1	1.01	5.54e−2	0.99	9.58e−1	1.01	0.3304
	0.0577	1441909	9.115	8.89e−1	0.92	5.11e−2	1.01	8.91e−1	0.92	0.3326
	0.0536	1799281	9.107	8.24e−1	1.02	4.74e−2	0.99	8.26e−1	1.02	0.3298
	0.0500	2211301	9.100	7.73e−1	0.93	4.43e−2	1.01	7.75e−1	0.93	0.3318
	0.0469	2681857	9.094	7.24e−1	1.02	4.15e−2	0.99	7.25e−1	1.02	0.3293
	0.0441	3214837	9.088	6.82e−1	0.98	3.91e−2	1.00	6.83e−1	0.98	0.3291
	0.0417	3814129	9.083	6.45e−1	0.98	3.69e−2	1.00	6.46e−1	0.98	0.3289
	0.0395	4483621	9.079	6.11e−1	1.00	3.50e−2	1.00	6.12e−1	1.00	0.3280
	0.0375	5227201	9.075	5.81e−1	0.99	3.32e−2	1.00	5.82e−1	0.99	0.3272
1	0.7500	3133	43.514	3.46e−0	–	1.08e−1	–	3.46e−0	–	0.2256
	0.3750	23761	41.252	1.74e−0	0.99	3.59e−2	1.59	1.74e−0	0.99	0.2444
	0.2500	78733	40.501	1.00e−0	1.36	1.77e−2	1.75	1.00e−0	1.36	0.2365
	0.1875	184897	40.125	6.24e−1	1.65	1.03e−2	1.87	6.24e−1	1.65	0.2383
	0.1500	359101	39.900	4.34e−1	1.63	6.51e−3	2.06	4.34e−1	1.63	0.2507
	0.1250	618193	39.750	3.11e−1	1.82	4.67e−3	1.82	3.11e−1	1.82	0.2388
	0.1071	979021	39.643	2.39e−1	1.71	3.46e−3	1.96	2.39e−1	1.71	0.2353
	0.0938	1458433	39.563	1.88e−1	1.78	2.66e−3	1.96	1.88e−1	1.78	0.2359
	0.0833	2073277	39.500	1.52e−1	1.83	2.11e−3	1.97	1.52e−1	1.83	0.2374
	0.0750	2840401	39.450	1.26e−1	1.77	1.69e−3	2.09	1.26e−1	1.77	0.2418
2	0.7500	7993	111.014	2.01e−0	–	3.81e−2	–	2.01e−0	–	0.1693
	0.3750	61345	106.502	7.66e−1	1.40	9.87e−3	1.95	7.66e−1	1.40	0.1788
	0.2500	204121	105.001	3.07e−1	2.25	3.37e−3	2.65	3.07e−1	2.25	0.1643
	0.1875	480385	104.250	1.50e−1	2.48	1.44e−3	2.96	1.51e−1	2.48	0.1605
	0.1500	934201	103.800	9.02e−2	2.29	7.39e−4	2.98	9.02e−2	2.29	0.1783
	0.1250	1609633	103.500	5.65e−2	2.56	4.28e−4	2.99	5.65e−2	2.56	0.1734

The cases $\nu = 0.4900$ and $\nu = 0.4999$ correspond to materials showing nearly incompressible behaviour.

The numerical results presented below were obtained using a C^{++} code. In turn, the linear systems were solved using the Conjugate Gradient method as main solver, and the individual errors are computed on each tetrahedron using a Gaussian quadrature rule. For the adaptive mesh generation, we use the software TetGen developed in [48]. The three examples to be considered in this section are described next. Example 1 is employed to illustrate the performance of the mixed finite element scheme and to confirm the reliability and efficiency of the a posteriori error estimator. Then, Examples 2 and 3 are utilized to show the behaviour of the adaptive algorithm associated with $\boldsymbol{\theta}$, which apply the following procedure from [42]:

(1) Start with a coarse mesh $\mathcal{T}_h$.
(2) Solve the discrete problem (3.3) for the actual mesh $\mathcal{T}_h$.
(3) Compute θ_T for each tetrahedron $T \in \mathcal{T}_h$.
(4) Evaluate stopping criterion ($\boldsymbol{\theta} \leq$ given tolerance) and decide to finish or go to next step.
(5) Use *blue–green* procedure to refine each $T' \in \mathcal{T}_h$ whose indicator $\theta_{T'}$ satisfies

$$\theta_{T'} \geq \frac{1}{2} \max \{\theta_T : T \in \mathcal{T}_h\}.$$

(6) Define resulting mesh as actual mesh $\mathcal{T}_h$ and go to step 2.

We take the domain Ω either as the unit cube $]0, 1[^3$, the L-shaped domain

$$]-1/2, 1/2[\times]0, 1[\times]-1/2, 1/2[\backslash \Big( ]0, 1/2[\times]0, 1[\times]0, 1/2[\Big),$$

or the T-shaped domain

$$]-1, 1[\times]-1, 1[\times]0, 1[\backslash \Big( ]-1, -1/3[\times]-1, 1/2[\times]0, 1[\cup]1/3, 1[\times]-1, 1/2[\times]0, 1[\Big),$$

Table 5.4
Example 2, quasi-uniform scheme for the postprocessed unknowns: $\boldsymbol{\sigma}_h$ and $\boldsymbol{\sigma}_h^\star$.

k	h	N	$\mathrm{e}_0(\boldsymbol{\sigma})$	$\mathrm{r}_0(\boldsymbol{\sigma})$	$\mathrm{e}_{\mathbf{div}}(\boldsymbol{\sigma})$	$\mathrm{r}_{\mathbf{div}}(\boldsymbol{\sigma})$	$\mathrm{e}_0^\star(\boldsymbol{\sigma})$	$\mathrm{r}_0^\star(\boldsymbol{\sigma})$	$\mathrm{e}_{\mathbf{div}}^\star(\boldsymbol{\sigma})$	$\mathrm{r}_{\mathbf{div}}^\star(\boldsymbol{\sigma})$
0	0.7500	757	2.17e−0	–	7.16e−0	–	2.12e−0	–	6.78e−0	–
	0.3750	5 617	1.33e−0	0.71	5.06e−0	0.50	1.33e−0	0.67	4.44e−0	0.61
	0.2500	18 469	9.39e−1	0.86	4.12e−0	0.51	9.39e−1	0.86	3.28e−0	0.75
	0.1875	43 201	7.23e−1	0.91	3.65e−0	0.42	7.22e−1	0.91	2.64e−0	0.75
	0.1500	83 701	5.88e−1	0.93	3.36e−0	0.36	5.85e−1	0.94	2.21e−0	0.79
	0.1250	143 857	4.99e−1	0.90	3.15e−0	0.36	4.98e−1	0.89	1.86e−0	0.94
	0.1071	227 557	4.30e−1	0.96	3.02e−0	0.28	4.30e−1	0.96	1.62e−0	0.91
	0.0938	338 689	3.78e−1	0.97	2.93e−0	0.23	3.78e−1	0.97	1.43e−0	0.92
	0.0833	481 141	3.37e−1	0.97	2.86e−0	0.20	3.37e−1	0.97	1.28e−0	0.93
	0.0750	658 801	3.03e−1	1.00	2.81e−0	0.16	3.03e−1	1.01	1.17e−0	0.90
	0.0682	875 557	2.76e−1	0.98	2.77e−0	0.15	2.76e−1	0.98	1.06e−0	0.96
	0.0625	1 135 297	2.54e−1	0.96	2.74e−0	0.13	2.54e−1	0.95	9.75e−1	1.01
	0.0577	1 441 909	2.35e−1	1.01	2.72e−0	0.11	2.34e−1	1.02	9.06e−1	0.92
	0.0536	1 799 281	2.18e−1	0.97	2.70e−0	0.10	2.18e−1	0.95	8.40e−1	1.02
	0.0500	2 211 301	2.04e−1	1.01	2.68e−0	0.08	2.03e−1	1.02	7.88e−1	0.93
	0.0469	2 681 857	1.91e−1	0.97	2.67e−0	0.08	1.91e−1	0.96	7.38e−1	1.02
	0.0441	3 214 837	1.80e−1	0.99	2.66e−0	0.07	1.80e−1	0.99	6.95e−1	0.98
	0.0417	3 814 129	1.70e−1	0.99	2.65e−0	0.06	1.70e−1	0.99	6.57e−1	0.98
	0.0395	4 483 621	1.61e−1	1.00	2.64e−0	0.05	1.61e−1	1.00	6.23e−1	0.99
	0.0375	5 227 201	1.53e−1	1.00	2.64e−0	0.04	1.53e−1	1.00	5.92e−1	0.99
1	0.7500	3 133	1.02e−0	–	6.04e−0	–	1.04e−0	–	3.56e−0	–
	0.3750	23 761	4.42e−1	1.21	4.99e−0	0.28	4.57e−1	1.18	1.78e−0	1.00
	0.2500	78 733	2.36e−1	1.54	4.41e−0	0.30	2.45e−1	1.54	1.02e−0	1.37
	0.1875	184 897	1.42e−1	1.77	3.67e−0	0.64	1.47e−1	1.76	6.35e−1	1.65
	0.1500	359 101	9.53e−2	1.79	3.07e−0	0.80	9.84e−2	1.81	4.41e−1	1.63
	0.1250	618 193	6.90e−2	1.77	2.78e−0	0.55	7.16e−2	1.75	3.16e−1	1.82
	0.1071	979 021	5.18e−2	1.86	2.53e−0	0.60	5.38e−2	1.86	2.43e−1	1.71
	0.0938	1 458 433	4.03e−2	1.89	2.28e−0	0.80	4.18e−2	1.89	1.91e−1	1.78
	0.0833	2 073 277	3.22e−2	1.90	2.05e−0	0.89	3.34e−2	1.90	1.54e−1	1.84
	0.0750	2 840 401	2.63e−2	1.92	1.86e−0	0.91	2.72e−2	1.94	1.28e−1	1.77
2	0.7500	7 993	5.49e−1	–	5.00e−0	–	5.70e−1	–	2.07e−0	–
	0.3750	61 345	1.90e−1	1.53	3.58e−0	0.48	2.00e−1	1.51	7.84e−1	1.40
	0.2500	204 121	7.44e−2	2.32	2.40e−0	0.99	7.96e−2	2.27	3.14e−1	2.26
	0.1875	480 385	3.42e−2	2.70	1.60e−0	1.41	3.68e−2	2.68	1.53e−1	2.49
	0.1500	934 201	1.90e−2	2.64	1.05e−0	1.90	2.03e−2	2.67	9.17e−2	2.31
	0.1250	1 609 633	1.17e−2	2.67	7.38e−1	1.91	1.27e−2	2.56	5.74e−2	2.56

Table 5.5
Example 2, adaptive scheme.

k	h	N	N/m	$\mathrm{e}(\boldsymbol{\rho})$	$\mathrm{r}(\boldsymbol{\rho})$	$\mathrm{e}(\mathbf{u})$	$\mathrm{r}(\mathbf{u})$	$\mathrm{e}(\boldsymbol{\rho}, \mathbf{u})$	$\mathrm{r}(\boldsymbol{\rho}, \mathbf{u})$	$\mathtt{eff}(\boldsymbol{\theta})$
0	0.7500	757	10.514	6.58e−0	–	6.65e−1	–	6.62e−0	–	0.3313
	0.7500	2 473	9.892	4.72e−0	0.56	4.42e−1	0.69	4.74e−0	0.56	0.3334
	0.5000	8 380	9.534	3.13e−0	0.67	3.10e−1	0.58	3.15e−0	0.67	0.3193
	0.5000	10 348	9.529	2.94e−0	0.58	2.81e−1	0.96	2.96e−0	0.59	0.3231
	0.4146	36 898	9.337	1.89e−0	0.70	1.69e−1	0.80	1.89e−0	0.70	0.3139
	0.2864	93 637	9.254	1.40e−0	0.63	1.36e−1	0.46	1.41e−0	0.63	0.3100
	0.2795	202 747	9.213	1.07e−0	0.70	9.41e−2	0.96	1.07e−0	0.71	0.3092
	0.1768	485 527	9.147	8.05e−1	0.65	7.69e−2	0.46	8.09e−1	0.65	0.3094
	0.1768	1 033 678	9.123	6.23e−1	0.68	5.50e−2	0.89	6.25e−1	0.68	0.3080
	0.1250	2 251 543	9.094	4.81e−1	0.66	4.48e−2	0.53	4.83e−1	0.66	0.3082
1	0.7500	3 133	43.514	3.46e−0	–	1.08e−1	–	3.46e−0	–	0.2256
	0.7071	9 586	41.498	1.97e−0	1.01	7.00e−2	0.78	1.97e−0	1.01	0.2243
	0.5590	27 331	40.732	9.21e−1	1.45	3.51e−2	1.32	9.22e−1	1.45	0.2008
	0.5590	41 794	40.656	6.34e−1	1.76	2.62e−2	1.38	6.34e−1	1.76	0.1891
	0.5000	101 143	40.232	3.65e−1	1.25	1.58e−2	1.14	3.66e−1	1.25	0.1846
	0.3692	156 802	40.072	2.61e−1	1.53	1.21e−2	1.24	2.61e−1	1.53	0.1806
	0.3668	300 970	39.858	1.81e−1	1.13	7.31e−3	1.54	1.81e−1	1.13	0.1848
	0.2613	583 252	39.704	1.07e−1	1.58	4.16e−3	1.70	1.07e−1	1.58	0.1843
2	0.7500	7 993	111.014	2.01e−0	–	3.81e−2	–	2.01e−0	–	0.1693
	0.7071	25 447	106.920	8.44e−1	1.50	1.44e−2	1.68	8.44e−1	1.50	0.1716
	0.7071	53 473	105.887	3.19e−1	2.62	7.52e−3	1.74	3.19e−1	2.62	0.1234
	0.7071	78 949	105.688	1.97e−1	2.48	6.06e−3	1.12	1.97e−1	2.48	0.1070
	0.4566	141 883	104.943	1.21e−1	1.66	2.37e−3	3.20	1.21e−1	1.66	0.1253
	0.4566	256 903	104.475	6.72e−2	1.98	1.75e−3	1.02	6.72e−2	1.98	0.1172
	0.3604	383 023	104.224	4.53e−2	1.98	1.10e−3	2.34	4.53e−2	1.98	0.1151

Table 5.6
Example 2, adaptive scheme for the postprocessed unknowns: $\boldsymbol{\sigma}_h$ and $\boldsymbol{\sigma}_h^\star$.

k	h	N	$\mathtt{e}_0(\boldsymbol{\sigma})$	$\mathtt{r}_0(\boldsymbol{\sigma})$	$\mathtt{e}_{\mathbf{div}}(\boldsymbol{\sigma})$	$\mathtt{r}_{\mathbf{div}}(\boldsymbol{\sigma})$	$\mathtt{e}_0^\star(\boldsymbol{\sigma})$	$\mathtt{r}_0^\star(\boldsymbol{\sigma})$	$\mathtt{e}_{\mathbf{div}}^\star(\boldsymbol{\sigma})$	$\mathtt{r}_{\mathbf{div}}^\star(\boldsymbol{\sigma})$
0	0.7500	757	2.17e−0	–	7.16e−0	–	2.12e−0	–	6.78e−0	–
	0.7500	2 473	1.61e−0	0.50	5.44e−0	0.46	1.63e−0	0.44	4.89e−0	0.55
	0.5000	8 380	1.05e−0	0.70	4.08e−0	0.47	1.07e−0	0.70	3.23e−0	0.68
	0.5000	10 348	9.63e−1	0.83	3.93e−0	0.35	9.74e−1	0.86	3.04e−0	0.60
	0.4146	36 898	6.30e−1	0.67	3.20e−0	0.32	6.35e−1	0.67	1.95e−0	0.70
	0.2864	93 637	4.61e−1	0.67	2.93e−0	0.19	4.66e−1	0.66	1.45e−0	0.64
	0.2795	202 747	3.59e−1	0.65	2.79e−0	0.13	3.62e−1	0.66	1.10e−0	0.70
	0.1768	485 527	2.63e−1	0.71	2.69e−0	0.08	2.66e−1	0.71	8.30e−1	0.66
	0.1768	1 033 678	2.07e−1	0.64	2.64e−0	0.05	2.09e−1	0.64	6.42e−1	0.68
	0.1250	2 251 543	1.58e−1	0.70	2.61e−0	0.03	1.59e−1	0.70	4.96e−1	0.67
1	0.7500	3 133	1.02e−0	–	6.04e−0	–	1.04e−0	–	3.56e−0	–
	0.7071	9 586	5.53e−1	1.09	5.47e−0	0.18	5.76e−1	1.05	2.03e−0	1.01
	0.5590	27 331	2.88e−1	1.25	4.13e−0	0.54	2.99e−1	1.25	9.52e−1	1.44
	0.5590	41 794	1.90e−1	1.96	3.81e−0	0.38	1.99e−1	1.92	6.53e−1	1.78
	0.5000	101 143	1.12e−1	1.20	2.92e−0	0.60	1.17e−1	1.20	3.77e−1	1.24
	0.3692	156 802	7.86e−2	1.62	2.53e−0	0.66	8.19e−2	1.62	2.69e−1	1.54
	0.3668	300 970	5.30e−2	1.21	2.10e−0	0.57	5.52e−2	1.21	1.86e−1	1.13
	0.2613	583 252	2.97e−2	1.75	1.66e−0	0.72	3.11e−2	1.74	1.05e−1	1.73
2	0.7500	7 993	5.49e−1	–	5.00e−0	–	5.70e−1	–	2.07e−0	–
	0.7071	25 447	2.26e−1	1.53	3.71e−0	0.52	2.41e−1	1.48	8.67e−1	1.50
	0.7071	53 473	1.07e−1	2.01	2.39e−0	1.18	1.15e−1	2.00	3.32e−1	2.58
	0.7071	78 949	6.15e−2	2.86	1.90e−0	1.18	6.61e−2	2.83	2.04e−1	2.51
	0.4566	141 883	3.30e−2	2.13	1.40e−0	1.05	3.54e−2	2.13	1.24e−1	1.69
	0.4566	256 903	1.98e−2	1.72	9.62e−1	1.26	1.83e−2	2.22	6.94e−2	1.96
	0.3604	383 023	1.39e−2	1.78	6.92e−1	1.65	1.04e−2	2.84	3.99e−2	2.77

and choose $\mathbf{f}$ and $\mathbf{g}$ so that the Poisson ratio ν and the exact solution $\mathbf{u}$ are given as follows:

Example	Ω	ν	$\mathbf{u}(x_1, x_2, x_3)$
1	Unit cube	0.4900	$(x_1^2+1)(x_2^2+1)(x_3^2+1)e^{x_1+x_2+x_3}\begin{pmatrix}1\\1\\1\end{pmatrix}$
2	L-shaped	0.3000	$\begin{pmatrix} e^{x_2}\,(x_3-0.1)\,(x_1+1)^2\,/\,r \\ e^{x_2}\,(x_1+1)^2\,r \\ -e^{x_2}\,(x_1+1)\,(150x_1^2+25x_1+100x_3^2-20x_3-3)\,/\,(50r)\end{pmatrix}$
3	T-shaped	0.4999	$\begin{pmatrix}(x_1+0.38)/r_1+(x_1-0.38)/r_2\\(x_2-0.45)(1/r_1+1/r_2)\\(x_3-1.05)(1/r_1+1/r_2)\end{pmatrix}$

where $r := \sqrt{(x_1-0.1)^2+(x_3-0.1)^2}$ in Example 2, whereas

$$r_1 := \sqrt{(x_1+0.38)^2+(x_2-0.45)^2+(x_3-1.05)^2}$$

and

$$r_2 := \sqrt{(x_1-0.38)^2+(x_2-0.45)^2+(x_3-1.05)^2}$$

in Example 3. Note that the solution of Example 2 is singular at $(0.1, x_2, 0.1)$, and then we should expect regions of high gradients around that line, which is the line in the middle corner of the L along x_2-axis. Similarly, the solution of Example 3 is singular at $(-0.38, 0.45, 1.05)$ and $(0.38, 0.45, 1.05)$, which are the middle corners of the T with respect the plane $x_3 = 1$.

In Tables 5.1 and 5.2, we summarize the convergence history of the mixed finite element scheme (3.3) as applied to Example 1, for a sequence of quasi-uniform triangulations (generated as in [14]) of the domain. We notice there that the rate of convergence $O(h^{k+1})$ predicted by Theorems 3.2 and 3.3 (when $s = k+1$) is attained by all the unknowns. In particular, these results confirm that our new postprocessed stress $\boldsymbol{\sigma}_h^*$ clearly improves in one power the non-satisfactory order provided by the first approximation $\boldsymbol{\sigma}_h$ with respect to the broken $\mathbb{H}(\mathbf{div})$-norm. In addition, as observed in the eighth column of Table 5.1, the convergence of $\mathtt{e}(\mathbf{u})$ is a bit faster than expected, which is a special behaviour of this particular solution $\mathbf{u}$, as it is also mentioned in [14]. We also remark the good behaviour of the a posteriori error estimator $\boldsymbol{\theta}$ in this case. More precisely, in Table 5.1, we see that the effectivity indices $\mathtt{eff}(\boldsymbol{\theta})$ remain always bounded above and below, which illustrates the reliability and efficiency result provided by Theorem 4.1.

Next, in Tables 5.3–5.10, we provide the convergence history of the quasi-uniform and adaptive schemes as applied to Examples 2 and 3. The stopping criterion in the adaptive refinements is $\boldsymbol{\theta} \leq 1.8\,(k=0)$, $\boldsymbol{\theta} \leq 0.6\,(k=1)$, and $\boldsymbol{\theta} \leq 0.4\,(k=2)$

Table 5.7
Example 3, quasi-uniform scheme.

k	h	N	N/m	$\mathtt{e}(\boldsymbol{\rho})$	$\mathtt{r}(\boldsymbol{\rho})$	$\mathtt{e}(\mathbf{u})$	$\mathtt{r}(\mathbf{u})$	$\mathtt{e}(\boldsymbol{\rho},\mathbf{u})$	$\mathtt{r}(\boldsymbol{\rho},\mathbf{u})$	$\mathtt{eff}(\boldsymbol{\theta})$
0	0.6509	2 905	10.087	1.50e+4	–	4.48e+2	–	1.50e+4	–	0.5604
	0.3254	21 985	9.542	1.03e+4	0.55	1.68e+2	1.42	1.03e+4	0.55	0.5755
	0.2170	72 793	9.361	7.77e+3	0.69	8.74e+1	1.61	7.77e+3	0.69	0.5801
	0.1627	170 881	9.271	6.22e+3	0.77	5.36e+1	1.70	6.22e+3	0.77	0.5803
	0.1302	331 801	9.217	5.16e+3	0.84	3.63e+1	1.75	5.16e+3	0.84	0.5774
	0.1085	571 105	9.181	4.40e+3	0.88	2.62e+1	1.77	4.40e+3	0.88	0.5739
	0.0930	904 345	9.155	3.82e+3	0.91	1.99e+1	1.81	3.82e+3	0.91	0.5697
	0.0814	1 347 073	9.135	3.38e+3	0.93	1.56e+1	1.82	3.38e+3	0.93	0.5662
	0.0723	1 914 841	9.120	3.02e+3	0.94	1.25e+1	1.84	3.02e+3	0.94	0.5632
	0.0651	2 623 201	9.108	2.73e+3	0.96	1.03e+1	1.86	2.73e+3	0.96	0.5601
	0.0592	3 487 705	9.098	2.49e+3	0.99	8.61e−0	1.88	2.49e+3	0.99	0.5569
	0.0542	4 523 905	9.090	2.29e+3	0.94	7.33e−0	1.86	2.29e+3	0.94	0.5550
1	0.6509	12 169	42.253	8.74e+3	–	6.18e+1	–	8.75e+3	–	0.4299
	0.3254	93 601	40.625	4.40e+3	0.99	1.37e+1	2.18	4.40e+3	0.99	0.5118
	0.2170	311 689	40.083	2.66e+3	1.24	5.27e−0	2.35	2.66e+3	1.24	0.5460
	0.1627	733 825	39.813	1.78e+3	1.40	2.56e−0	2.51	1.78e+3	1.40	0.5622
	0.1302	1 427 401	39.650	1.26e+3	1.54	1.44e−0	2.58	1.26e+3	1.54	0.5678
	0.1085	2 459 809	39.542	9.36e+2	1.64	8.81e−1	2.69	9.36e+2	1.64	0.5697
	0.0930	3 898 441	39.464	7.27e+2	1.63	5.99e−1	2.50	7.27e+2	1.63	0.5637
2	0.6509	31 249	108.503	5.04e+3	–	1.87e+1	–	5.04e+3	–	0.3386
	0.3254	242 497	105.250	1.90e+3	1.40	2.94e−0	2.67	1.90e+3	1.40	0.4172
	0.2170	810 001	104.167	9.31e+2	1.76	9.18e−1	2.87	9.31e+2	1.76	0.4647
	0.1627	1 910 017	103.625	5.76e+2	1.67	4.00e−1	2.89	5.76e+2	1.67	0.4643
	0.1302	3 718 801	103.300	3.97e+2	1.67	2.10e−1	2.88	3.97e+2	1.67	0.4651

Table 5.8
Example 3, quasi-uniform scheme for the postprocessed unknown: $\boldsymbol{\sigma}_h$ and $\boldsymbol{\sigma}_h^\star$.

k	h	N	$\mathtt{e}_0(\boldsymbol{\sigma})$	$\mathtt{r}_0(\boldsymbol{\sigma})$	$\mathtt{e}_{\mathbf{div}}(\boldsymbol{\sigma})$	$\mathtt{r}_{\mathbf{div}}(\boldsymbol{\sigma})$	$\mathtt{e}_0^\star(\boldsymbol{\sigma})$	$\mathtt{r}_0^\star(\boldsymbol{\sigma})$	$\mathtt{e}_{\mathbf{div}}^\star(\boldsymbol{\sigma})$	$\mathtt{r}_{\mathbf{div}}^\star(\boldsymbol{\sigma})$
0	0.6509	2 905	4.48e+3	–	1.58e+4	–	4.37e+3	–	1.51e+4	–
	0.3254	21 985	2.63e+3	0.77	1.15e+4	0.46	2.56e+3	0.77	1.03e+4	0.55
	0.2170	72 793	1.84e+3	0.87	9.40e+3	0.50	1.80e+3	0.87	7.83e+3	0.69
	0.1627	170 881	1.42e+3	0.91	8.20e+3	0.47	1.38e+3	0.91	6.27e+3	0.77
	0.1302	331 801	1.15e+3	0.93	7.45e+3	0.43	1.12e+3	0.93	5.20e+3	0.84
	0.1085	571 105	9.69e+2	0.95	6.96e+3	0.37	9.47e+2	0.94	4.44e+3	0.88
	0.0930	904 345	8.36e+2	0.96	6.62e+3	0.32	8.17e+2	0.96	3.86e+3	0.91
	0.0814	1 347 073	7.35e+2	0.97	6.38e+3	0.28	7.18e+2	0.97	3.41e+3	0.93
	0.0723	1 914 841	6.55e+2	0.97	6.21e+3	0.24	6.40e+2	0.97	3.05e+3	0.94
	0.0651	2 623 201	5.91e+2	0.98	6.08e+3	0.20	5.77e+2	0.98	2.76e+3	0.96
	0.0592	3 487 705	5.37e+2	1.00	5.97e+3	0.18	5.24e+2	1.00	2.51e+3	0.99
	0.0542	4 523 905	4.93e+2	0.97	5.90e+3	0.15	4.82e+2	0.97	2.31e+3	0.94
1	0.6509	12 169	1.29e+3	–	1.03e+4	–	1.22e+3	–	8.76e+3	–
	0.3254	93 601	5.41e+2	1.26	6.24e+3	0.72	5.13e+2	1.25	4.41e+3	0.99
	0.2170	311 689	2.99e+2	1.46	4.52e+3	0.80	2.84e+2	1.45	2.67e+3	1.24
	0.1627	733 825	1.89e+2	1.60	3.53e+3	0.86	1.80e+2	1.60	1.78e+3	1.40
	0.1302	1 427 401	1.30e+2	1.68	2.93e+3	0.83	1.23e+2	1.68	1.26e+3	1.54
	0.1085	2 459 809	9.40e+1	1.77	2.49e+3	0.89	8.95e+1	1.77	9.37e+2	1.64
	0.0930	3 898 441	7.24e+1	1.69	2.16e+3	0.95	6.91e+1	1.68	7.33e+2	1.59
2	0.6509	31 249	5.54e+2	–	6.79e+3	–	5.12e+2	–	5.04e+3	–
	0.3254	242 497	1.66e+2	1.74	3.39e+3	1.00	1.55e+2	1.73	1.91e+3	1.40
	0.2170	810 001	7.36e+1	2.01	2.07e+3	1.21	6.85e+1	2.01	9.32e+2	1.76
	0.1627	1 910 017	4.44e+1	1.75	1.35e+3	1.48	4.12e+1	1.76	5.67e+2	1.72
	0.1302	3 718 801	3.06e+1	1.68	9.56e+2	1.56	2.82e+1	1.70	3.89e+2	1.69

for Example 2, whereas $\boldsymbol{\theta} \leq 4000$ ($k = 0$), $\boldsymbol{\theta} \leq 1200$ ($k = 1$), and $\boldsymbol{\theta} \leq 900$ ($k = 2$) for Example 3. We observe here that the errors of the adaptive methods decrease faster than those obtained by the quasi-uniform ones. This fact is better illustrated in Figs. 5.1 and 5.4 where we display the errors $\mathtt{e}(\boldsymbol{\rho}, \mathbf{u})$ and $\mathtt{e}_{\mathbf{div}}^\star(\boldsymbol{\sigma})$ vs. the degrees of freedom N for both refinements. In addition, the effectivity indices remain also bounded from above and below, which confirms the reliability and efficiency of $\boldsymbol{\theta}$ for the associated adaptive algorithm as well. Some intermediate meshes obtained with this procedure are displayed in Figs. 5.2 and 5.5. Notice here that the adapted meshes concentrate the refinements around the line $(0, x_2, 0)$ in Example 2, and around the points $(-1/3, 1/2, 1)$ and $(1/3, 1/2, 1)$ in Example 3, which means that the method is able to recognize the regions with high gradients of the solutions. Finally, in Figs. 5.3 and 5.6, we display iso-surfaces for some components of the pseudostress $\boldsymbol{\rho}_h$, the displacement $\mathbf{u}_h$, and the stress tensor $\boldsymbol{\sigma}_h$ (or $\boldsymbol{\sigma}_h^\star$), for both examples.

Table 5.9
Example 3, adaptive scheme.

k	h	N	N/m	$\mathtt{e}(\boldsymbol{\rho})$	$\mathtt{r}(\boldsymbol{\rho})$	$\mathtt{e}(\mathbf{u})$	$\mathtt{r}(\mathbf{u})$	$\mathtt{e}(\boldsymbol{\rho},\mathbf{u})$	$\mathtt{r}(\boldsymbol{\rho},\mathbf{u})$	$\mathtt{eff}(\boldsymbol{\theta})$
0	0.6509	2 905	10.087	1.50e+4	–	4.48e+2	–	1.50e+4	–	0.5604
	0.6509	4 657	9.825	1.04e+4	1.56	3.37e+2	1.21	1.04e+4	1.56	0.4900
	0.6509	6 868	9.756	7.38e+3	1.76	2.85e+2	0.86	7.39e+3	1.76	0.4144
	0.6509	13 672	9.601	5.90e+3	0.65	1.82e+2	1.30	5.90e+3	0.65	0.4091
	0.6009	42 169	9.396	4.05e+3	0.67	9.05e+1	1.24	4.05e+3	0.67	0.3960
	0.4167	81 979	9.307	3.19e+3	0.71	5.77e+1	1.35	3.19e+3	0.71	0.3827
	0.3560	204 958	9.221	2.28e+3	0.73	3.47e+1	1.11	2.28e+3	0.73	0.3644
	0.3125	412 942	9.183	1.83e+3	0.62	2.10e+1	1.44	1.83e+3	0.62	0.3659
	0.2763	861 778	9.137	1.41e+3	0.72	1.33e+1	1.23	1.41e+3	0.72	0.3555
1	0.6509	12 169	42.253	8.74e+3	–	6.18e+1	–	8.75e+3	–	0.4299
	0.6509	17 875	41.667	4.14e+3	3.89	2.65e+1	4.41	4.14e+3	3.89	0.4143
	0.6509	25 642	41.492	2.12e+3	3.71	1.85e+1	1.98	2.12e+3	3.71	0.3112
	0.6509	46 606	40.954	1.38e+3	1.44	1.30e+1	1.18	1.38e+3	1.44	0.3000
	0.6509	103 993	40.417	8.08e+2	1.33	5.13e−0	2.32	8.08e+2	1.33	0.3054
	0.6009	158 200	40.203	5.68e+2	1.68	3.13e−0	2.35	5.68e+2	1.68	0.3094
	0.4566	253 738	40.047	4.04e+2	1.45	1.78e−0	2.39	4.04e+2	1.45	0.3141
	0.4566	455 698	39.837	2.53e+2	1.59	1.05e−0	1.80	2.53e+2	1.59	0.2925
2	0.6509	31 249	108.503	5.04e+3	–	1.87e+1	–	5.04e+3	–	0.3386
	0.6509	46 759	107.245	1.75e+3	5.26	4.26e−0	7.34	1.75e+3	5.26	0.3854
	0.6509	66 439	106.987	5.62e+2	6.46	2.75e−0	2.50	5.62e+2	6.46	0.2274
	0.6509	100 765	105.957	3.87e+2	1.80	1.47e−0	3.01	3.87e+2	1.80	0.2547
	0.6509	160 993	105.224	2.24e+2	2.33	9.24e−1	1.98	2.24e+2	2.33	0.2456
	0.6509	270 037	104.909	1.35e+2	1.95	3.91e−1	3.32	1.35e+2	1.95	0.2523

Table 5.10
Example 3, adaptive scheme for the postprocessed unknown: $\boldsymbol{\sigma}_h$ and $\boldsymbol{\sigma}_h^\star$.

k	h	N	$\mathtt{e}_0(\boldsymbol{\sigma})$	$\mathtt{r}_0(\boldsymbol{\sigma})$	$\mathtt{e}_{\mathbf{div}}(\boldsymbol{\sigma})$	$\mathtt{r}_{\mathbf{div}}(\boldsymbol{\sigma})$	$\mathtt{e}_0^\star(\boldsymbol{\sigma})$	$\mathtt{r}_0^\star(\boldsymbol{\sigma})$	$\mathtt{e}_{\mathbf{div}}^\star(\boldsymbol{\sigma})$	$\mathtt{r}_{\mathbf{div}}^\star(\boldsymbol{\sigma})$
0	0.6509	2 905	4.48e+3	–	1.58e+4	–	4.37e+3	–	1.51e+4	–
	0.6509	4 657	3.70e+3	0.82	1.17e+4	1.29	3.62e+3	0.80	1.05e+4	1.54
	0.6509	6 868	3.24e+3	0.68	9.20e+3	1.23	3.17e+3	0.67	7.53e+3	1.72
	0.6509	13 672	2.55e+3	0.69	8.05e+3	0.39	2.50e+3	0.69	6.03e+3	0.65
	0.6009	42 169	1.66e+3	0.76	6.80e+3	0.30	1.62e+3	0.77	4.15e+3	0.66
	0.4167	81 979	1.29e+3	0.76	6.33e+3	0.22	1.26e+3	0.77	3.28e+3	0.71
	0.3560	204 958	9.35e+2	0.70	5.92e+3	0.15	9.14e+2	0.70	2.35e+3	0.73
	0.3125	412 942	7.21e+2	0.74	5.75e+3	0.08	7.04e+2	0.74	1.89e+3	0.62
	0.2763	861 778	5.56e+2	0.71	5.63e+3	0.06	5.42e+2	0.71	1.45e+3	0.72
1	0.6509	12 169	1.29e+3	–	1.03e+4	–	1.22e+3	–	8.76e+3	–
	0.6509	17 875	6.62e+2	3.48	6.31e+3	2.54	6.32e+2	3.41	4.16e+3	3.88
	0.6509	25 642	4.53e+2	2.10	4.68e+3	1.65	4.32e+2	2.11	2.14e+3	3.69
	0.6509	46 606	3.06e+2	1.31	3.58e+3	0.89	2.91e+2	1.32	1.39e+3	1.44
	0.6509	103 993	1.78e+2	1.35	2.76e+3	0.65	1.69e+2	1.35	8.15e+2	1.33
	0.6009	158 200	1.26e+2	1.67	2.29e+3	0.90	1.19e+2	1.68	5.73e+2	1.68
	0.4566	253 738	8.67e+1	1.58	1.92e+3	0.73	8.20e+1	1.58	4.07e+2	1.45
	0.4566	455 698	5.86e+1	1.33	1.53e+3	0.78	5.55e+1	1.33	2.56e+2	1.59
2	0.6509	31 249	5.54e+2	–	6.79e+3	–	5.12e+2	–	5.05e+3	–
	0.6509	46 759	1.69e+2	5.91	3.38e+3	3.46	1.57e+2	5.87	1.75e+3	5.26
	0.6509	66 439	9.03e+1	3.55	1.81e+3	3.55	8.40e+1	3.55	5.65e+2	6.44
	0.6509	100 765	5.78e+1	2.15	1.37e+3	1.35	5.34e+1	2.18	3.88e+2	1.80
	0.6509	160 993	3.32e+1	2.36	1.00e+3	1.32	3.07e+1	2.36	2.25e+2	2.33
	0.6509	270 037	2.02e+1	1.92	7.33e+2	1.22	1.86e+1	1.94	1.36e+2	1.95

References

[1] D.N. Arnold, F. Brezzi, J. Douglas, PEERS: A new mixed finite element method for plane elasticity, Japan J. Appl. Math. 1 (2) (1984) 347–367.
[2] R. Stenberg, A family of mixed finite elements for the elasticity problem, Numer. Math. 53 (5) (1988) 513–538.
[3] R. Stenberg, Two low-order mixed methods for the elasticity problem, in: The Mathematics of Finite Elements and Applications, VI (Uxbridge, 1987), Academic Press, London, 1988, pp. 271–280.
[4] D.N. Arnold, R.S. Falk, R. Winther, Differential complexes and stability of finite element methods. II: The elasticity complex, in: D.N. Arnold, P. Bochev, R. Lehoucq, R. Nicolaides, M. Shashkov (Eds.), Compatible Spatial Discretizations, in: IMA Volumes in Mathematics and its Applications, vol. 142, Springer Verlag, 2005, pp. 47–67.
[5] D.N. Arnold, R.S. Falk, R. Winther, Finite element exterior calculus, homological techniques, and applications, Acta Numer. 15 (2006) 1–155.
[6] D.N. Arnold, R.S. Falk, R. Winther, Mixed finite element methods for linear elasticity with weakly imposed symmetry, Math. Comp. 76 (260) (2007) 1699–1723.
[7] D.N. Arnold, R. Winther, Mixed finite elements for elasticity, Numer. Math. 92 (3) (2002) 401–419.
[8] S. Adams, B. Cockburn, A mixed finite element method for elasticity in three dimensions, J. Sci. Comput. 25 (3) (2005) 515–521.
[9] D. Boffi, F. Brezzi, M. Fortin, Reduced symmetry elements in linear elasticity, Commun. Pure Appl. Anal. 8 (1) (2009) 95–121.

[10] Z. Cai, C. Tong, P.S. Vassilevski, C. Wang, Mixed finite element methods for incompressible flow: stationary Stokes equations, Numer. Methods Partial Differential Equations 26 (4) (2010) 957–978.
[11] G.N. Gatica, A. Márquez, M.A. Sánchez, Analysis of a velocity–pressure-pseudostress formulation for the stationary Stokes equations, Comput. Methods Appl. Mech. Engrg. 199 (17–20) (2010) 1064–1079.
[12] G.N. Gatica, Analysis of a new augmented mixed finite element method for linear elasticity allowing $\mathbb{RT}_0 - \mathbb{P}_1 - \mathbb{P}_0$ approximations, M2AN Math. Model. Numer. Anal. 40 (1) (2006) 1–28.
[13] G.N. Gatica, An augmented mixed finite element method for linear elasticity with non-homogeneous Dirichlet conditions, Electron. Trans. Numer. Anal. 26 (2007) 421–438.
[14] G.N. Gatica, A. Márquez, S. Meddahi, An augmented mixed finite element method for 3D linear elasticity problems, J. Comput. Appl. Math. 231 (2) (2009) 526–540.
[15] L. Figueroa, G.N. Gatica, A. Márquez, Augmented mixed finite element methods for the stationary Stokes equations, SIAM J. Sci. Comput. 31 (2) (2008–2009) 1082–1119.
[16] G.N. Gatica, M. González, S. Meddahi, A low-order mixed finite element method for a class of quasi-Newtonian Stokes flows. I. A priori error analysis, Comput. Methods Appl. Mech. Engrg. 193 (9–11) (2004) 881–892.
[17] V.J. Ervin, J.S. Howell, I. Stanculescu, A dual-mixed approximation method for a three-field model of a nonlinear generalized Stokes problem, Comput. Methods Appl. Mech. Engrg. 197 (33–40) (2008) 2886–2900.
[18] J.S. Howell, Dual-mixed finite element approximation of Stokes and nonlinear Stokes problems using trace-free velocity gradients, J. Comput. Appl. Math. 231 (2) (2009) 780–792.
[19] V.J. Ervin, E.W. Jenkins, S. Sun, Coupled generalized nonlinear Stokes flow with flow through a porous medium, SIAM J. Numer. Anal. 47 (2) (2009) 929–952.
[20] G.N. Gatica, A. Márquez, R. Oyarzúa, R. Rebolledo, Analysis of an augmented fully-mixed approach for the coupling of quasi-Newtonian fluids and porous media, Comput. Methods Appl. Mech. Engrg. 270 (2014) 76–112.
[21] Z. Cai, C. Wang, S. Zhang, Mixed finite element methods for incompressible flow: stationary Navier–Stokes equations, SIAM J. Numer. Anal. 48 (1) (2010) 79–94.
[22] Z. Cai, S. Zhang, Mixed methods for stationary Navier–Stokes equations based on pseudostress-pressure-velocity formulation, Math. Comp. 81 (280) (2012) 1903–1927.
[23] J.S. Howell, N.J. Walkington, Dual-mixed finite element methods for the Navier–Stokes equations, ESAIM Math. Model. Numer. Anal. 47 (3) (2013) 789–805.
[24] J. Camaño, R. Oyarzua, G. Tierra, Analysis of an augmented mixed-FEM for the Navier Stokes problem, Preprint 2014-33, Centro de Investigación en Ingeniería Matemática (CI^2MA), Universidad de Concepción, Chile, 2014.
[25] E. Colmenares, G.N. Gatica, R. Oyarzua, Analysis of an augmented mixed-primal formulation for the stationary Boussinesq problem, Preprint 2015-07, Centro de Investigación en Ingeniería Matemática (CI^2MA), Universidad de Concepción, Chile, 2015.
[26] J. Camaño, G.N. Gatica, R. Oyarzua, G. Tierra, An augmented mixed finite element method for the Navier–Stokes equations with variable viscosity, Preprint 2015-09, Centro de Investigación en Ingeniería Matemática (CI^2MA), Universidad de Concepción, Chile, 2015.
[27] D.N. Arnold, R.S. Falk, A new mixed formulation for elasticity, Numer. Math. 53 (1–2) (1988) 13–30.
[28] G.N. Gatica, L.F. Gatica, F.A. Sequeira, A $\mathbb{RT}_k$–$\mathbf{P}_k$ approximation for linear elasticity yielding a broken $H(\mathbf{div})$ convergent postprocessed stress, Appl. Math. Lett. 49 (2015) 133–140.
[29] F. Brezzi, M. Fortin, Mixed and Hybrid Finite Element Methods, Springer Verlag, 1991.
[30] V. Girault, P.A. Raviart, Finite Element Methods for Navier–Stokes Equations. Theory and Algorithms, Springer Verlag, 1986.
[31] G.N. Gatica, A Simple Introduction to the Mixed Finite Element Method. Theory and Applications, in: SpringerBriefs in Mathematics, Springer, Cham, Heidelberg, New York, Dordrecht, London, 2014.
[32] D.N. Arnold, J. Douglas, Ch.P. Gupta, A family of higher order mixed finite element methods for plane elasticity, Numer. Math. 45 (1) (1984) 1–22.
[33] R. Hiptmair, Finite elements in computational electromagnetism, Acta Numer. 11 (2002) 237–339.
[34] P.G. Ciarlet, The Finite Element Method for Elliptic Problems, North-Holland, 1978.
[35] P. Clément, Approximation by finite element functions using local regularization, RAIRO Anal. Numer. 9 (R-2) (1975) 77–84.
[36] G.N. Gatica, R. Oyarzúa, F.J. Sayas, A residual-based a posteriori error estimator for a fully-mixed formulation of the Stokes–Darcy coupled problem, Comput. Methods Appl. Mech. Engrg. 200 (21–22) (2011) 1877–1891.
[37] R. Verfürth, A Posteriori Error Estimation Techniques for Finite Element Methods, Oxford University Press, 2013.
[38] C. Amrouche, C. Bernardi, M. Dauge, V. Girault, Vector potentials in three-dimensional non-smooth domains, Math. Methods Appl. Sci. 21 (9) (1998) 823–864.
[39] C. Carstensen, A posteriori error estimate for the mixed finite element method, Math. Comp. 66 (218) (1997) 465–476.
[40] C. Carstensen, G. Dolzmann, A posteriori error estimates for mixed FEM in elasticity, Numer. Math. 81 (2) (1998) 187–209.
[41] G.N. Gatica, A note on the efficiency of residual-based a-posteriori error estimators for some mixed finite element methods, Electron. Trans. Numer. Anal. 17 (2004) 218–233.
[42] R. Verfürth, A Review of a Posteriori Error Estimation and Adaptive-Mesh-Refinement Techniques, Wiley-Teubner, Chichester, 1996.
[43] R. Verfürth, A posteriori error estimation and adaptive-mesh-refinement techniques, J. Comput. Appl. Math. 50 (1–3) (1994) 67–83.
[44] D.N. Arnold, An interior penalty finite element method with discontinuous elements, SIAM J. Numer. Anal. 19 (4) (1982) 742–760.
[45] T.P. Barrios, G.N. Gatica, M. González, N. Heuer, A residual based a posteriori error estimator for an augmented mixed finite element method in linear elasticity, M2AN Math. Model. Numer. Anal. 40 (5) (2006) 843–869 (2007).
[46] G.N. Gatica, L.F. Gatica, A. Márquez, Analysis of a pseudostress-based mixed finite element method for the Brinkman model of porous media flow, Numer. Math. 126 (4) (2014) 635–677.
[47] M. Lonsing, R. Verfürth, On the stability of BDMS and PEERS elements, Numer. Math. 99 (1) (2004) 131–140.
[48] H. Si, TetGen: A quality tetrahedral mesh generator and 3D delaunay triangulator v.1.5 user's manual, Technical Report 13, Weierstrass Institute for Applied Analysis and Stochastics, Berlin, 2013.